Supporting Information

Contents

1. Instrumentation and Materials

Commercially available solvents and reagents were used without further purification unless otherwise noted. Dichloromethane was passed through Alumina plug. The spectroscopic grade solvents were used as solvents for all spectroscopic studies. Silica gel column chromatography was performed on Wakogel C-300 and C-400. Thin-layer chromatography (TLC) was carried out on aluminum sheets coated with silica gel 60 F254 (Merck 5554). UV/Visible absorption spectra were recorded on Shimadzu UV-3600 spectrometers. ^{1}H, ^{13}C and ^{19}F NMR spectra were recorded on a JEOL ECA-600 spectrometer (operating as 600 MHz for ^{1}H, 151 MHz for ^{13}C and 564 MHz for ^{19}F) using the residual solvent as the internal reference for ^{1}H (δ = 7.26 ppm in $CDCl_3$, δ = 2.50 ppm in DMSO-d_6, δ = 1.39 ppm in cyclohexane-d_{12}) and for ^{13}C (δ = 77.16 ppm in $CDCl_3$, δ = 39.52 ppm in DMSO-d_6), and hexafluorobenzene as an external reference for ^{19}F (δ = –162.9 ppm). High-resolution atmospheric-pressure-chemical-ionization time-of-flight mass-spectrometry (HR-APCI-TOF-MS) was recorded on a BRUKER micrOTOF model using positive mode. Single-crystal X-ray diffraction analysis data were collected at –180 °C with a Rigaku XtaLAB P200 by using graphite monochromated Cu-$K\alpha$ radiation (λ = 1.54187 Å). The structures were solved by direct methods (SHELXS-2013/1 or SHELXT-2014/5) and refined with full-matrix least square technique (SHELXL-2014/7).

2. Experimental Section

1,14-dibromo-5,10-diphenyltripyrrane (**2**)

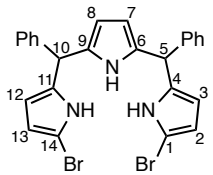

A solution of 5,10-diphenyltripyrrane **1** (755.0 mg, 2.00 mmol) in dry THF (40 mL) under Ar was cooled to –78 °C, to which *N*-bromosuccinimide (733 mg, 4.1 mmol) was added in two portions over 2.5 h. The reaction was quenched at –78 °C with an aqueous $Na_2S_2O_3$ solution. Dichloromethane was added and the organic layer was separated. The organic extract was washed by water and dried with anhydrous Na_2SO_4. The solvent was evaporated to dryness. The crude product was purified by column chromatography on silica gel (C-300: *n*-hexane/dichloromethane = 1/2) to afford **2** (766.7 mg, 1.45 mmol, 72%).

^{1}H NMR ($CDCl_3$, r.t.) δ (ppm): 7.81 (s, 2H, NH), 7.67 (s, 1H, NH), 7.33 (t, J = 7.3 Hz, 4H, Ph-H), 7.28 (t, J = 7.3 Hz, 4H, Ph-H), 7.18 (d, J = 7.3 Hz, 2H, Ph-H), 6.06 (m, 2H, β-H), 5.79 (m, 4H, β-H), and 5.31 (s, 2H, methylene-H).

The product is unstable in ambient conditions and used in the next step immediately.

1,14-dibromo-5,10-diphenyltripyrrin (**3**)

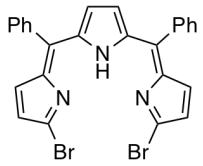

A solution of **2** (1.77 g, 3.31 mmol) in dry dichloromethane (400 mL) under Ar was cooled to 0 °C, to which DDQ (1.57 g, 6.93 mmol) was added and the reaction mixture was stirred at 0 °C for 10 min. The reaction mixture was filtered through a short pad of alumina with dichloromethane as an eluent and the filtrate was concentrated under reduced pressure. The crude product was purified by recrystallization from dichloromethane/methanol to give **3** (1.53 g, 2.98 mmol, 87%) as brown solids.

^{1}H NMR ($CDCl_3$, r.t.) δ (ppm): 13.44 (s, 1H, NH), 7.49 (m, 2H, Ph-H), 7.45 (s, 4H, Ph-H), 7.45 (s, 4H, Ph-H), 6.75 (d, J = 4.6 Hz, 2H, β-H), 6.54 (d, J = 4.6 Hz, 2H, β-H), and 6.31 (s, 2H, β-H).

^{13}C NMR ($CDCl_3$, r.t.) δ (ppm): 150.90, 150.33, 139.37, 138.43, 137.09, 136.52, 131.14, 129.38, 128.95, 127.99, and 122.69.

HR APCI-TOF-MS (positive): m/z calcd for $[C_{26}H_{18}N_3{}^{79}Br_2]^+$: 529.9862 $[M + H]^+$; found: 529.9844.

UV/vis (CH_2Cl_2): λ_{max} [nm] (ε [M^{-1} cm^{-1}]) = 344 (37000), 363 (34000), 536 (24000), and 573 (28000).

1,14-dianilino-5,10-diphenyltripyrrin (4)

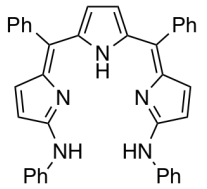

A mixture of **3** (15.9 mg, 30 μmol) and aniline (11 μL, 0.12 mmol) in dry THF (3 mL) was stirred at room temperature for 14 h under Ar. After quenching with water, the solution was extracted with ethyl acetate. The organic fraction was washed by water and dried with anhydrous Na_2SO_4. The solvent was evaporated to dryness. The crude product was purified by column chromatography on silica gel (C-400: dichloromethane/ethyl acetate = 100/3) to afford **4** (10.7 mg, 96%) as black solids.

^{1}H NMR ($CDCl_3$, r.t., 4.8 mM) δ (ppm): 12.34 (s, 4H, dimer, aniline-NH), 11.93 (s, 2H, dimer, NH), 7.49 (m, 4H, monomer, Ph-H), 7.42 (m, 6H, monomer, Ph-H), 7.27 (m, 4H, dimer, Ph-H), 7.11 (m, 16H, dimer, Ph-H), 6.94 (t, J = 7.4 Hz, 4H, dimer, Ph-H), 6.89 (br, 2H, monomer, Ph-H), 6.83 (d, J = 5.0 Hz, monomer, 2H, β-H), 6.75 (br, 8H, dimer, Ph-H), 6.52 (d, J = 7.8 Hz, 8H, dimer, Ph-H), 6.45 (d, J = 4.6 Hz, 4H, dimer, β-H), 6.40 (d, J = 4.6 Hz, 4H, dimer, β-H), 6.36 (br, 2H, monomer, β-H), 6.12 (br, 2H, monomer, β-H), and 6.00 (d, J = 2.3 Hz, 4H, dimer, β-H). (The signals assignable to NH protons of monomeric **4** were not observed presumably because of their broadness or equilibrium between monomer and dimer.)

^{1}H NMR (DMSO-d_6, r.t.) δ (ppm): 13.06 (s, 1H, NH), 9.55 (s, 2H, aniline-NH), 7.62 (d, J = 7.8 Hz, 4H, Ph-H), 7.5–7.4 (m, 10H, Ph-H), 6.87 (d, J = 7.8 Hz, 4H, Ph-H), 6.77 (d, J = 4.6 Hz, 2H, β-H), 6.72 (t, J = 7.3 Hz, 2H, Ph-H), 6.53 (d, J = 4.6 Hz, 2H, β-H), and 5.97 (d, J = 2.3 Hz, 2H, β-H).

^{13}C NMR ($CDCl_3$, r.t.) δ (ppm): 166.67, 166.52, 163.92, 149.11, 148.88, 141.42, 139.21, 138.54, 138.04, 136.94, 132.16, 131.59, 129.27, 129.07, 128.92, 128.40, 128.22, 127.99, 127.88, 127.43, 122.78, 121.90, 119.96, 119.79, 119.56, 119.38, 118.99, and 117.74. (Some signals were not observed because of equilibrium between monomer and dimer.)

^{13}C NMR (DMSO-d_6, r.t.) δ (ppm): 163.94, 150.52, 139.97, 138.28, 136.24, 134.86, 131.30, 128.10, 127.83, 126.48, 123.36, 121.22, 118.59, and 116.51. (A signal was not observed presumably because of their broadness or overlapping with the major conformer.)

HR APCI-TOF-MS (positive): m/z calcd for $[C_{38}H_{30}N_5]^+$: 556.2496 [M]$^-$; found: 556.2478.

UV/vis (n-hexane, 1.0 × 10^{-5} M): λ_{max} [nm] (ε [M^{-1} cm^{-1}]) = 399 (48000) and 588 (13000).

UV/vis ($CHCl_3$, 1.0 × 10^{-5} M): λ_{max} [nm] (ε [M^{-1} cm^{-1}]) = 400 (46000) and 585 (13000).

UV/vis (CH_2Cl_2, 1.0 × 10^{-5} M): λ_{max} [nm] (ε [M^{-1} cm^{-1}]) = 398 (49000) and 576 (14000).

UV/vis (MeOH, 1.0 × 10^{-5} M): λ_{max} [nm] (ε [M^{-1} cm^{-1}]) = 401 (38000), 571 (8000), and 608 (7900).

UV/vis (DMSO, 1.0 × 10^{-5} M): λ_{max} [nm] (ε [M^{-1} cm^{-1}]) = 409 (42000), 573 (9600), and 613 (9600).

1-anilino-5,10-diphenyl-14-bromotripyrrin (**S1**)

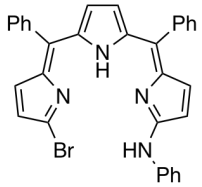

A mixture of **3** (116.9 mg, 0.22 mmol), dry acetonitrile (66 mL), and aniline (20 μL, 0.22 mmol) in dry THF (22 mL) was stirred at room temperature for 14 h under Ar. After quenching with water, the aqueous layer was extracted with ethyl acetate. The organic extract was washed by water and dried with anhydrous Na_2SO_4. The solvent was evaporated to dryness. The crude product was purified by column chromatography on silica gel (C-400: *n*-hexane/dichloromethane = 1/2) to afford **S1** (107 mg, 90%) as black solids.

^{1}H NMR ($CDCl_3$, r.t.) δ (ppm): 14.36 (s, 1H, NH), 8.19 (s, 1H, aniline-NH), 7.5–7.4 (10H, Ph-H), 7.36 (t, *J* = 7.8 Hz, 2H, Ph-H), 7.26 (d, *J* = 4.6 Hz, 2H, Ph-H), 7.14 (d, *J* = 7.3 Hz, 1H, Ph-H), 6.86 (d, *J* = 4.6 Hz, 1H, *β*-H), 6.68 (d, *J* = 4.6 Hz, 2H, *β*-H), 6.44 (d, *J* = 4.1 Hz, 1H, *β*-H), 6.28 (d, *J* = 2.3 Hz, 1H, *β*-H), and 6.13 (d, *J* = 2.8 Hz, 1H, *β*-H).

^{13}C NMR ($CDCl_3$, r.t.) δ (ppm): 166.43, 151.71, 147.96, 145.78, 143.32, 140.39, 139.59, 138.75, 137.42, 136.97, 136.34, 136.00, 131.20, 131.12, 129.68, 129.11, 128.23, 127.92, 127.76, 127.34, 125.89, 124.39, 124.29, 121.22, 119.75, and 118.65.

HR APCI-TOF-MS (positive): *m*/*z* calcd for $[C_{32}H_{24}N_4{}^{79}Br]^+$: 543.1179 [*M*+H]$^-$; found: 543.1160.

1,14-bis(*p*-trifluoromethylanilino)-5,10-diphenyltripyrrin (**5**)

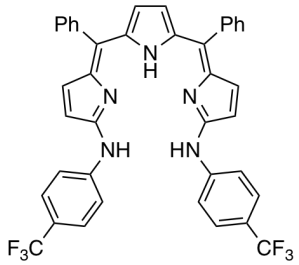

A mixture of **3** (79.7 mg, 0.15 mmol) and *p*-trifluoromethylaniline (75 μL, 0.60 mmol) in dry THF (30 mL) was stirred at room temperature for 12 h under Ar. After quenching with water, the solution was extracted with ethyl acetate. The organic extract was washed by water and dried with anhydrous Na_2SO_4. The solvent was evaporated to dryness. The crude product was purified by column chromatography on silica gel (C-400: dichloromethane) to afford **5** (101.4 mg, 98%) as black solids.

^{1}H NMR ($CDCl_3$, r.t., 4.8 mM) δ (ppm): 12.90 (s, 1H, monomer, NH), 12.48 (s, 4H, dimer, aniline-NH), 11.89 (s, 2H, dimer, NH), 7.52 (m, 4H, monomer, Ph-H), 7.45 (m, 6H, monomer,

Ph-H), 7.42 (br, 8H, dimer, Ph-H), 7.37 (d, *J* = 8.2 Hz, 8H, dimer, Ar-H), 7.33 (t, *J* = 7.8 Hz, 4H, dimer, Ph-H), 7.0–7.3 (br, 8H, dimer, Ph-H), 7.14 (br, 4H, monomer, Ar-H), 6.90 (d, *J* = 4.6 Hz, 2H, monomer, *β*-H), 6.60 (d, *J* = 8.2 Hz, 8H, dimer, Ar-H), 6.54 (d, *J* = 4.6 Hz, 4H, dimer, *β*-H), 6.47 (br, 4H, monomer, Ar-H), 6.40 (d, *J* = 5.0 Hz, 4H, dimer, *β*-H), 6.27 (d, *J* = 3.7 Hz, 2H, monomer, *β*-H), 6.20 (s, 2H, monomer, *β*-H), and 6.07 (d, *J* = 2.3 Hz, 4H, dimer, *β*-H). (The signals assignable to NH protons of monomeric **5** were not observed presumably because of their broadness or equilibrium between monomer and dimer.)

^{1}H NMR (DMSO-d_6, r.t.) δ (ppm): 12.96 (s, 1H, NH), 9.86 (s, 2H, aniline-NH), 7.66 (d, *J* = 8.7 Hz, 4H, Ar-H), 7.4–7.6 (m, 10H, Ph-H), 7.10 (d, *J* = 8.7 Hz, 4H, Ar-H), 6.79 (d, *J* = 4.6 Hz, 2H, *β*-H), 6.47 (d, *J* = 4.6 Hz, 2H, *β*-H), and 6.04 (d, *J* = 2.3 Hz, 2H, *β*-H).

^{19}F NMR (DMSO-d_6, r.t.) δ (ppm): –60.23 (s, CF_3).

HR APCI-TOF-MS (positive): *m*/*z* calcd for $[C_{40}H_{28}N_5F_6]^+$: 692.2243 $[M + H]^+$; found: 692.2249.

UV/vis (*n*-hexane, 1.0 × 10^{-5} M): λ_{max} [nm] (ε [M^{-1} cm^{-1}]) = 392 (58000), 561 (13000), and 605 (15000).

UV/vis (CH_2Cl_2, 1.0 × 10^{-5} M): λ_{max} [nm] (ε [M^{-1} cm^{-1}]) = 396 (59000), 565 (11000), and 604 (13000).

UV/vis (DMSO, 1.0 × 10^{-5} M): λ_{max} [nm] (ε [M^{-1} cm^{-1}]) = 405 (59000), 570 (11000), and 613 (12000).

1,14-bis(*p*-methoxyanilino)-5,10-diphenyltripyrrin (**6**)

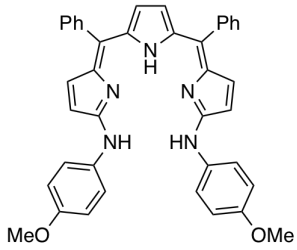

A mixture of **3** (79.7 mg, 0.15 mmol) and *p*-anisidine (73.9 mg, 0.60 mmol) in dry THF (30 mL) was stirred at room temperature for 24 h under Ar. After quenching with water, the solution was extracted with ethyl acetate. The organic extract was washed by water and dried with anhydrous Na_2SO_4. The solvent was evaporated to dryness. The crude product was purified by column chromatography on silica gel (C-400: dichloromethane/ethyl acetate = 10/1). Recrystallization from dichloromethane/*n*-hexane gave **6** (86.5 mg, 93%) as black solids.

^{1}H NMR ($CDCl_3$, r.t., 4.8 mM) δ (ppm): 12.26 (s, 4H, dimer, aniline-NH), 11.92 (s, 2H, dimer, NH), 7.48 (m, 4H, monomer, Ph-H), 7.41 (m, 6H, monomer, Ph-H), 7.28 (m, 4H, dimer, Ph-H), 7.14 (t, *J* = 7.3 Hz, 8H, dimer, Ph-H), 7.0–7.2 (m, 4H, monomer, Ar-H), 6.80 (m, {8H, dimer, Ph-H} + {2H, monomer, *β*-H}), 6.68 (m, {8H, dimer, Ar-H} + {4H, monomer, Ar-H}), 6.42 (m, {4H, dimer, *β*-H} + {8H, dimer, Ar-H)), 6.33 (d, *J* = 4.6 Hz, 4H, dimer, *β*-H), 6.30 (br, 2H, monomer, *β*-H), 6.09 (brs, 2H, monomer, *β*-H), 6.00 (brs, 4H, dimer, *β*-H), 3.77 (s, 12H, dimer, MeO-H), and

3.72 (s, 6H, monomer, MeO-H). (The signals assignable to NH protons of monomeric **6** were not observed presumably because of their broadness or equilibrium between monomer and dimer.)
^{1}H NMR (DMSO-d_6, r.t.) δ (ppm): 13.09 (s, 1H, NH), 9.51 (s, 2H, aniline-NH), 7.60 (d, J = 8.7 Hz, 4H, Ar-H), 7.4–7.5 (m, 10H, Ph-H), 6.75 (d, J = 4.6 Hz, 2H, β-H), 6.48 (d, J = 4.6 Hz, 2H, β-H), 6.44 (d, J = 8.7 Hz, 4H, Ar-H), 5.93 (d, J = 2.3 Hz, 2H, β-H), and 3.59 (s, 6H, MeO-H).
^{13}C NMR ($CDCl_3$, r.t.) δ (ppm): 166.73, 164.22, 164.17, 155.31, 149.23, 139.42, 137.87, 136.82, 135.13, 132.17, 131.61, 128.13, 127.86, 127.39, 127.16, 121.13, 118.91, 117.30, 114.45, 114.09, 55.90, and 55.61. (Some signals were not observed because of poor solubility and equilibrium of monomer and dimer.)
HR APCI-TOF-MS (positive): m/z calcd for $[C_{40}H_{33}N_5O_2]^+$: 615.2629 $[M]^+$; found: 615.2606.
UV/vis (CH_2Cl_2, 1.0 × 10^{-5} M): λ_{max} [nm] (ε [M^{-1} cm^{-1}]) = 406 (43000) and 585 (13000).
UV/vis (DMSO, 1.0 × 10^{-5} M): λ_{max} [nm] (ε [M^{-1} cm^{-1}]) = 419 (41000), 588 (9800), and 629 (9300).

1,14-bis(*m*-di-*tert*-butylanilino)-5,10-diphenyltripyrrin (**7**)

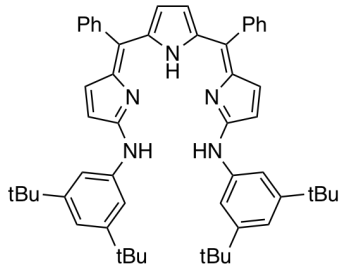

A mixture of **3** (79.7 mg, 0.15 mmol) and 3,5-di-*tert*-butylaniline (123.2 mg, 0.60 mmol) in dry THF (30 mL) was stirred at room temperature for 12 h under Ar. After quenching with water, the solution was extracted with ethyl acetate. The organic extract was washed by water and dried with anhydrous Na_2SO_4. The solvent was evaporated to dryness. The crude product was purified by column chromatography on silica gel (C-400: dichloromethane/ethyl acetate = 100/2). Recrystallization from dichloromethane/*n*-hexane gave **7** (104.4 mg, 89%) as black solids.

^{1}H NMR ($CDCl_3$, r.t., 4.8 mM) δ (ppm): 12.07 (s, 4H, dimer, aniline-NH), 11.81 (s, 2H, dimer, NH), 7.48 (m, 4H, monomer, Ph-H), 7.42 (m, 6H, monomer, Ph-H), 7.23 (t, J = 7.7 Hz, 4H, dimer, Ph-H), 7.0–7.1 (br, 8H, dimer, Ph-H), 7.04 (brs, 2H, monomer, *p*-Ar-H), 7.02 (m, 4H, dimer, *p*-Ar-H), 6.7–7.0 (br, 8H, dimer, Ph-H), 6.79 (br, 4H, monomer, *o*-Ar-H), 6.45 (brs, 8H, dimer, *o*-Ar-H), 6.42 (d, J = 4.2 Hz, 4H, dimer, β-H), 6.37 (d, J = 4.6 Hz, 4H, dimer, β-H), 6.0–6.3 (br, 2H, monomer, β-H), 5.97 (d, J = 2.3 Hz, 4H, dimer, β-H), 1.20 (s, 72H, dimer, *t*-Bu-H), and 1.16 (s, 36H, monomer, *t*-Bu-H). (Some signals of monomeric **7** were not observed because of their broadness or equilibrium of monomer and dimer.)
^{1}H NMR (cyclohexane-d_{12}, r.t.) δ (ppm): 12.12 (s, 4H, aniline-NH), 11.85 (s, 2H, NH), 7.13 (t, J = 7.8 Hz, 4H, Ph-H), 7.03 (s, 4H, *p*-Ar-H), 6.99 (br, 8H, Ph-H), 6.7–6.9 (br, 8H, Ph-H), 6.48 (brs, 8H,

o-Ar-H), 6.44 (d, *J* = 4.6 Hz, 4H, *β*-H), 6.42 (d, *J* = 5.0 Hz, 4H, *β*-H), 5.90 (d, *J* = 2.3 Hz, 4H, *β*-H), and 1.21 (s, 72H, *t*-Bu-H).

^{13}C NMR ($CDCl_3$, r.t.) δ (ppm): 166.57, 151.67, 149.23, 140.77, 139.81, 137.41, 136.79, 132.11, 131.34, 128.09, 127.97, 127.75, 127.71, 127.29, 119.57, 117.96, 117.82, 116.27, 114.04, 35.03, 34.87, and 31.51. (Some signals were not observed because of equilibrium of monomer and dimer.)

HR APCI-TOF-MS (positive): *m*/*z* calcd for $[C_{54}H_{61}N_5]^+$: 779.4921 [*M*]$^+$; found: 779.4909.

UV/vis (*n*-hexane, 1.0 × 10^{-5} M): λ_{max} [nm] (ε [M^{-1} cm^{-1}]) = 409 (46000) and 577 (15000).

UV/vis (CH_2Cl_2, 1.0 × 10^{-5} M): λ_{max} [nm] (ε [M^{-1} cm^{-1}]) = 400 (47000) and 591 (18000).

UV/vis (DMSO, 1.0 × 10^{-5} M): λ_{max} [nm] (ε [M^{-1} cm^{-1}]) = 409 (30000) and 601 (13000).

1,14-bis(*m*-di-trifluoromethylanilino)-5,10-diphenyltripyrrin (**8**)

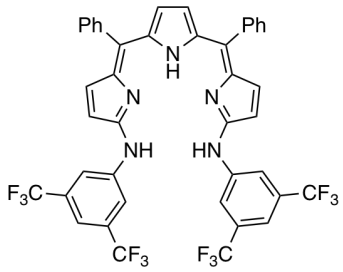

A mixture of **3** (79.7 mg, 0.15 mmol) and 3,5-bis(trifluoromethyl)aniline (94 mL, 0.60 mmol) in dry THF (30 mL) was refluxed for 6 h under Ar. After quenching with water, the solution was extracted with ethyl acetate. The organic extract was washed by water and dried with anhydrous Na_2SO_4. The solvent was evaporated to dryness. The crude product was purified by column chromatography on silica gel (C-400: *n*-hexane/dichloromethane = 1/1) to afford **8** (112.6 mg, 91%) as black solids.

^{1}H NMR ($CDCl_3$, r.t., 4.8 mM) δ (ppm): 12.74 (s, 4H, dimer, aniline-NH), 11.79 (s, 2H, dimer, NH), 7.4–7.5 (m, 10H, monomer, Ph-H), 7.42 (s, 4H, dimer, *p*-Ar-H), 7.37 (t, *J* = 7.8 Hz, 4H, dimer, Ph-H), 7.19 (br, 8H, dimer, Ph-H), 6.97 (s, 8H, dimer, *o*-Ar-H), 6.5-6.8 (br, 8H, dimer, Ph-H), 6.60 (d, *J* = 4.6 Hz, 4H, dimer, *β*-H), 6.42 (d, *J* = 4.6 Hz, 4H, dimer, *β*-H), 6.14 (brs, 2H, monomer, *β*-H), and 6.09 (d, *J* = 1.8 Hz, 4H, dimer, *β*-H). (Some signals of monomeric **8** were not observed because of their broadness or equilibrium of monomer and dimer.)

^{1}H NMR (cyclohexane-d_{12}, r.t.) δ (ppm): 12.85 (s, 4H, aniline-NH), 11.84 (s, 2H, NH), 7.40 (s, 4H, *p*-Ar-H), 7.29 (t, *J* = 7.8 Hz, 4H, Ph-H), 7.13 (brs, 8H, Ph-H), 6.99 (s, 8H, *o*-Ar-H), 6.5-6.9 (br, 8H, Ph-H), 6.55 (d, *J* = 5.0 Hz, 4H, *β*-H), 6.40 (d, *J* = 5.0 Hz, 4H, *β*-H), and 6.08 (d, *J* = 2.3 Hz, 4H, *β*-H).

^{19}F NMR (DMSO-d_6, r.t.) δ (ppm): –61.94 (s, CF_3).

HR APCI-TOF-MS (positive): *m*/*z* calcd for $[C_{42}H_{26}F_{12}N_5]^+$: 828.1991 [*M*+H]$^+$; found: 828.1982.

UV/vis (*n*-hexane, 1.0 × 10^{-5} M): λ_{max} [nm] (ε [M^{-1} cm^{-1}]) = 392 (55000) and 575 (16000).

UV/vis (CH_2Cl_2, 1.0 × 10^{-5} M): λ_{max} [nm] (ε [M^{-1} cm^{-1}]) = 394 (63000) and 595 (14000).

1,14-bis(*a*-naphthylamino)-5,10-diphenyltripyrrin (9)

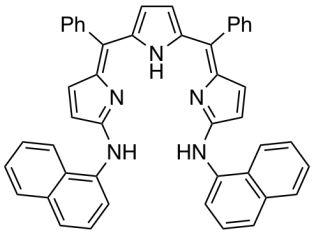

A mixture of **3** (79.7 mg, 0.15 mol) and 1-naphthylamine (85.9 mg, 0.60 mmol) in dry THF (30 mL) was stirred at room temperature for 48 h under Ar. After quenching with water, the solution was extracted with ethyl acetate. The organic extract was washed by water and dried with anhydrous Na_2SO_4. The solvent was evaporated to dryness. The crude product was purified by column chromatography on silica gel (C-400: dichloromethane/ethyl acetate = 100/3). Recrystallization from dichloromethane/*n*-hexane gave **9** (78.8 mg, 80%) as black solids.

^{1}H NMR ($CDCl_3$, r.t., 4.8 mM) δ (ppm): 11.9 (s, 1H, NH), 7.6–7.8 (br, 2H, naphthyl-H), 7.50 (m, {4H, Ph-H} + {2H, naphthyl-H}), 7.42 (m, 6H, Ph-H), 7.35 (d, *J* = 8.2 Hz, 2H, naphthyl-H), 7.18 (t, *J* = 7.8 Hz, 2H, naphthyl-H), 7.11 (br, 4H, naphthyl-H), 6.78 (d, *J* = 4.1 Hz, 2H, β-H), 6.72 (br, 2H, naphthyl-H), 6.28 (brs, 2H, β-H), and 6.12 (brs, 2H, β-H). (The signals assigned to aniline-NH protons were not observed because of their broadness.)
^{1}H NMR (DMSO-d_6, r.t.) δ (ppm): 13.31 (s, 1H, NH), 9.27 (s, 2H, amine-NH), 8.80 (d, *J* = 7.3 Hz, 2H, Naphthyl-H), 7.84 (d, *J* = 8.7 Hz, 2H, Naphthyl-H), 7.70 (d, *J* = 8.2 Hz, 2H, Naphthyl-H), 7.49 (m, 10H, Ph-H), 7.31 (m, 4H, Naphthyl-H), 7.15 (t, *J* = 7.6 Hz, 2H, Naphthyl-H), 6.91 (t, *J* = 7.8 Hz, 2H, Naphthyl-H), 6.86 (d, *J* = 4.8 Hz, 2H, β-H), 6.82 (d, *J* = 4.8 Hz, 2H, β-H), and 5.98 (d, *J* = 3.2 Hz, 2H, β-H).
^{13}C NMR ($CDCl_3$, r.t.) δ (ppm): 164.86, 137.58, 136.77, 136.45, 133.99, 131.34, 131.06, 128.67, 128.25, 128.06, 127.39, 125.68, 125.38, 125.00, 124.11, 122.84, 118.80, 118.16, and 116.95. (Some signals were not observed because of their broadness or overlapping with the major signals.)
HR APCI-TOF-MS (positive): *m*/*z* calcd for $[C_{46}H_{33}N_5]^+$: 655.2730 $[M]^+$; found: 655.2694.
UV/vis (*n*-hexane): λ_{max} [nm] (ε [M^{-1} cm^{-1}]) = 398 (56000) and 603 (11000).
UV/vis (CH_2Cl_2): λ_{max} [nm] (ε [M^{-1} cm^{-1}]) = 400 (48000) and 580 (15000).
UV/vis (DMSO): λ_{max} [nm] (ε [M^{-1} cm^{-1}]) = 347 (32000), 418 (45000), and 582 (11000).

1,14-dimesithylamino-5,10-diphenyltripyrrin (10)

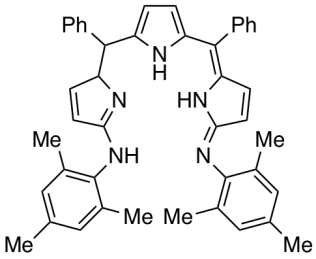

A mixture of **3** (79.7 mg, 0.15 mmol) and 2,4,6-trimethylaniline (0.17 mL, 1.2 mmol) in dry THF (30 mL) was refluxed for 48 h under Ar. After quenching with water, the solution was extracted with ethyl acetate. The organic extract was washed by water and dried with anhydrous Na_2SO_4. The solvent was evaporated to dryness. The crude product was purified by column chromatography on silica gel (C-400: dichloromethane/ethyl acetate = 100/3) to afford **10** (93.1 mg, 80%) as black solids.

^{1}H NMR ($CDCl_3$, r.t.) δ (ppm): 11.90 (s, 1H, NH), 7.45–7.5 (m, 4H, Ph-H), 7.35–7.45 (m, 6H, Ph-H), 6.75 (s, 4H, Mes-H), 6.70 (d, 2H, J = 5.0 Hz, β-H), 6.07 (s, 2H, β-H), 5.76 (d, 2H, J = 5.0 Hz, β-H), 2.22 (s, 6H, Me-H), and 2.06 (s, 12H, Me-H). (The signals assigned to aniline-NH protons were not observed because of their broadness.)

^{1}H NMR (cyclohexane-d_{12}, r.t.) δ (ppm): 12.14 (s, 1H, NH), 7.35–7.45 (m, 4H, Ph-H), 7.25–7.35 (m, 6H, Ph-H), 6.67 (s, 4H, Mes-H), 6.60 (d, J = 5.0 Hz, 2H, β-H), 5.91 (s, 2H, β-H), 5.64 (d, 2H, J = 5.0 Hz, β-H), 2.15 (s, 6H, Me-H), and 2.03 (s, 12H, Me-H). (The signals assigned to aniline-NH protons were not observed because of their broadness.)

^{13}C NMR ($CDCl_3$, r.t.) δ (ppm): 165.67, 137.69, 136.93, 136.09, 134.21, 133.12, 131.31, 128.76, 127.99, 117.43, 116.23, 20.97, and 18.44. (Some signals were not observed because of their broadness or overlapping with the major signals.)

HR APCI-TOF-MS (positive): m/z calcd for $[C_{44}H_{42}N_5]^+$: 640.3435 $[M + H]^+$; found: 640.3407.

UV/vis (n-hexane): λ_{max} [nm] (ε [M^{-1} cm^{-1}]) = 384 (52000) and 575 (12000).

UV/vis (CH_2Cl_2): λ_{max} [nm] (ε [M^{-1} cm^{-1}]) = 384 (45000) and 563 (14000).

UV/vis (DMSO): λ_{max} [nm] (ε [M^{-1} cm^{-1}]) = 388 (27000) and 539 (21000).

1,14-bis(*N*-methylanilino)-5,10-diphenyltripyrrin (**11**)

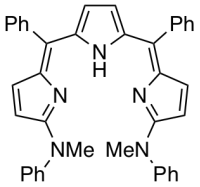

A mixture of **3** (79.7 mg, 0.15 mmol) and *N*-methylaniline (65 μL, 0.60 mmol) in dry THF (30 mL) was stirred at room temperature for 12 h under Ar. After quenching with water, the solution was extracted with ethyl acetate. The organic extract was washed by water and dried with anhydrous Na_2SO_4. The solvent was evaporated to dryness. The crude product was

purified by column chromatography on silica gel (C-400: dichloromethane/ethyl acetate = 20/1). Recrystallization from *n*-hexane gave **11** (82.9 mg, 95%) as black solids.

^{1}H NMR ($CDCl_3$, r.t.) δ (ppm): 13.22 (s, 1H, NH), 7.5–7.45 (m, 4H, Ph-H), 7.3–7.45 (m, 10H, Ph-H), 7.15–7.25 (m, 6H, Ph-H), 6.68 (d, J = 4.6 Hz, 2H, β-H), 6.2–6.6 (br, 2H, β-H), and 6.21 (d, J = 4.6 Hz, 2H, β-H).
^{13}C NMR ($CDCl_3$, r.t.) δ (ppm): 167.97, 149.78, 145.57, 138.75, 137.26, 137.10, 131.52, 129.39, 128.36, 127.93, 127.76, 125.56, 125.19, 119.37, 118.55, and 39.09.
HR APCI-TOF-MS (positive): m/z calcd for $[C_{40}H_{34}N_5]^+$: 584.2809 $[M + H]^+$; found: 584.2800.
UV/vis (*n*-hexane): λ_{max} [nm] (ε [M^{-1} cm^{-1}]) = 393 (43000) and 576 (23000).
UV/vis (CH_2Cl_2): λ_{max} [nm] (ε [M^{-1} cm^{-1}]) = 397 (46000) and 580 (29000).
UV/vis (DMSO): λ_{max} [nm] (ε [M^{-1} cm^{-1}]) = 400 (41000) and 584 (25000).

3. NMR Spectra

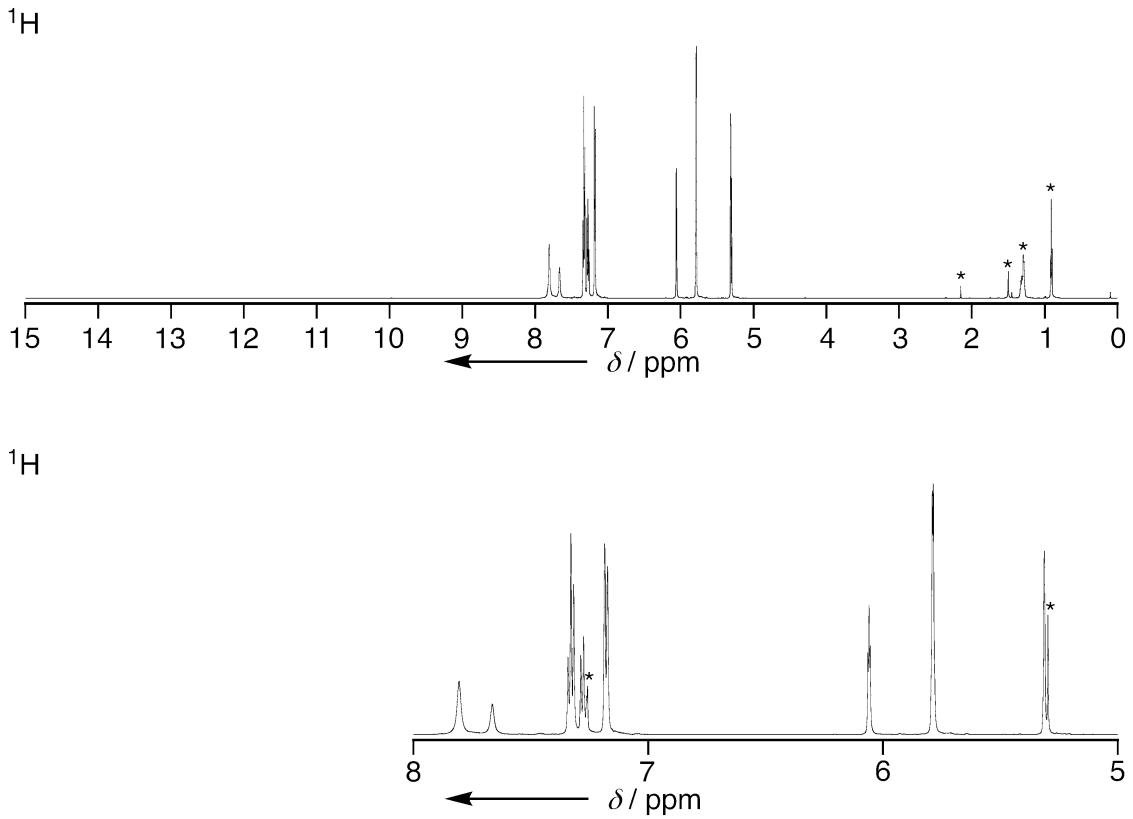

Figure S3-1. ^{1}H NMR spectrum of **2** in $CDCl_3$ at room temperature. * means residual solvent peaks.

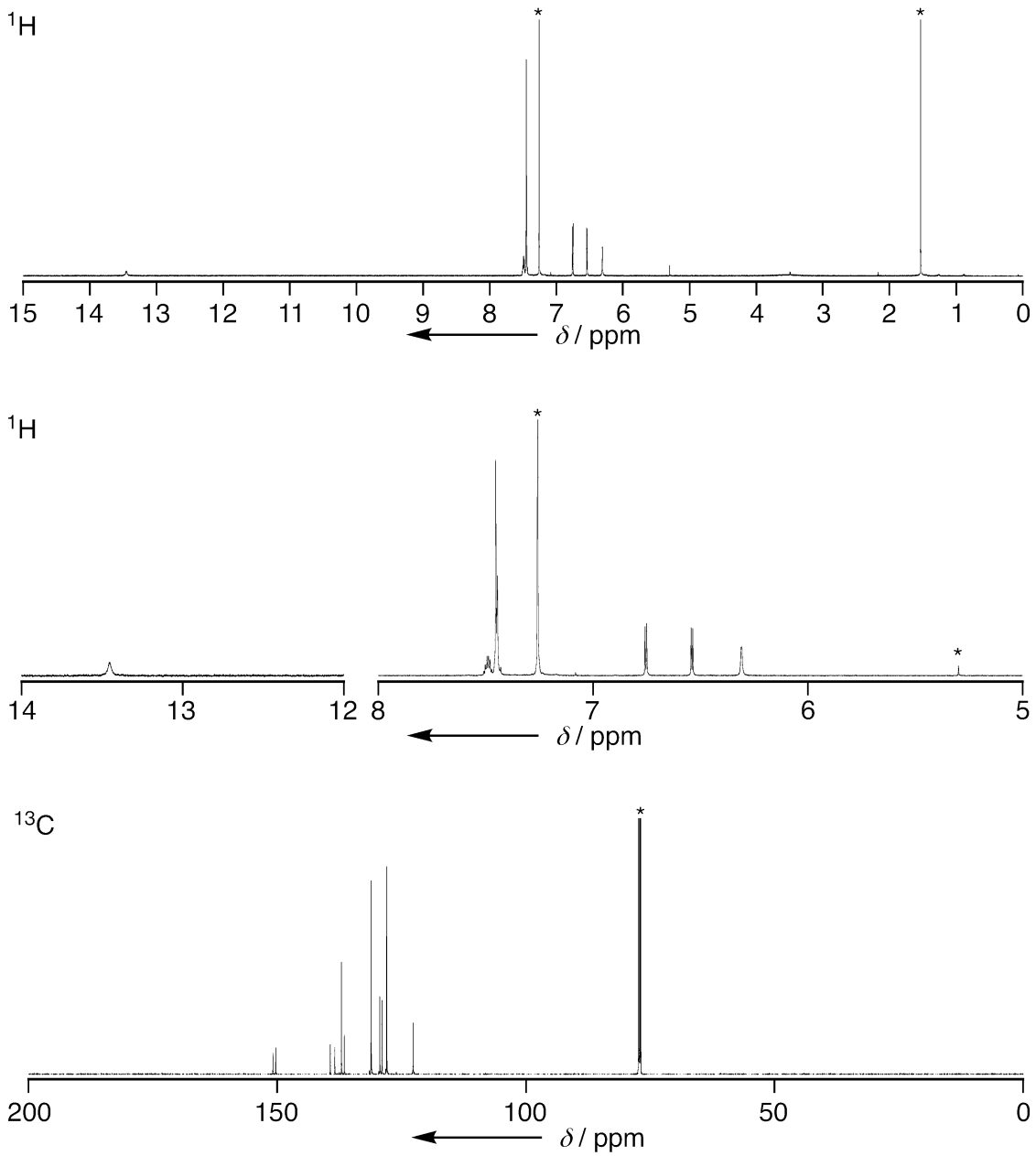

Figure S3-2. ^{1}H and ^{13}C NMR spectra of **3** in $CDCl_3$ at room temperature. * means residual solvent peaks.

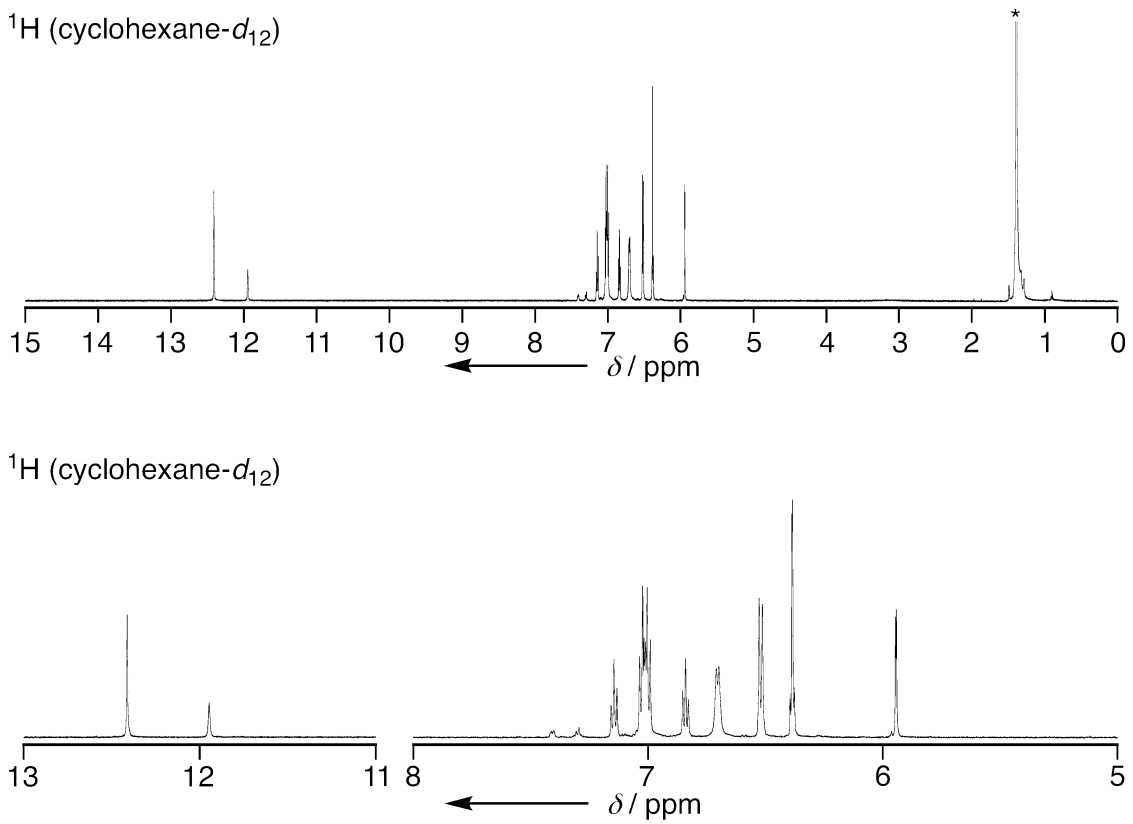

Figure S3-3. ^{1}H NMR spectrum of **4** in cyclohexane-d_{12} at room temperature. * means residual solvent peaks.

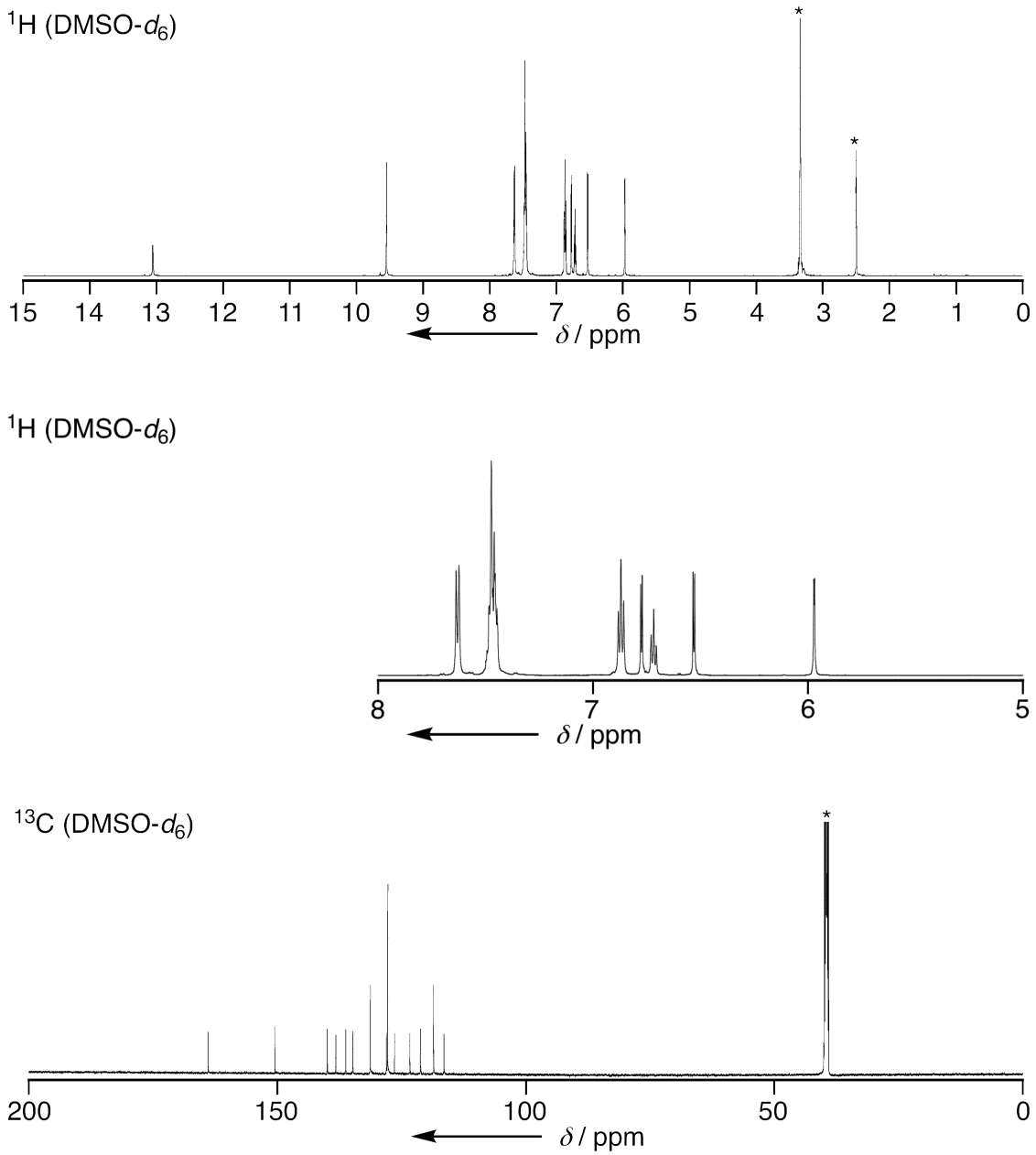

Figure S3-4. ^{1}H and ^{13}C NMR spectra of **4** in DMSO-d_6 at room temperature. * means residual solvent peaks.

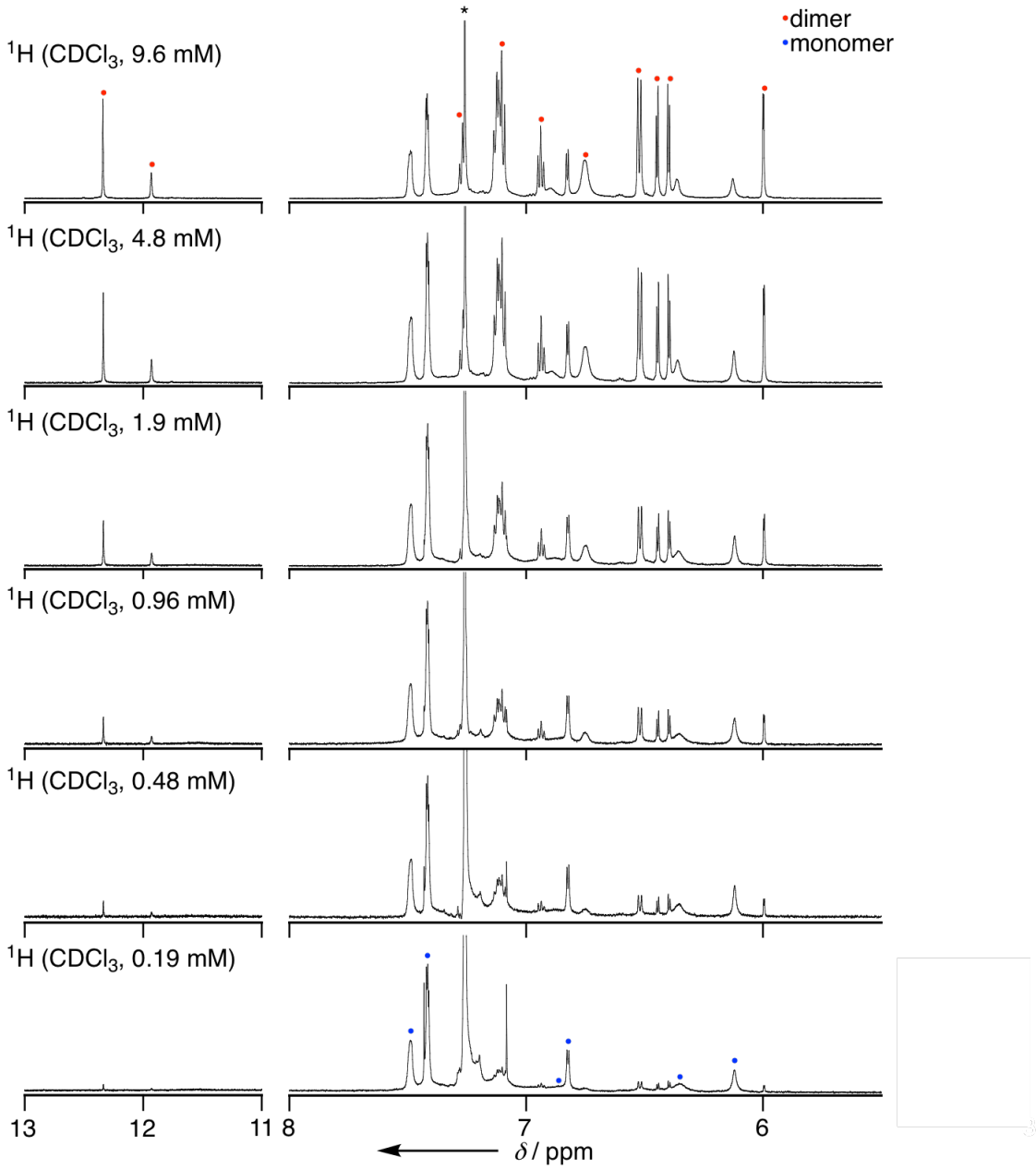

Figure S3-5. Concentration dependent ^{1}H NMR spectra of **4** in $CDCl_3$ at room temperature. * means residual solvent peaks.

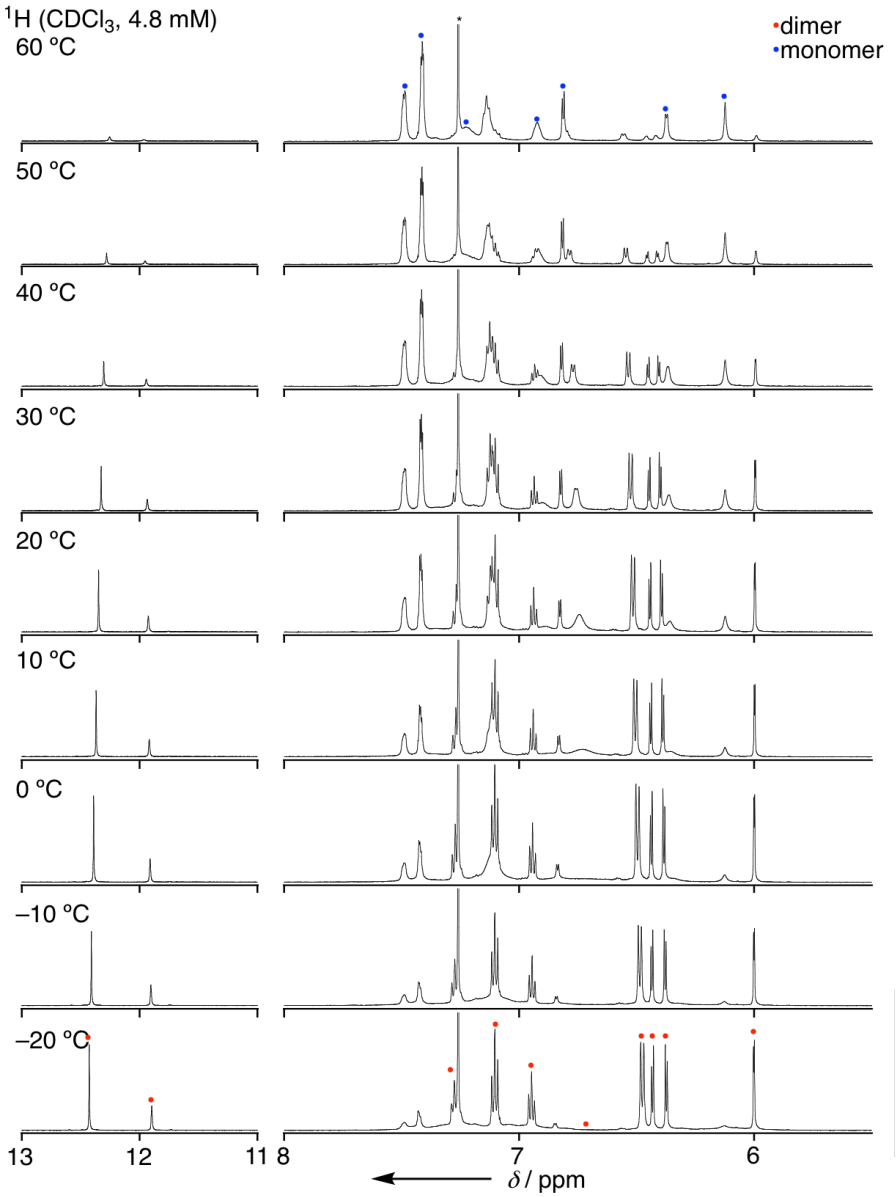

$$2(\mathbf{4}) \underset{\text{CDCl}_3\,(4.8\text{ mM})}{\overset{K_{dim}}{\rightleftharpoons}} (\mathbf{4})_2$$

$$K_{dim} = [(\mathbf{4})_2]/[\mathbf{4}]^2$$

$$\ln(K_{dim}) = -\Delta H/RT + \Delta S/R$$

T (K)	[**4**] (mM)	[(**4**)$_2$] (mM)	K_{dim} (M^{-1})	ln(K_{dim})
333	4.01	0.39	24.39	3.194
323	3.60	0.59	45.66	3.821
313	3.08	0.86	90.27	4.503
303	2.52	1.34	178.9	5.187
293	1.95	1.42	375.1	5.927
283	1.56	1.61	659.4	6.491
273	0.91	1.94	2336	7.756
263	0.73	2.03	3804	8.244

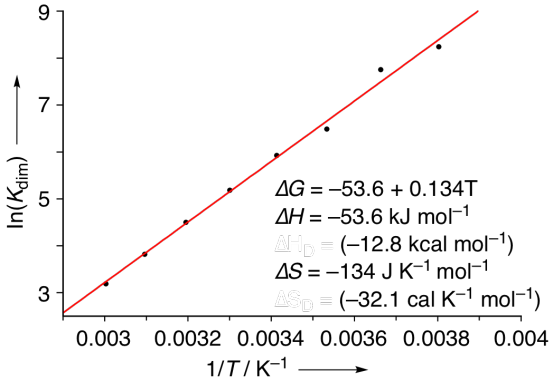

Figure S3-6. Temperature dependent ^{1}H NMR spectra of **4** in $CDCl_3$ and van't Hoff plot for **4**. * means residual solvent peaks.

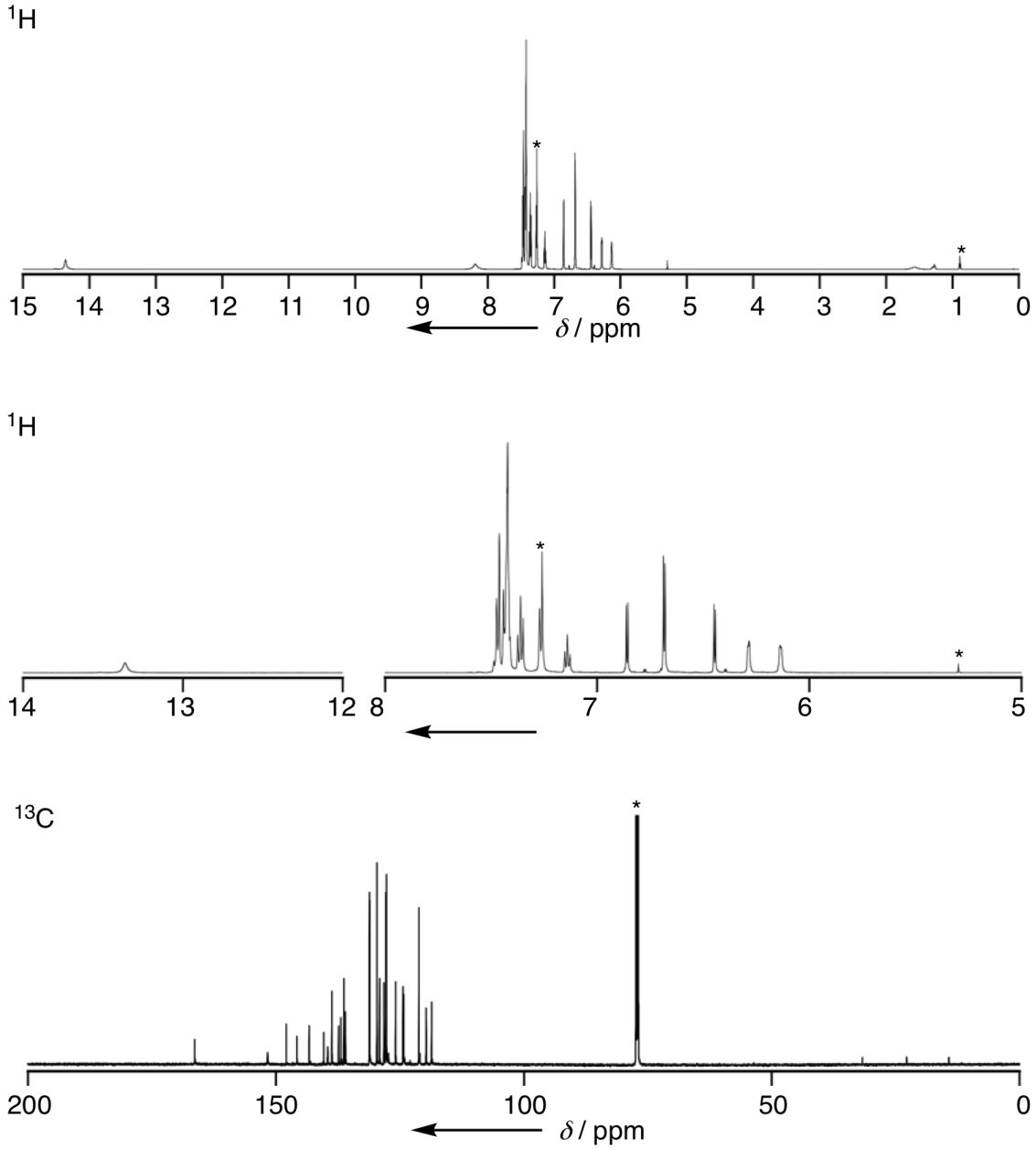

Figure S3-7. ^{1}H and ^{13}C NMR spectra of **S1** in $CDCl_3$ at room temperature. * means residual solvent peaks.

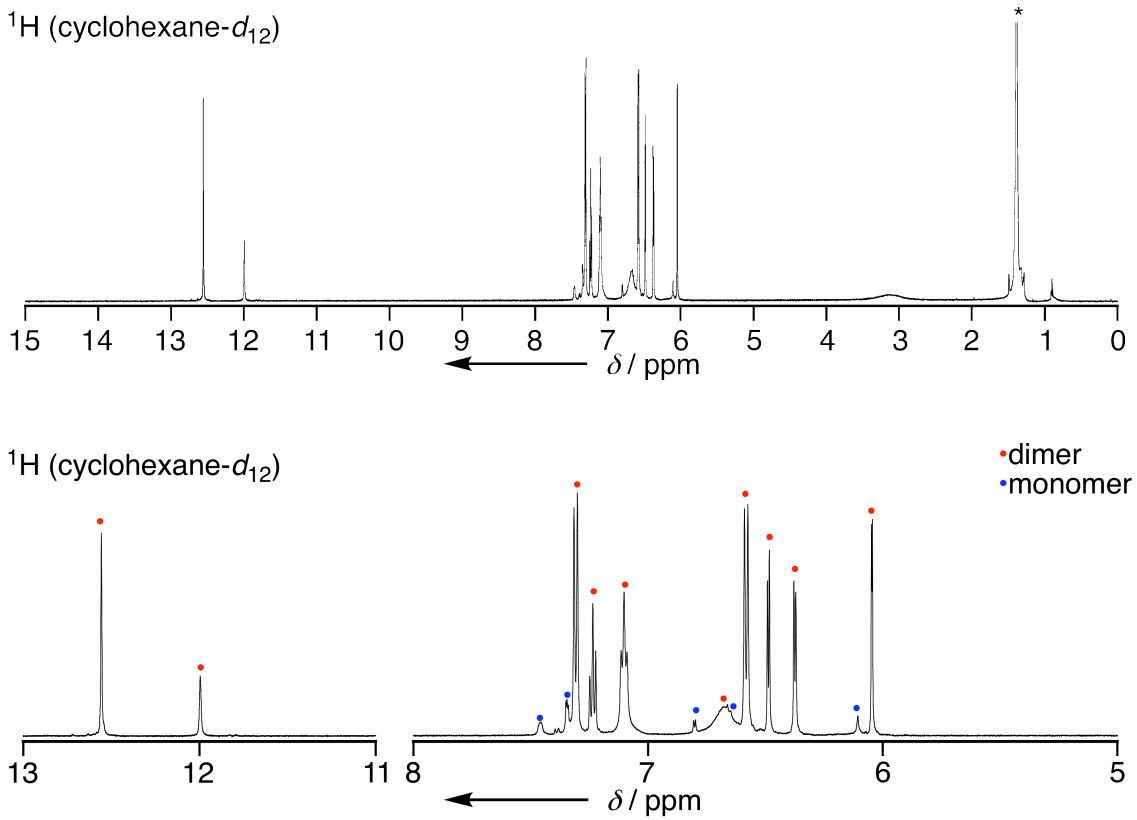

Figure S3-8. ^{1}H NMR spectrum of **5** in cyclohexane-d_{12} at room temperature. * means residual solvent peaks.

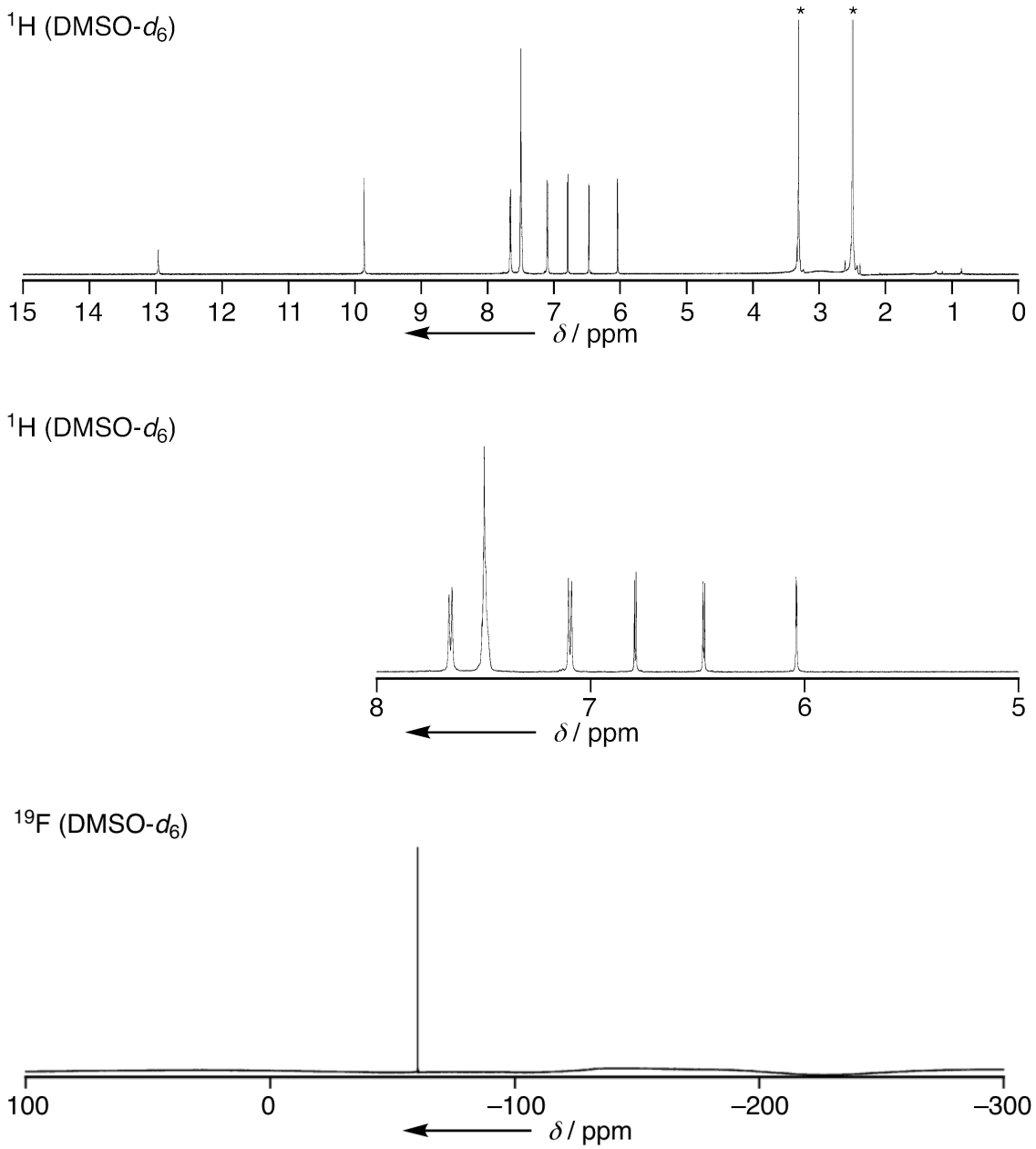

Figure S3-9. ^{1}H and ^{19}F NMR spectra of **5** in DMSO-d_6 at room temperature. * means residual solvent peaks.

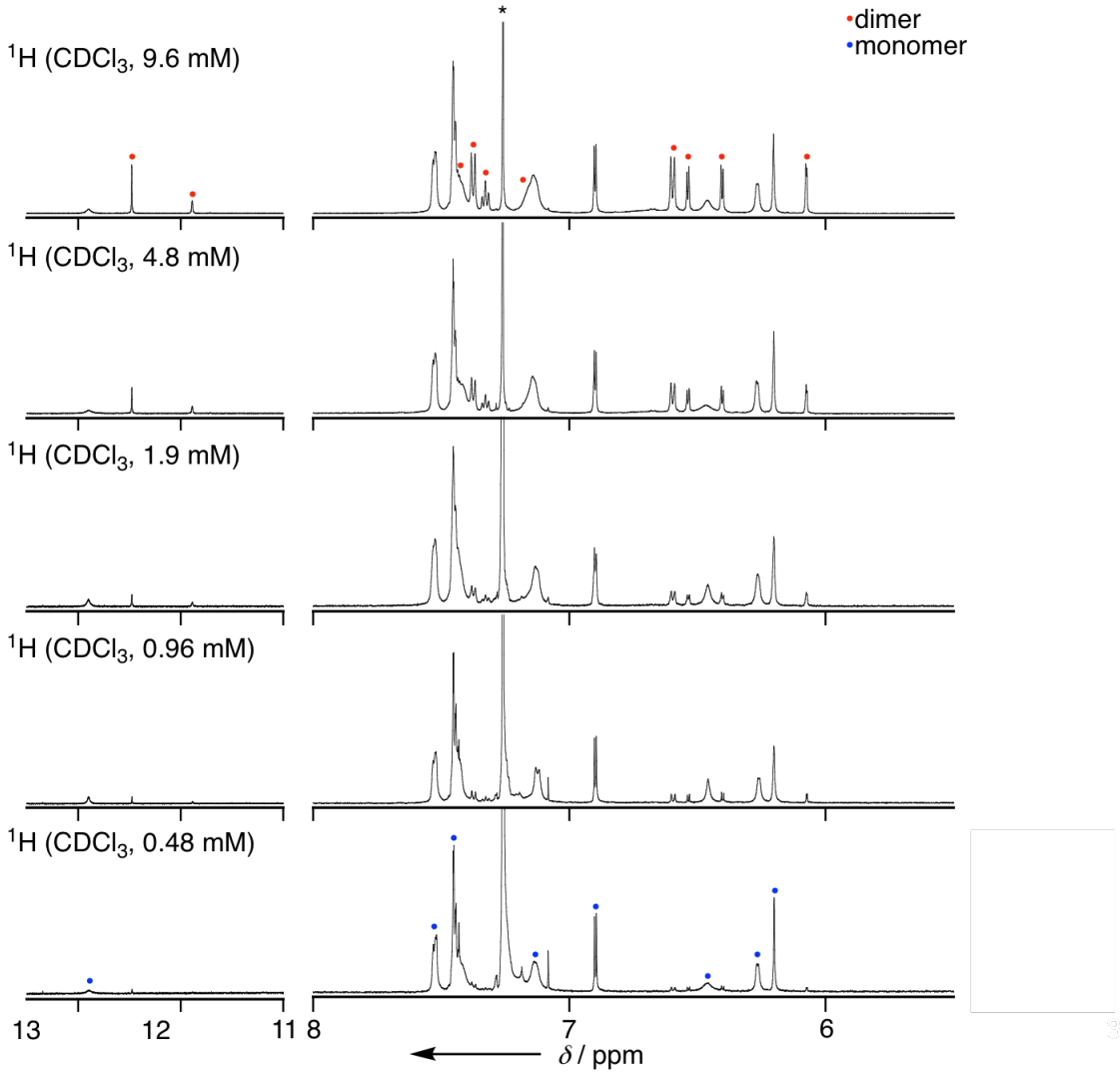

Figure S3-10. Concentration dependent ^{1}H NMR spectra of **5** in $CDCl_3$ at room temperature. * means residual solvent peaks.

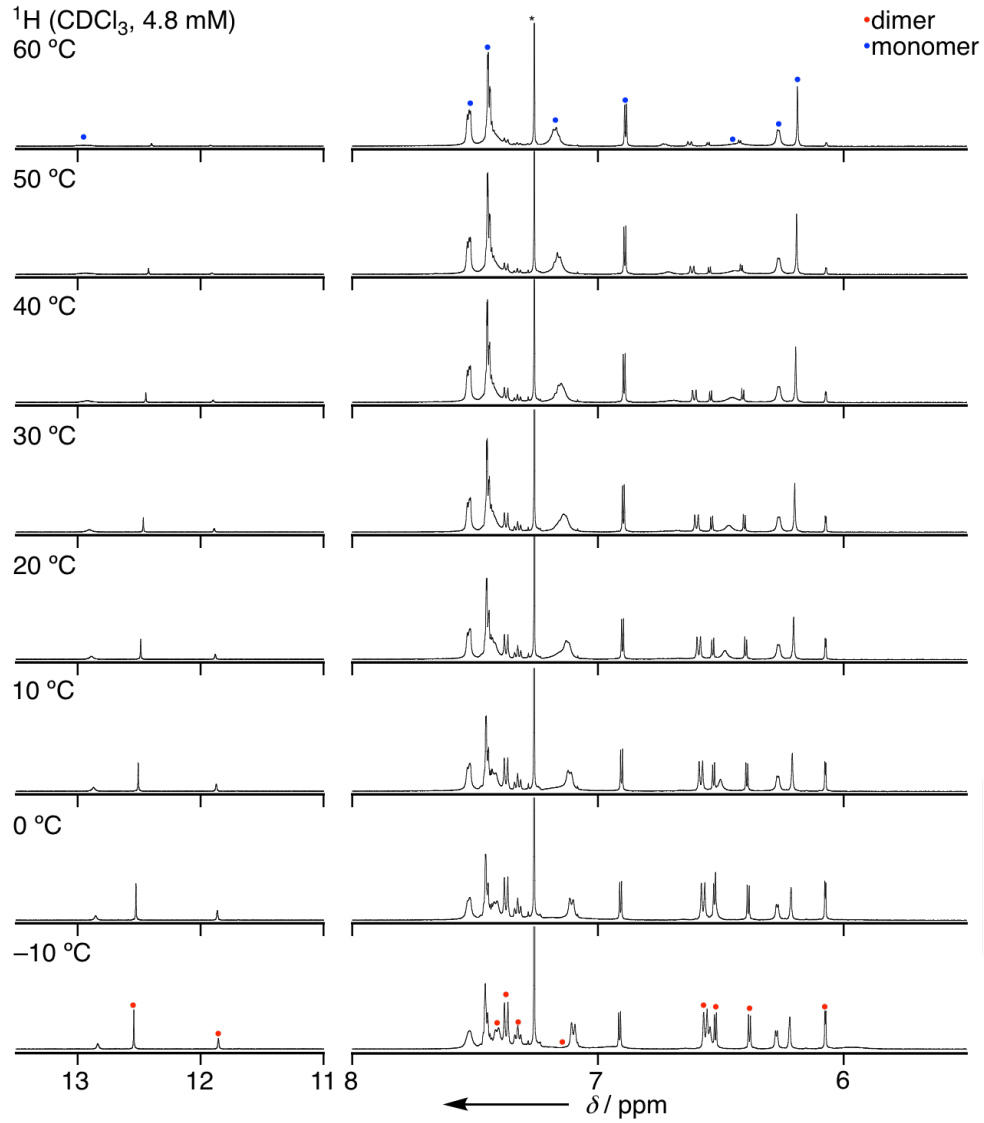

$$2(\mathbf{5}) \underset{CDCl_3\ (4.8\ mM)}{\overset{K_{dim}}{\rightleftharpoons}} (\mathbf{5})_2$$

$$K_{dim} = [(\mathbf{5})_2]/[\mathbf{5}]^2$$

$$\ln(K_{dim}) = -\Delta H/RT + \Delta S/R$$

T (K)	[**5**] (mM)	[(**5**)$_2$] (mM)	K_{dim} (M^{-1})	ln(K_{dim})
313	4.11	0.34	20.36	3.014
303	3.69	0.55	40.54	3.702
293	3.19	0.81	79.22	4.372
283	2.50	1.15	183.3	5.211
273	1.98	1.41	361.6	5.890
263	1.52	1.64	706.1	6.560

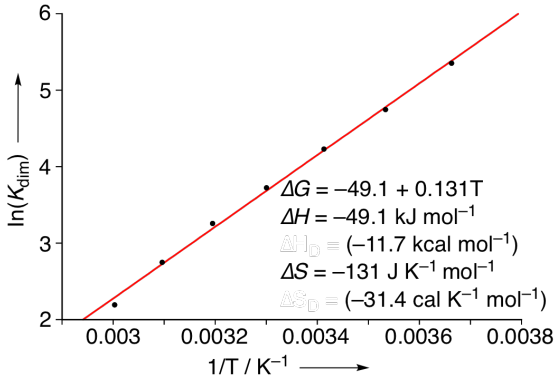

Figure S3-11. Temperature dependent ^{1}H NMR spectra of **5** in $CDCl_3$ and van't Hoff plot for **5**. * means residual solvent peaks.

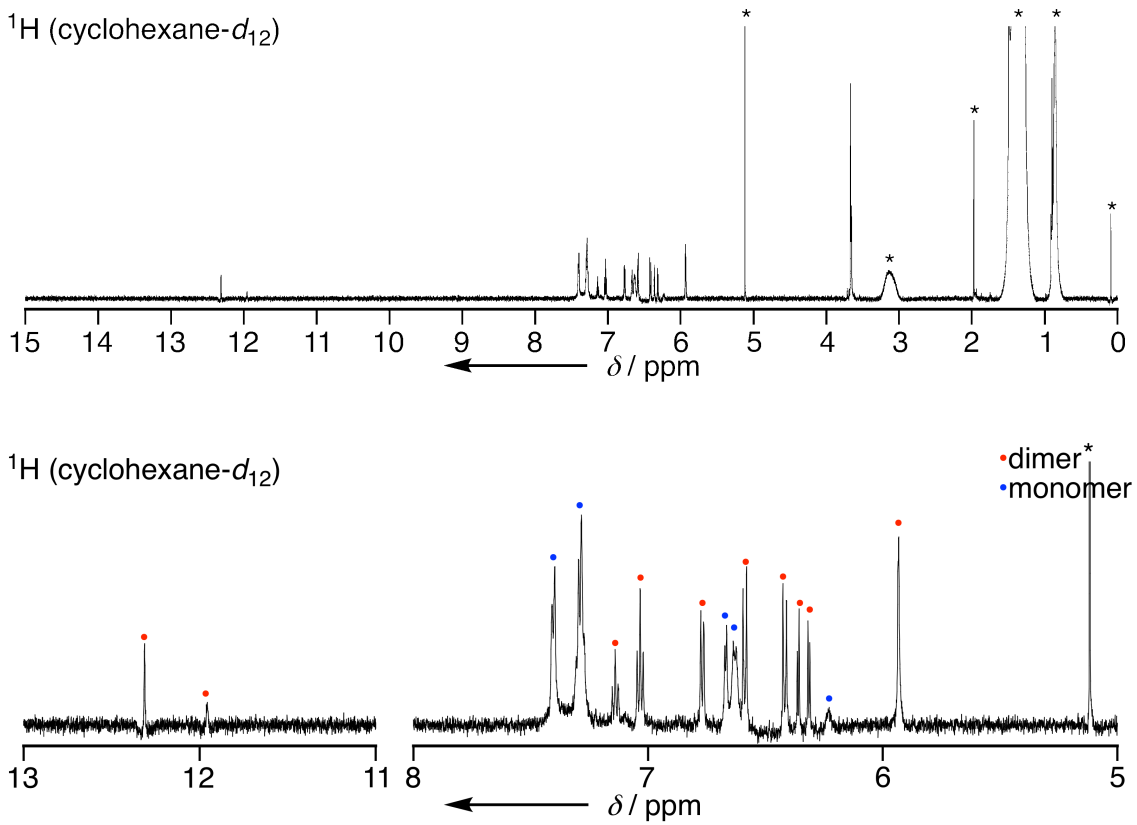

Figure S3-12. ^{1}H NMR spectrum of **6** in cyclohexane-d_{12} at room temperature. * means residual solvent peaks.

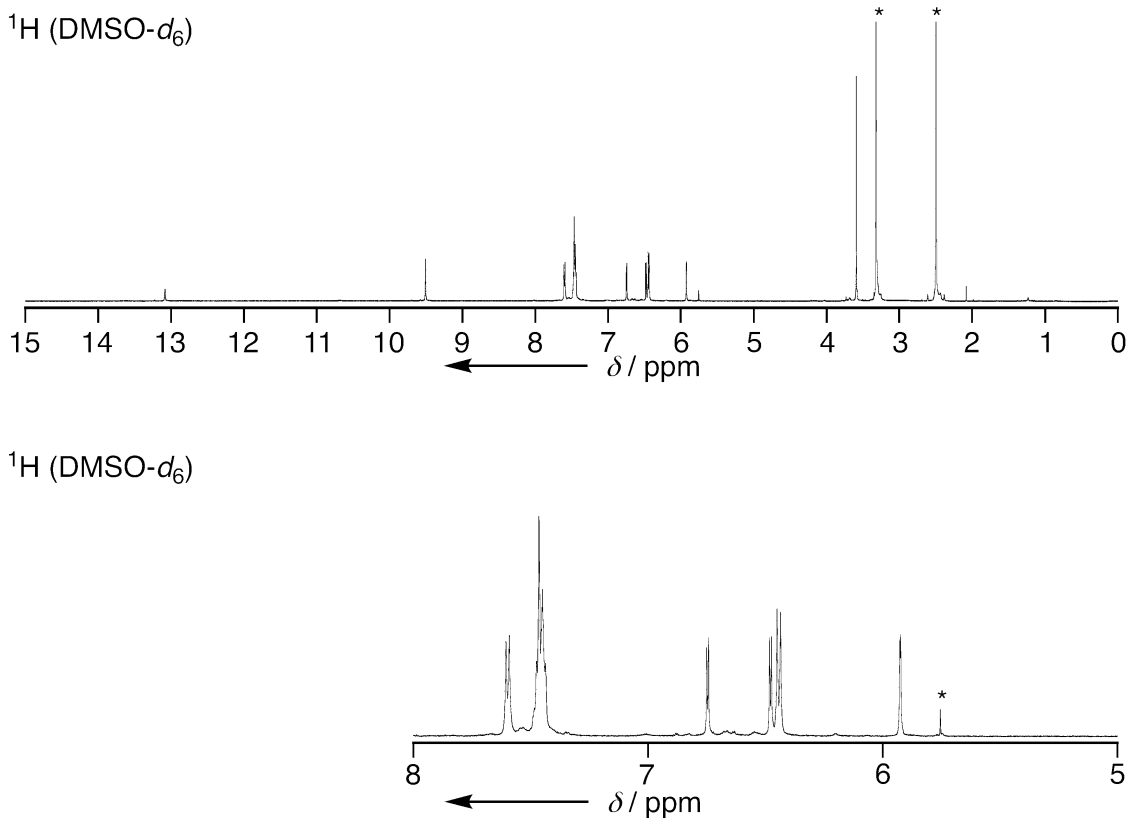

Figure S3-13. ^{1}H NMR spectrum of **6** in DMSO-d_6 at room temperature. * means residual solvent peaks.

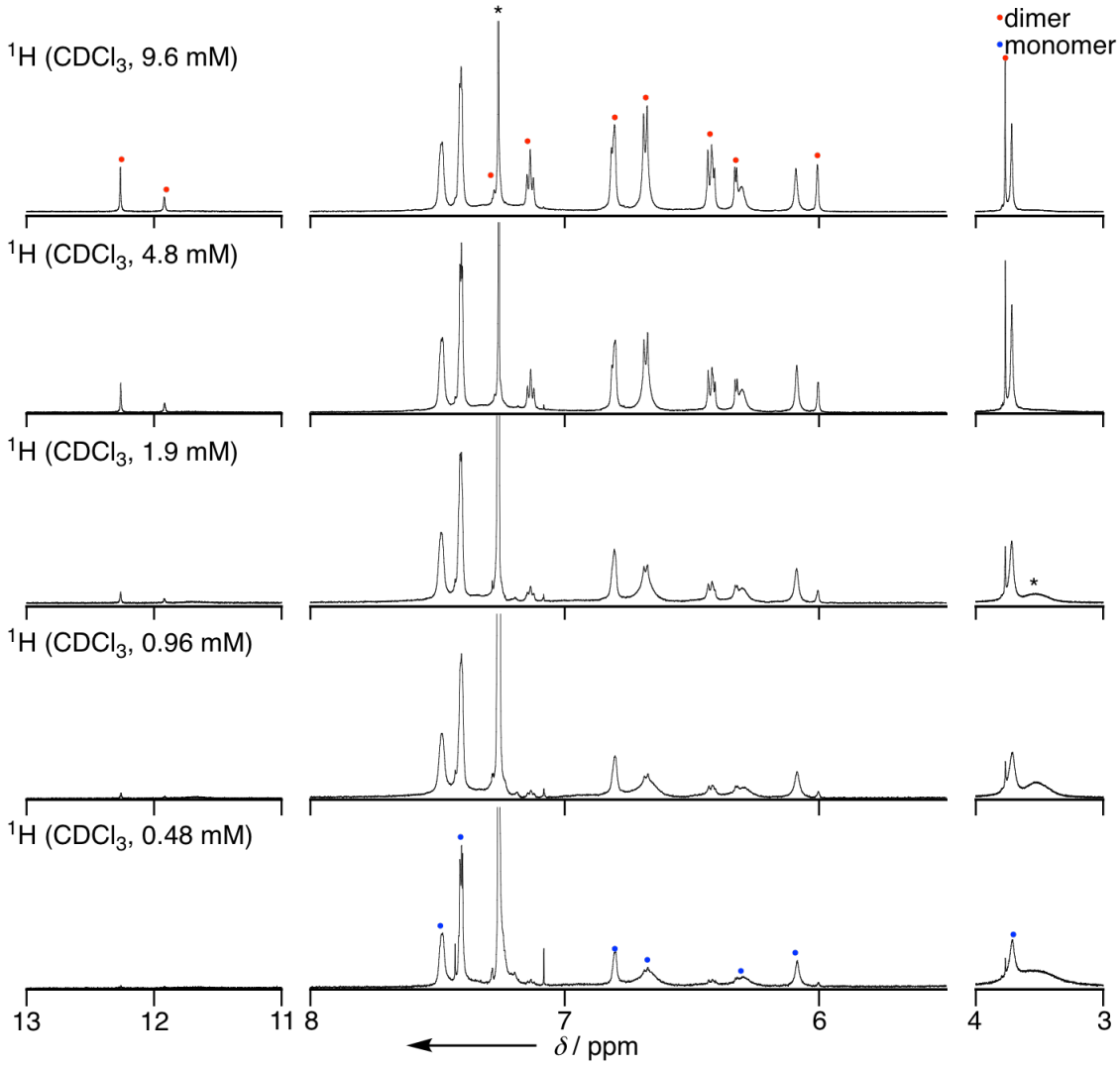

Figure S3-14. Concentration dependent ^{1}H NMR spectra of **6** in $CDCl_3$ at room temperature. * means residual solvent peaks.

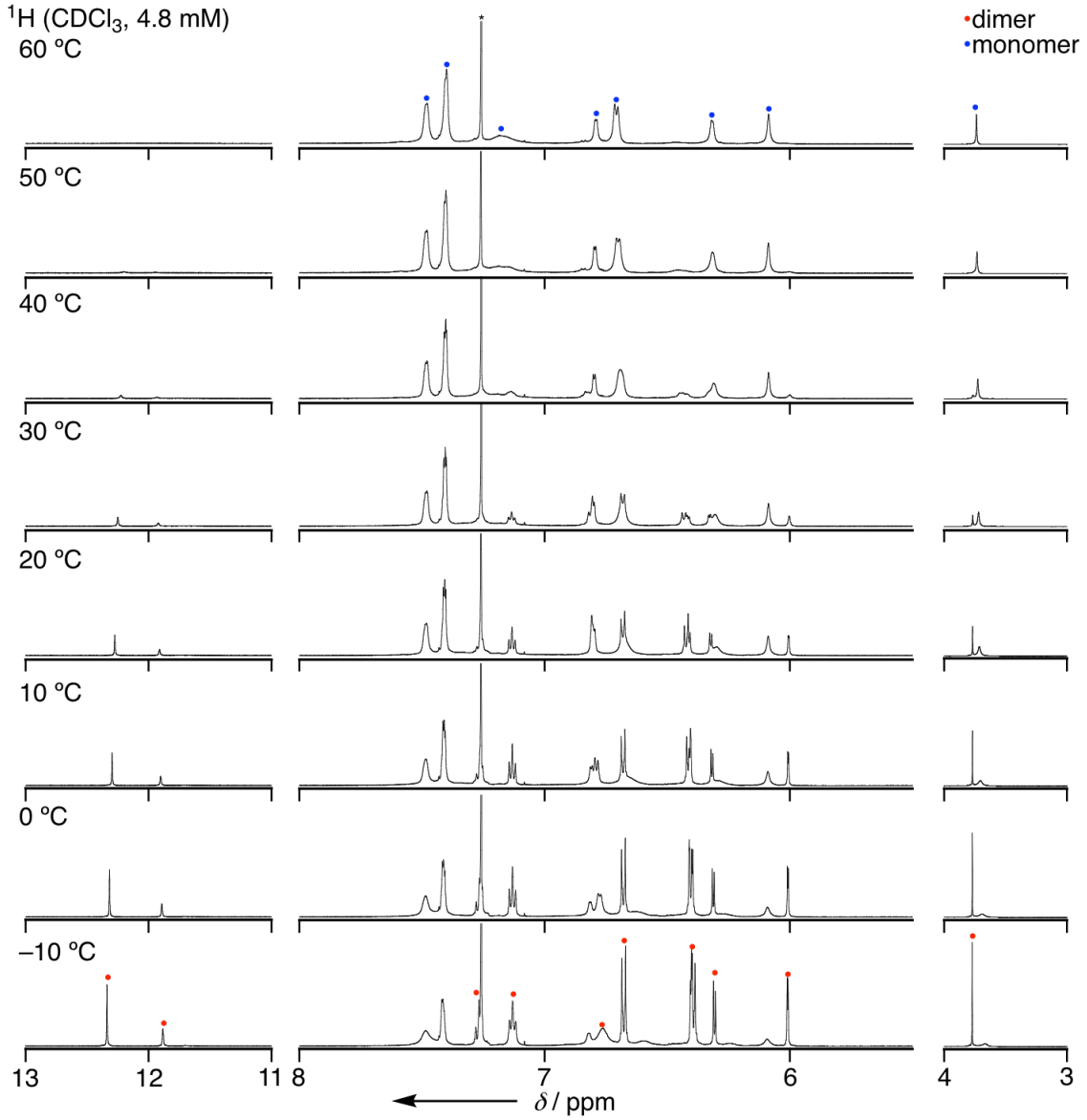

$$2(\mathbf{6}) \underset{CDCl_3\ (4.8\ mM)}{\overset{K_{dim}}{\rightleftharpoons}} (\mathbf{6})_2$$

$$K_{dim} = [(\mathbf{6})_2]/[\mathbf{6}]^2$$

$$\ln(K_{dim}) = -\Delta H/RT + \Delta S/R$$

T (K)	[**6**] (mM)	[(**6**)$_2$] (mM)	K_{dim} (M^{-1})	ln(K_{dim})
313	4.13	0.34	19.75	2.983
303	3.69	0.56	40.99	3.713
293	3.17	0.82	81.53	4.401
283	2.65	1.08	153.31	5.032
273	2.08	1.37	316.9	5.759
263	1.59	1.61	634.6	6.453

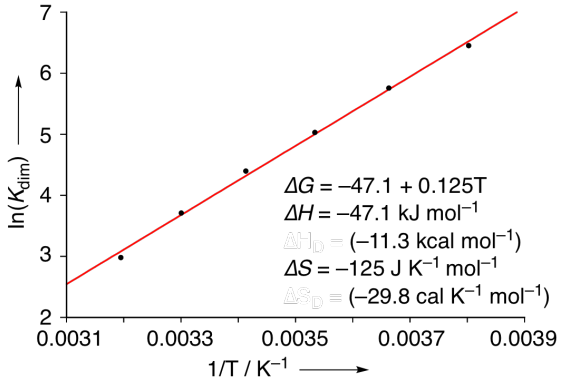

Figure S3-15. Temperature dependent ^{1}H NMR spectra of **6** in $CDCl_3$ and van't Hoff plot for **6**. * means residual solvent peaks.

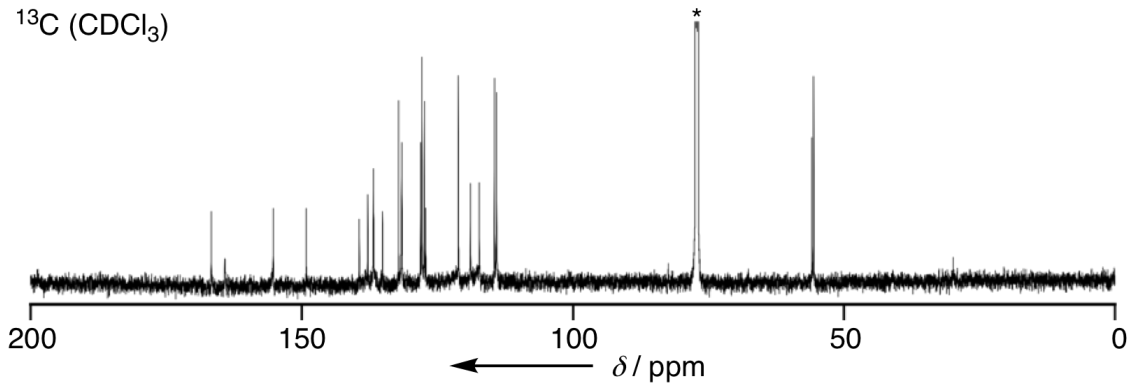

Figure S3-16. ^{13}C NMR spectrum of **6** in $CDCl_3$ at room temperature. * means residual solvent peaks.

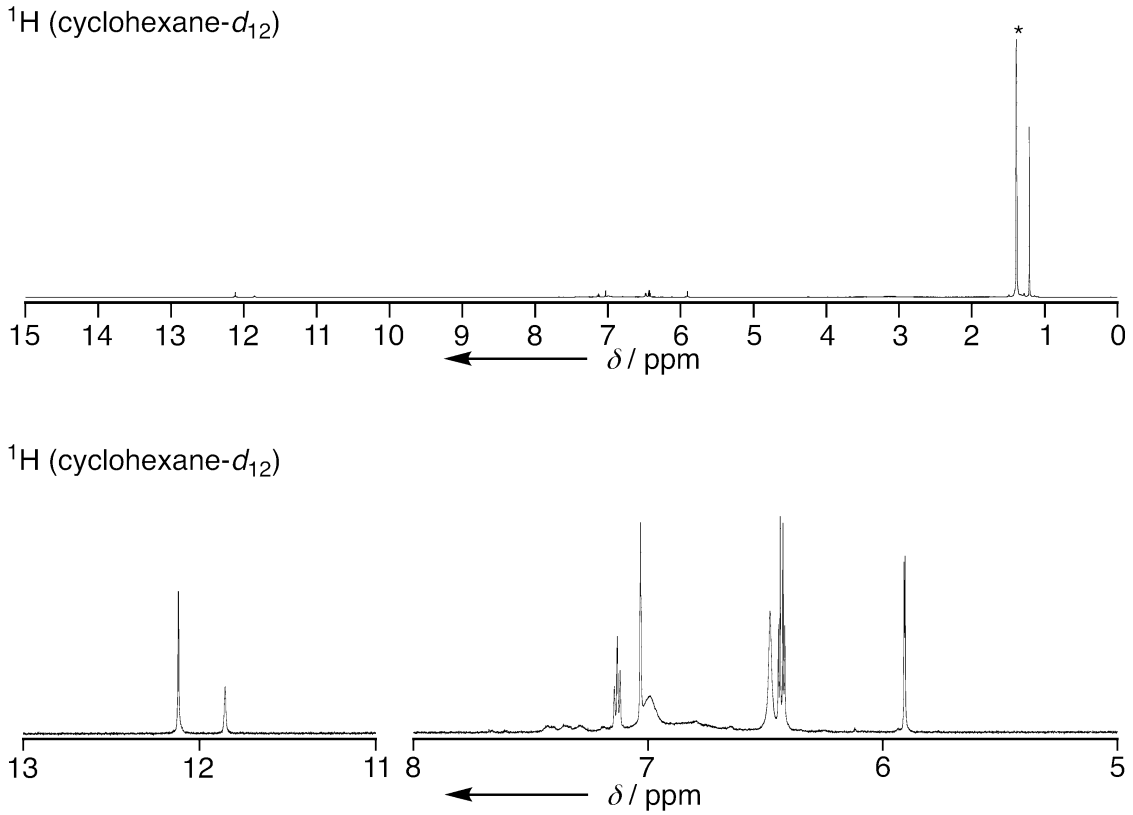

Figure S3-17. ^{1}H NMR spectrum of **7** in cyclohexane-d_{12} at room temperature. * means residual solvent peaks.

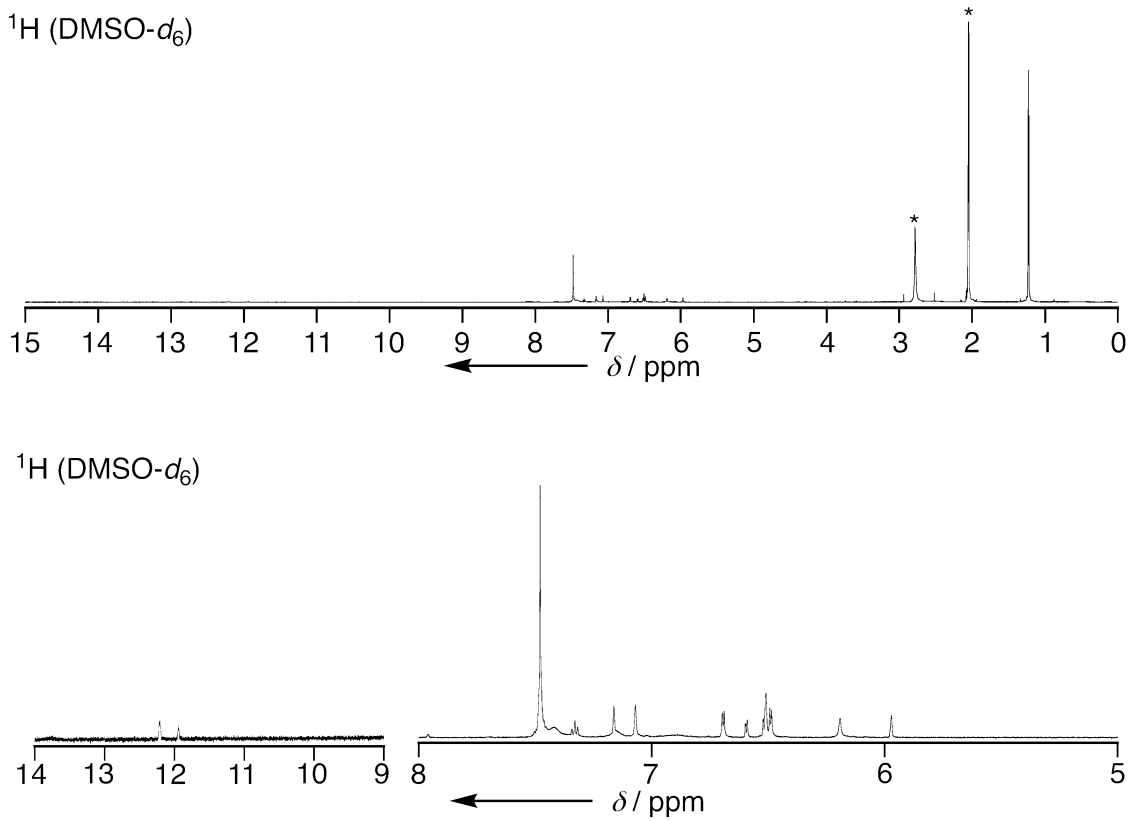

Figure S3-18. ^{1}H NMR spectrum of **7** in DMSO-d_6 at room temperature. * means residual solvent peaks.

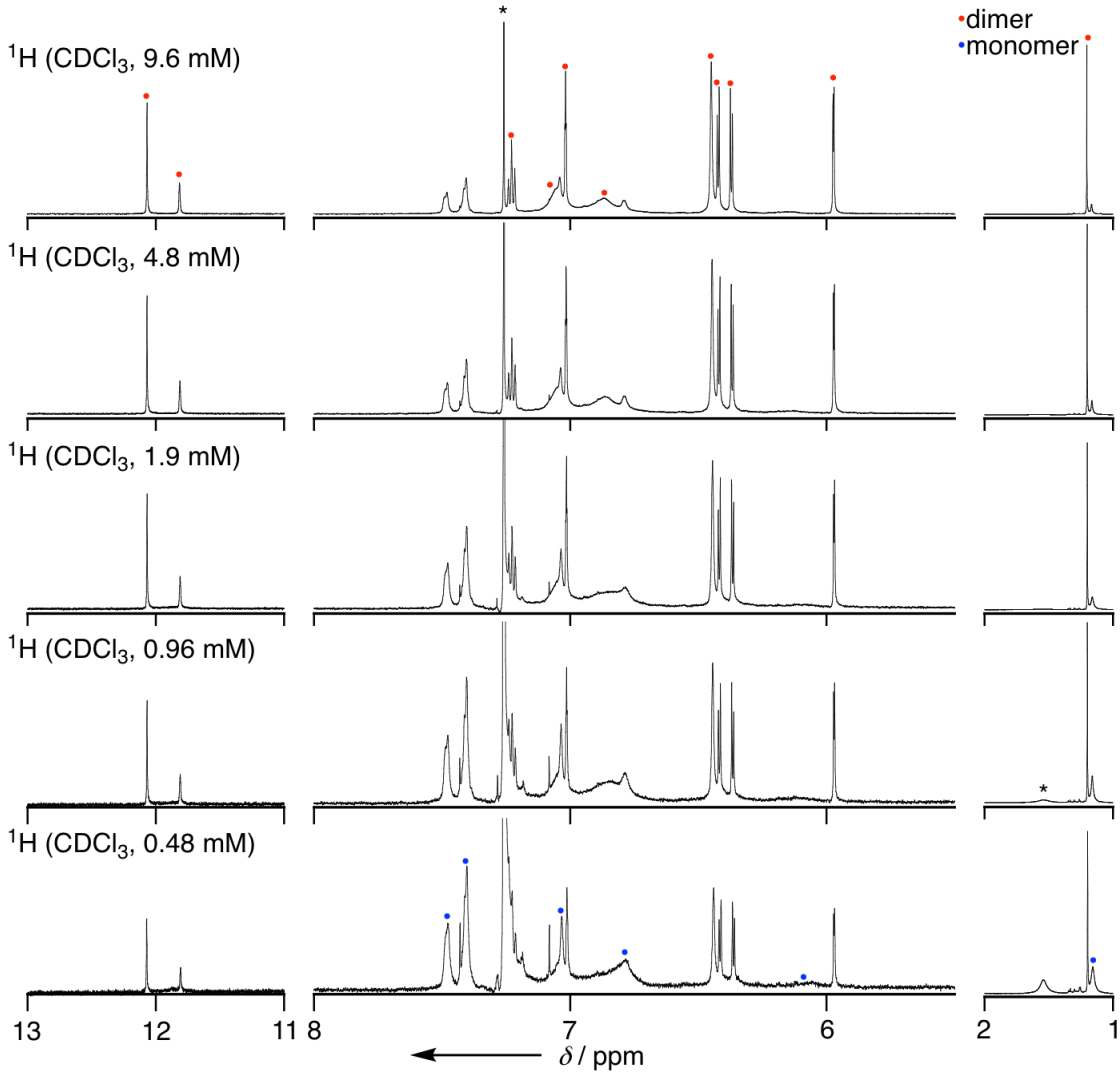

Figure S3-19. Concentration dependent ^{1}H NMR spectra of **7** in $CDCl_3$ at room temperature. * means residual solvent peaks.

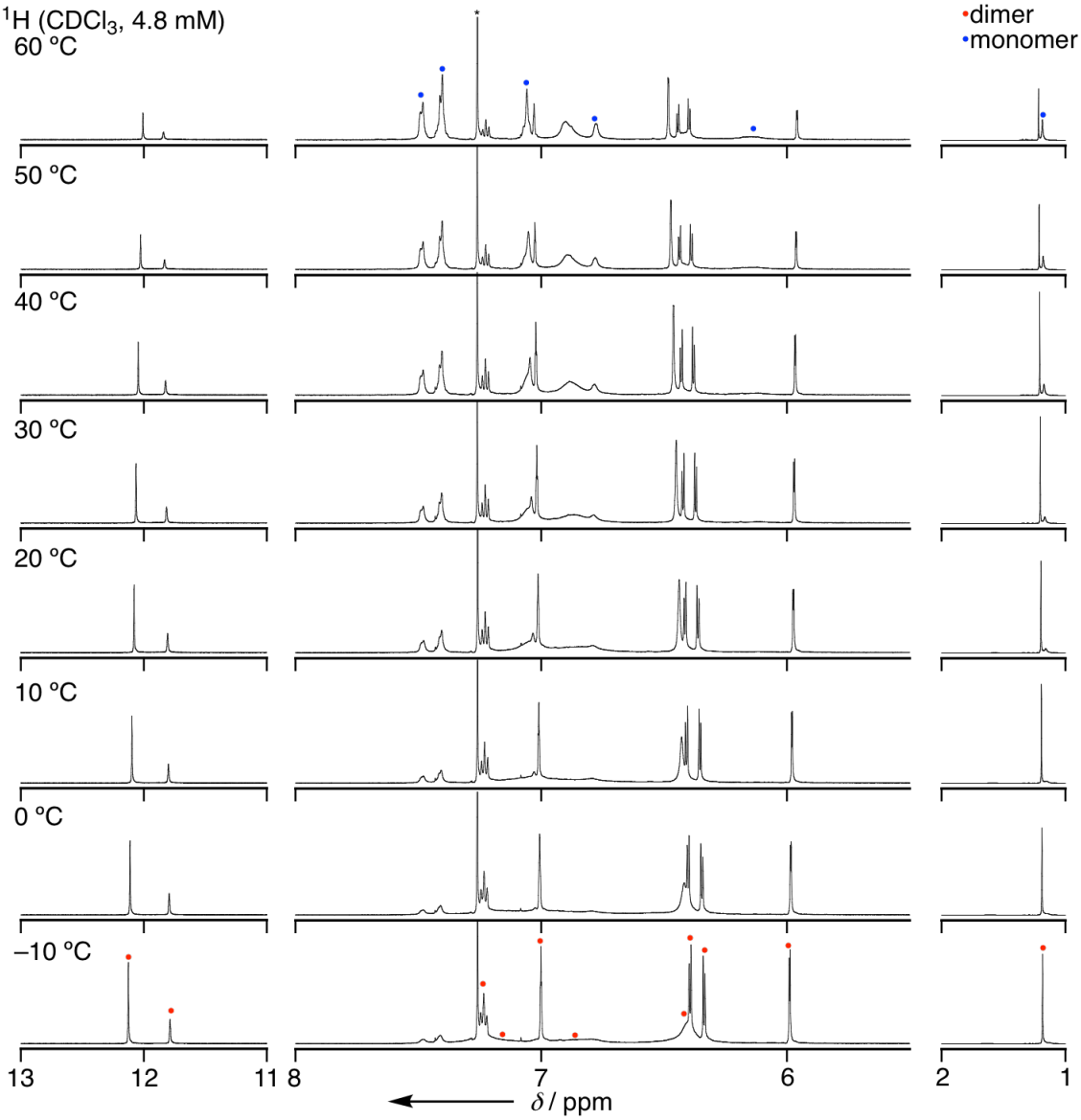

$$2(\mathbf{7}) \underset{CDCl_3\ (4.8\ mM)}{\overset{K_{dim}}{\rightleftharpoons}} (\mathbf{7})_2$$

$$K_{dim} = [(\mathbf{7})_2]/[\mathbf{7}]^2$$

$$\ln(K_{dim}) = -\Delta H/RT + \Delta S/R$$

T (K)	[**7**] (mM)	[(**7**)$_2$] (mM)	K_{dim} (M^{-1})	ln(K_{dim})
333	3.00	0.90	99.44	4.600
323	2.35	1.22	221.8	5.402
313	1.93	1.43	383.4	5.949
303	1.37	1.71	912.6	6.816
293	1.02	1.89	1817	7.505
283	0.731	2.03	3798	8.242
273	0.456	2.17	10450	9.255

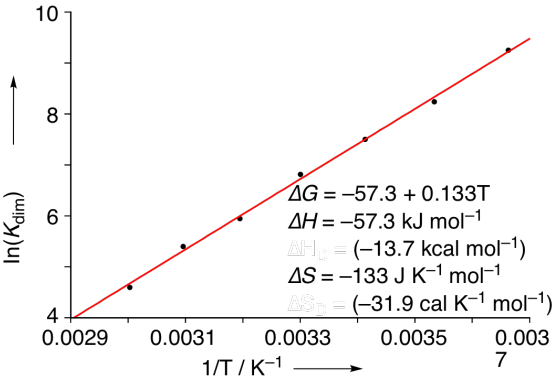

Figure S3-20. Temperature dependent ^{1}H NMR spectra of **7** in $CDCl_3$ and van't Hoff plot for **7**.
* means residual solvent peaks.

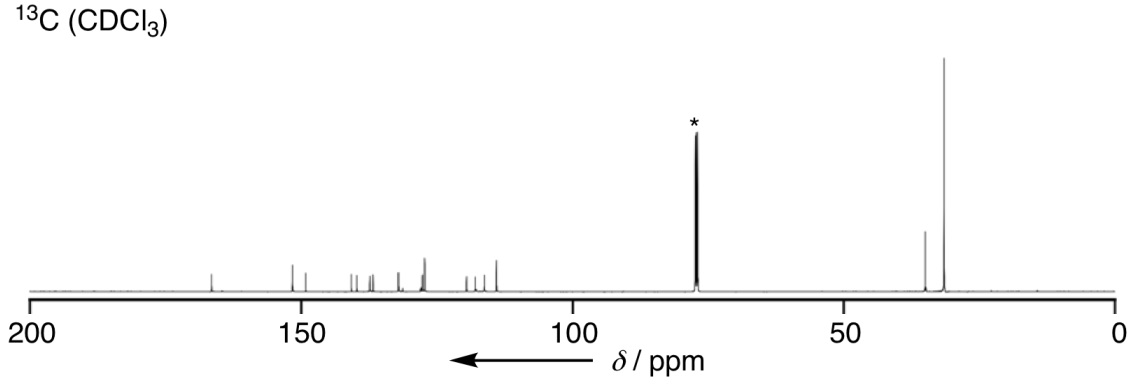

Figure S3-21. ^{13}C NMR spectrum of **7** in $CDCl_3$ at room temperature. * means residual solvent peaks.

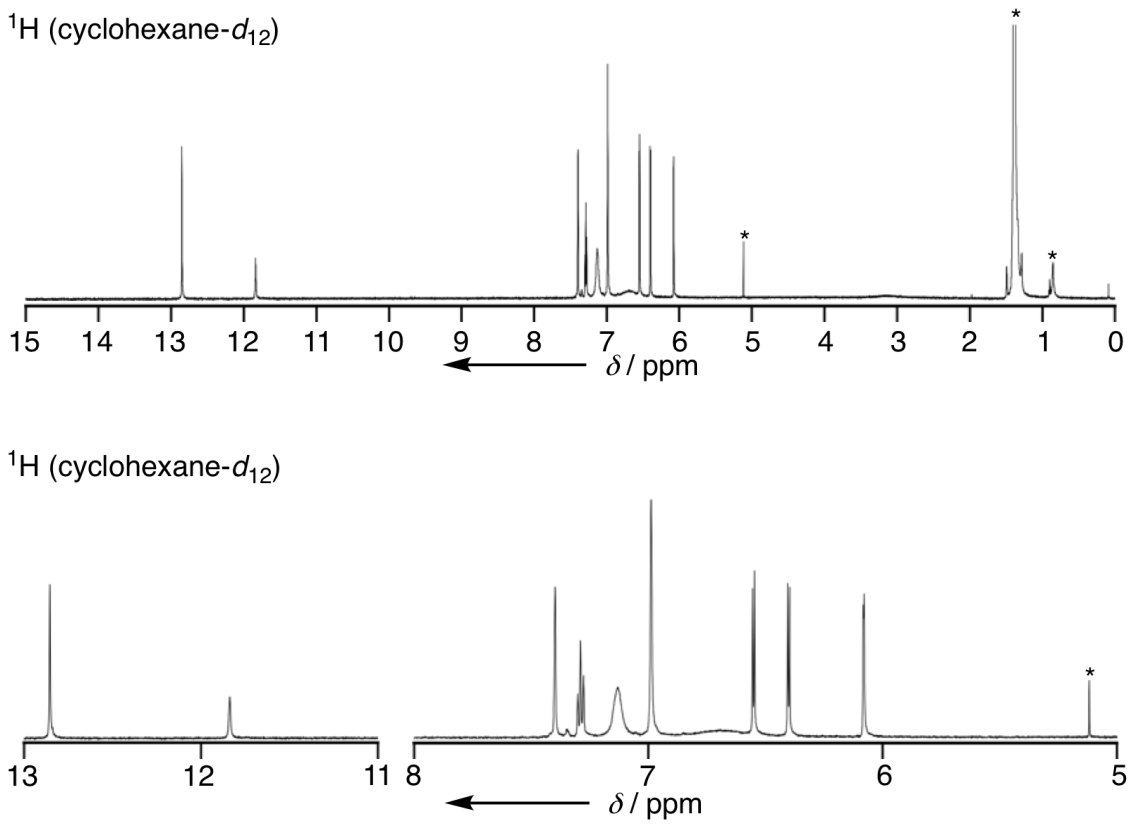

Figure S3-22. ^{1}H NMR spectrum of **8** in cyclohexane-d_{12} at room temperature. * means residual solvent peaks.

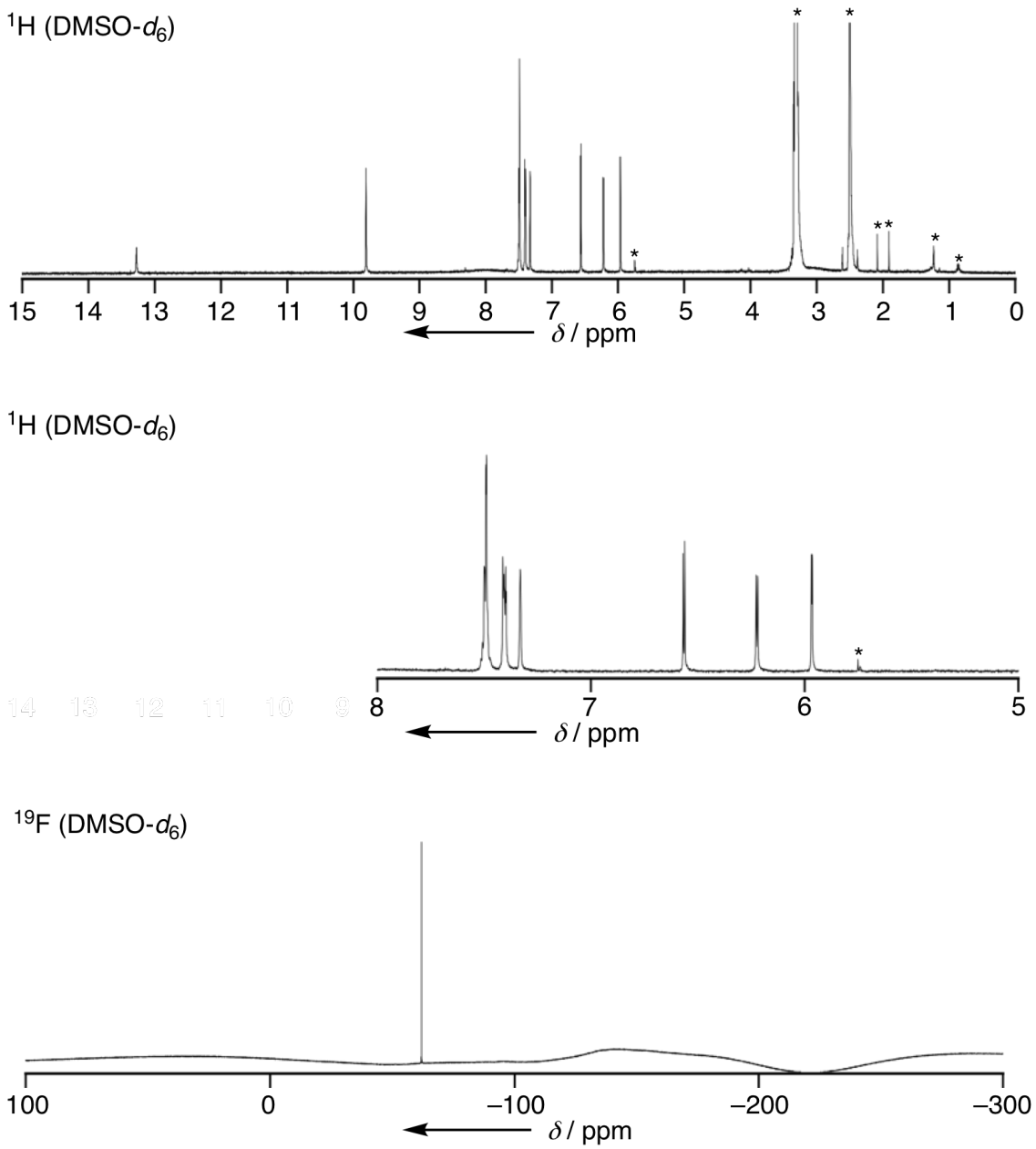

Figure S3-23. ^{1}H and ^{19}F NMR spectra of **8** in DMSO-d_6 at room temperature. * means residual solvent peaks.

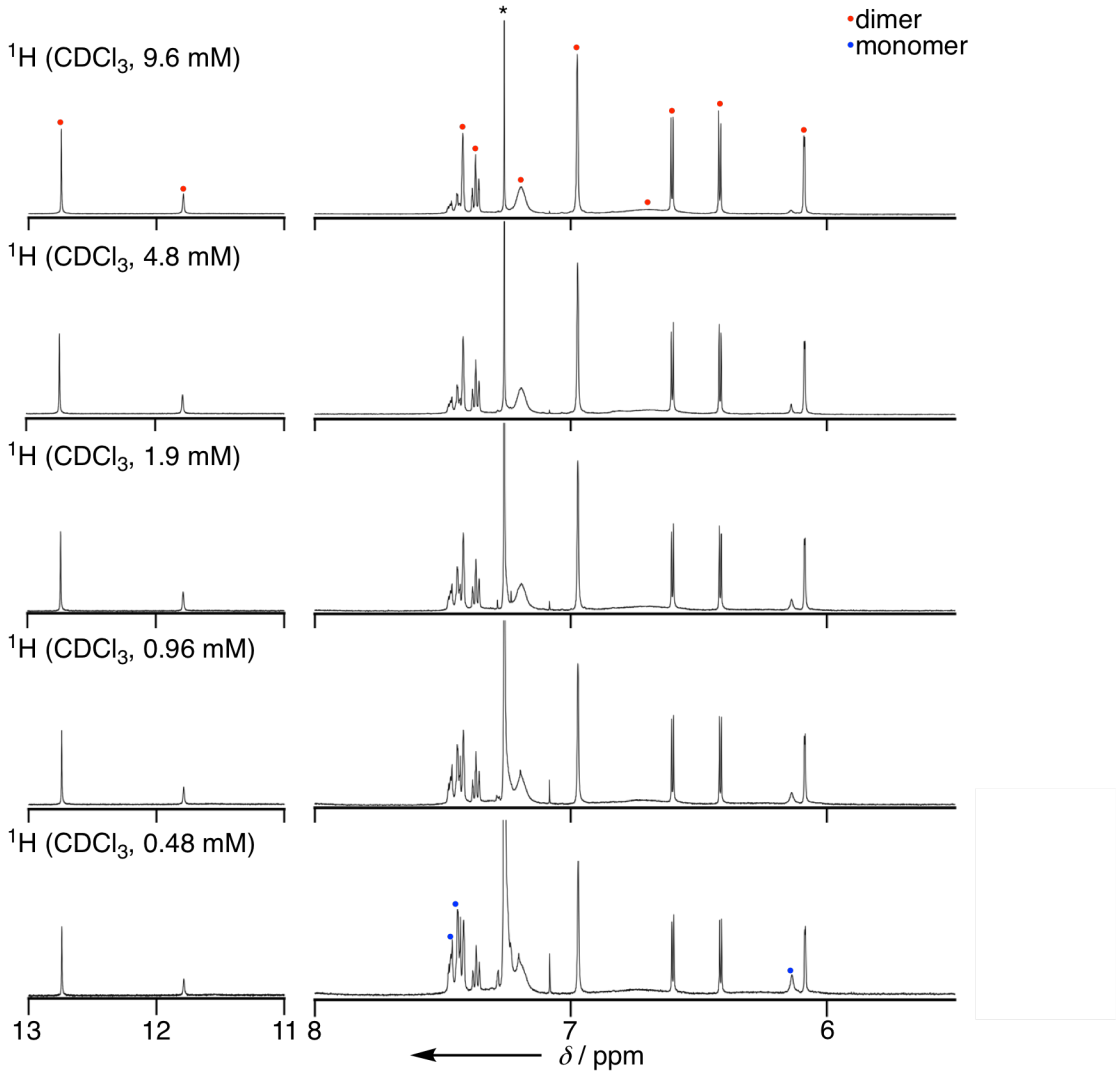

Figure S3-24. Concentration dependent ^{1}H NMR spectra of **8** in $CDCl_3$ at room temperature. * means residual solvent peaks.

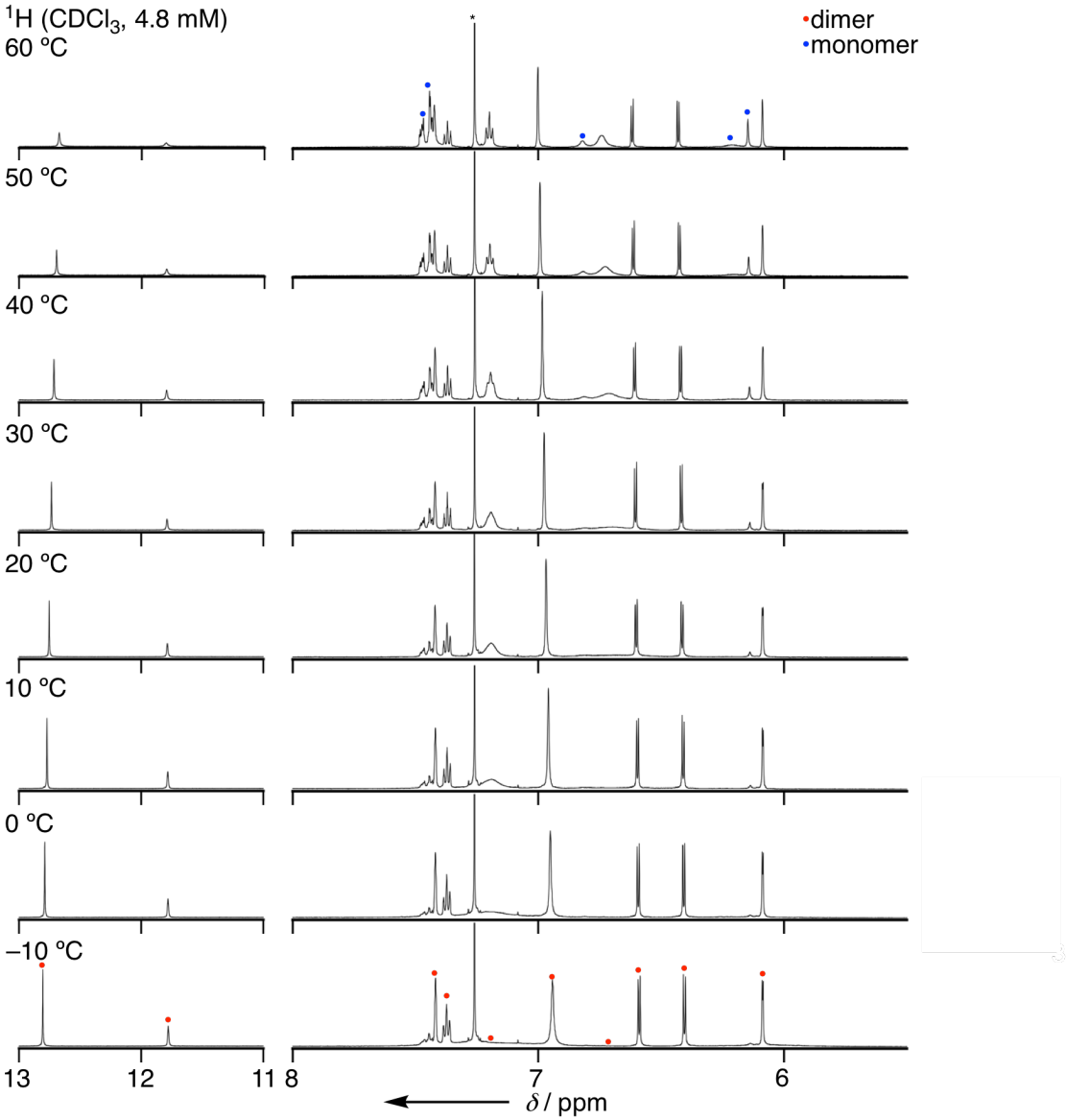

$$2(\mathbf{8}) \underset{CDCl_3\ (4.8\ mM)}{\overset{K_{dim}}{\rightleftharpoons}} (\mathbf{8})_2$$

$$K_{dim} = [(\mathbf{8})_2]/[\mathbf{8}]^2$$

$$\ln(K_{dim}) = -\Delta H/RT + \Delta S/R$$

T (K)	[**8**] (mM)	[(**8**)$_2$] (mM)	K_{dim} (M^{-1})	ln(K_{dim})
333	1.98	1.41	357.6	5.879
323	1.53	1.63	693.7	6.542
313	1.18	1.81	1308	7.176
303	0.865	1.97	2628	7.874
293	0.589	2.10	6063	8.710
283	0.416	2.19	12648	9.445

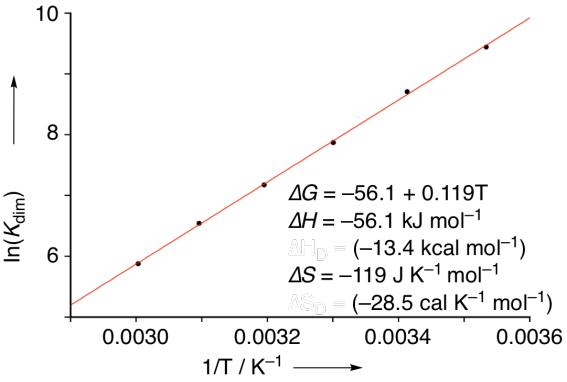

Figure S3-25. Temperature dependent ^{1}H NMR spectra of **8** in CDCl$_3$ and van't Hoff plot for **8**. * means residual solvent peaks.

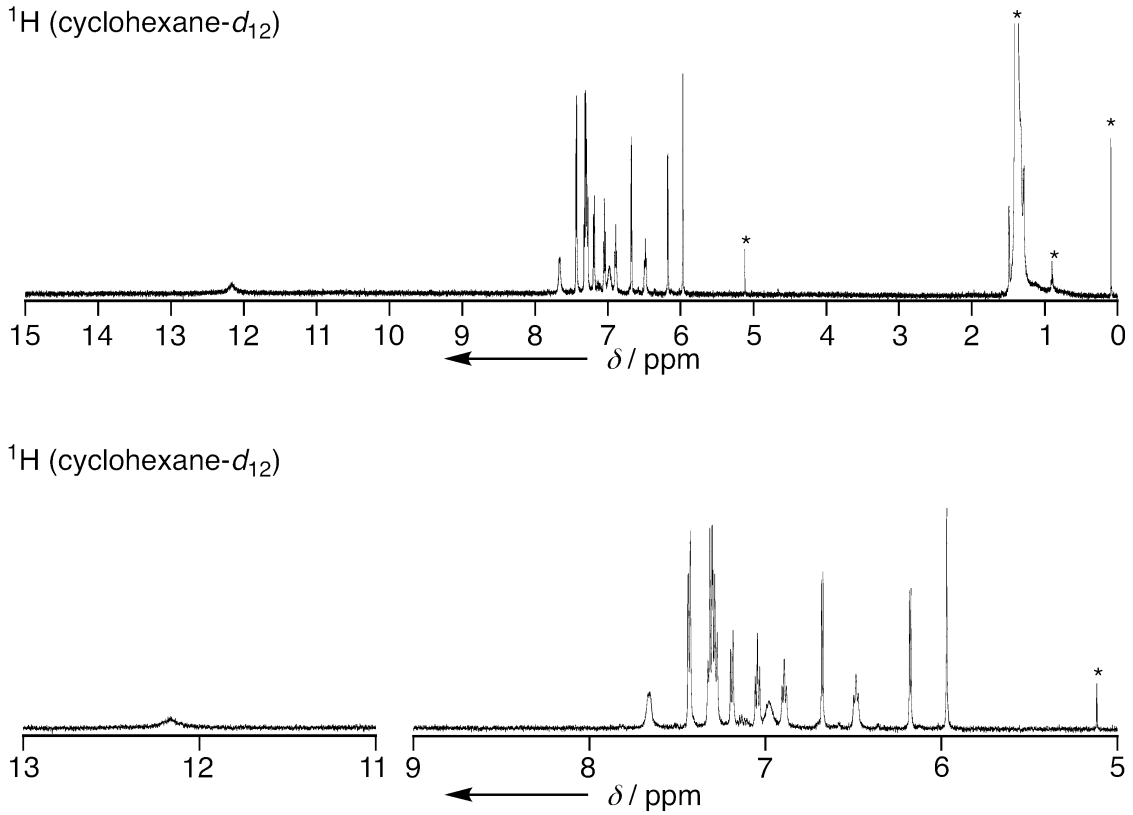

Figure S3-26. ^{1}H NMR spectrum of **9** in cyclohexane-d_{12} at room temperature. * means residual solvent peaks.

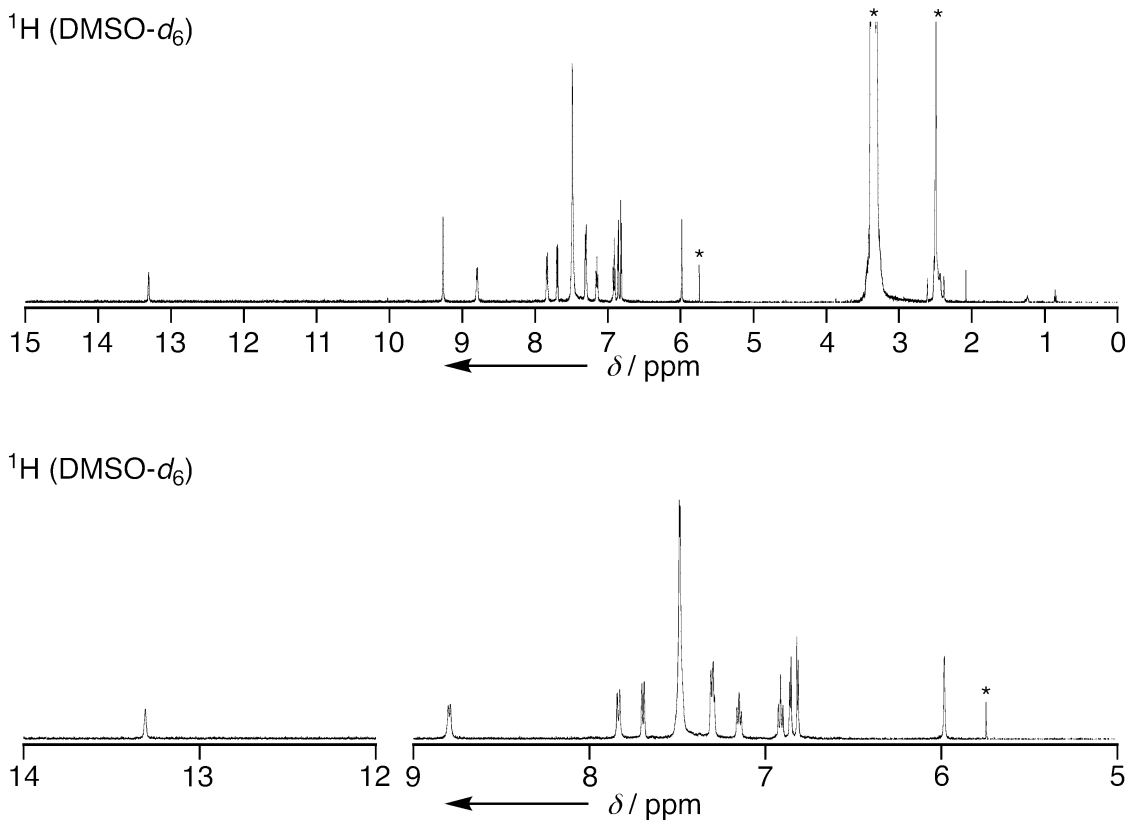

Figure S3-27. ^{1}H NMR spectrum of **9** in DMSO-d_6 at room temperature. * means residual solvent peaks.

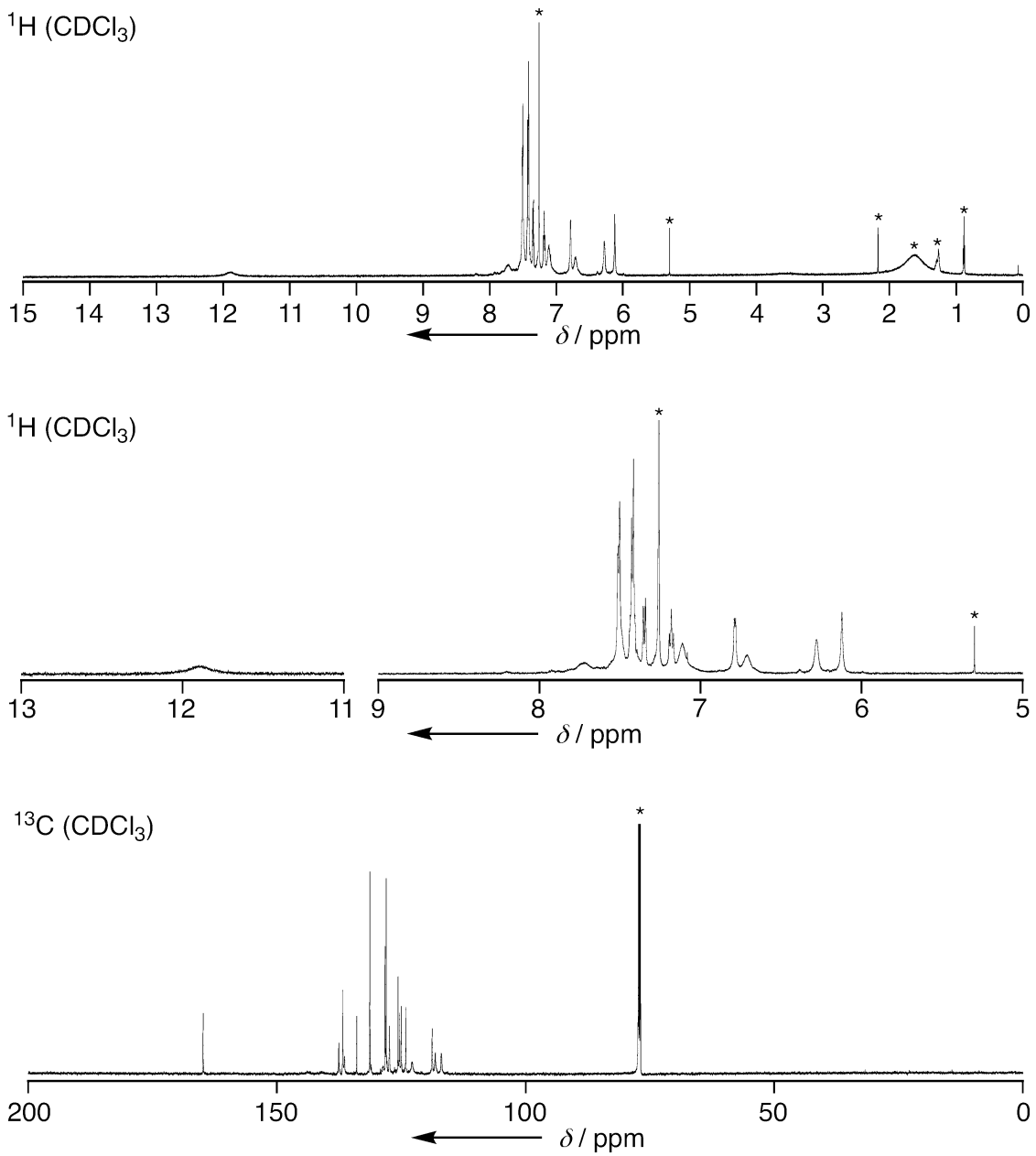

Figure S3-28. ^{1}H and ^{13}C NMR spectra of **9** in $CDCl_3$ at room temperature. * means residual solvent peaks.

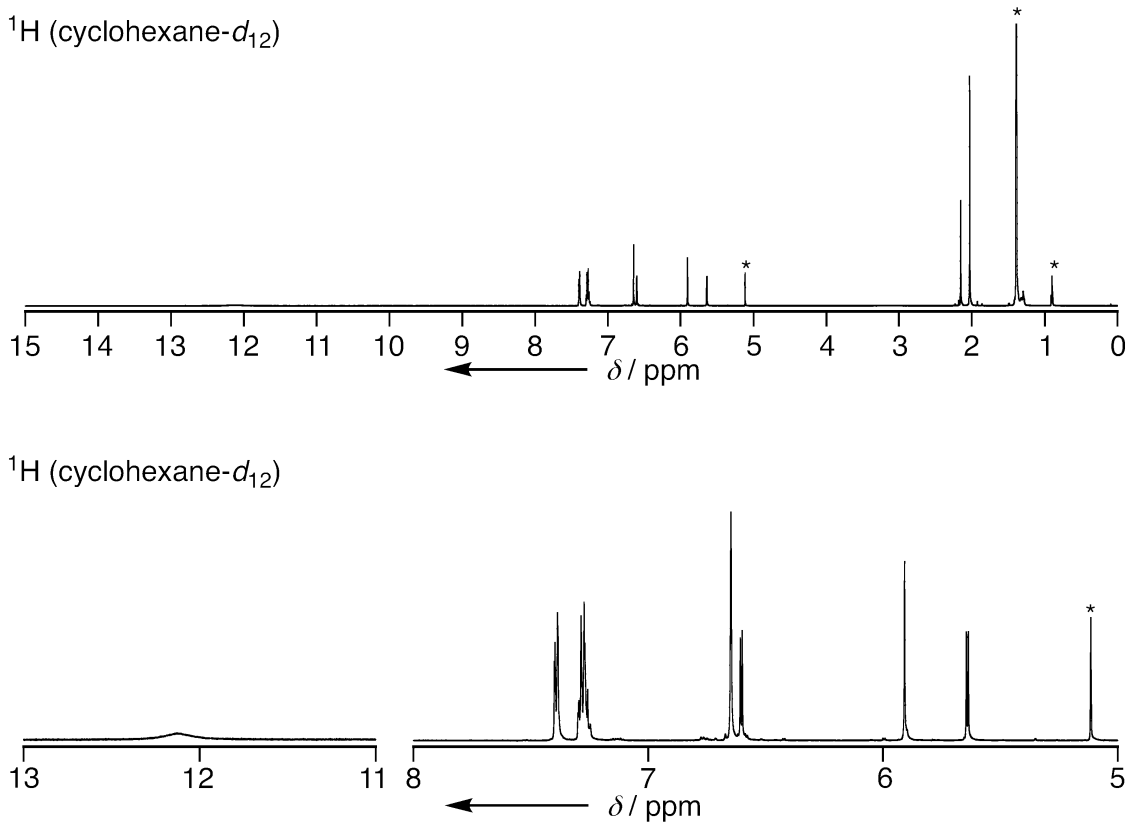

Figure S3-29. ^{1}H NMR spectrum of **10** in cyclohexane-d_{12} at room temperature. * means residual solvent peaks.

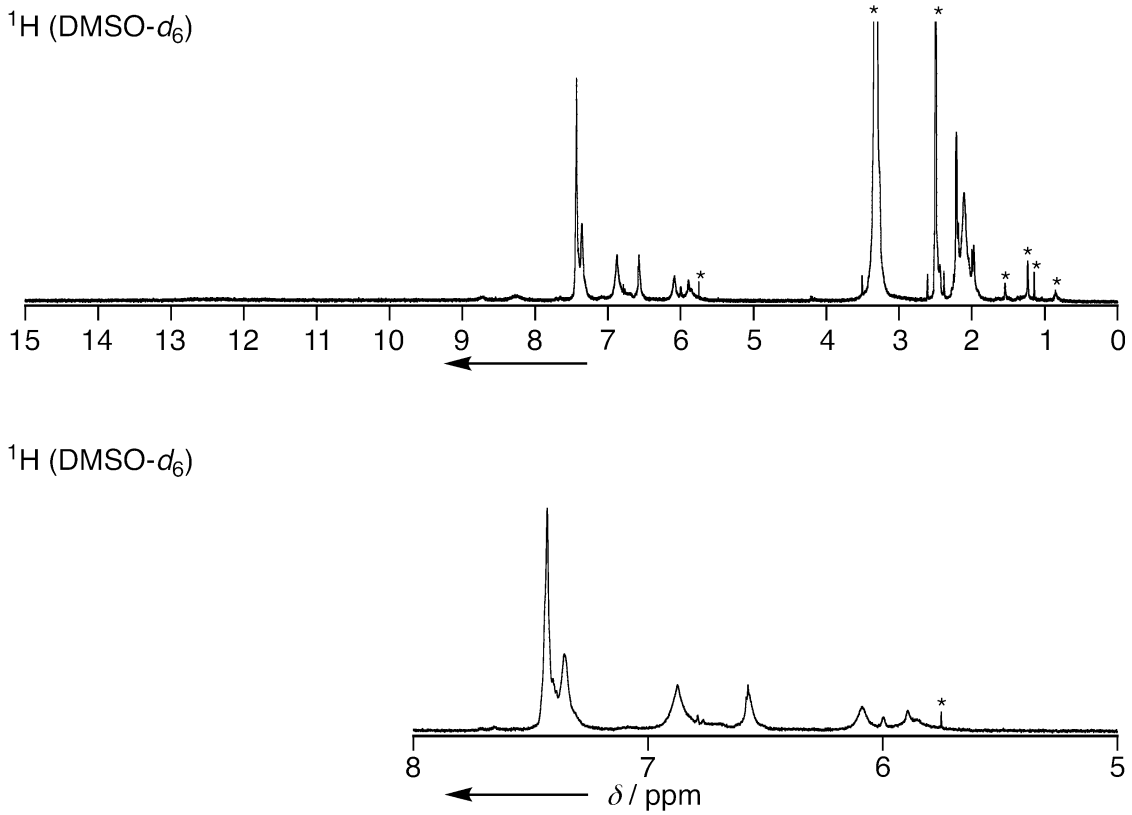

Figure S3-30. ^{1}H NMR spectrum of **10** in DMSO-d_6 at room temperature. * means residual solvent peaks.

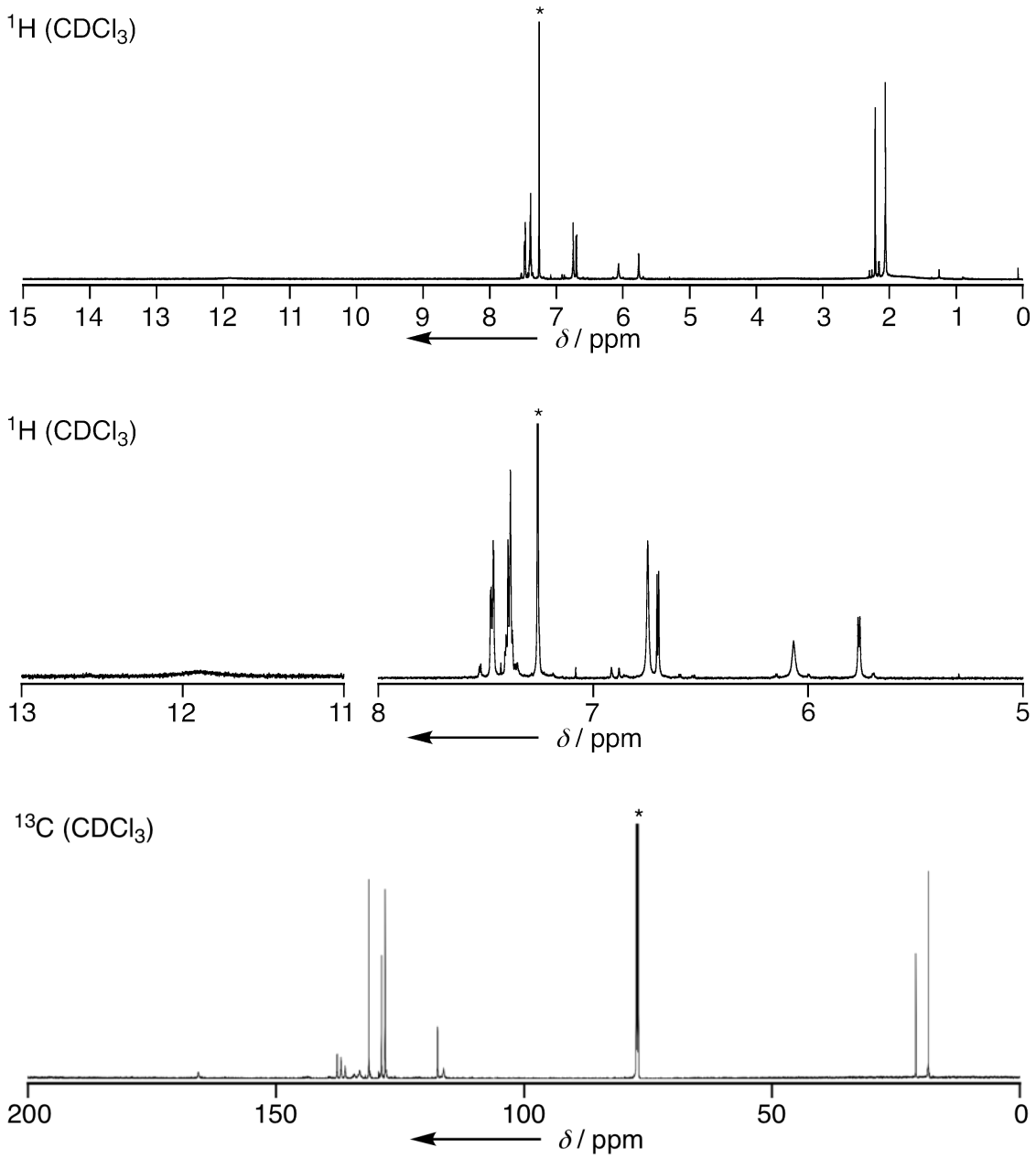

Figure S3-31. ^{1}H and ^{13}C NMR spectra of **10** in $CDCl_3$ at room temperature. * means residual solvent peaks.

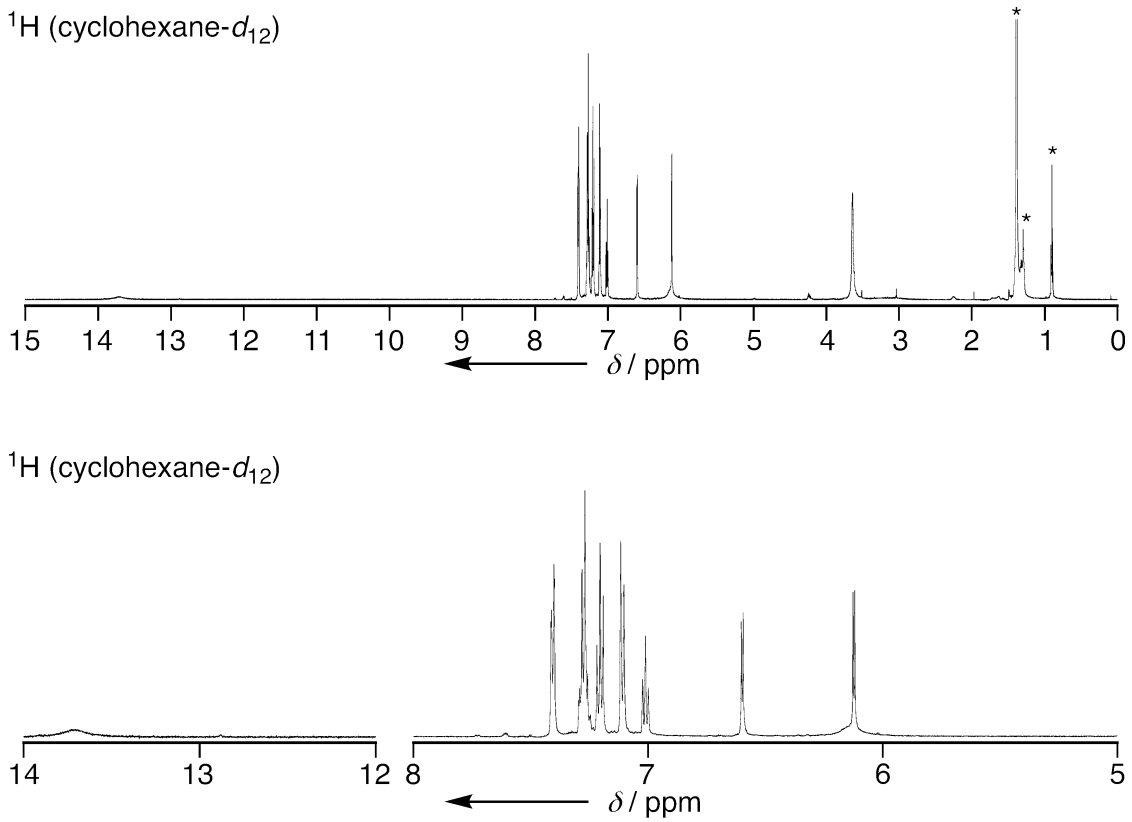

Figure S3-32. ^{1}H NMR spectrum of **11** in cyclohexane-d_{12} at room temperature. * means residual solvent peaks.

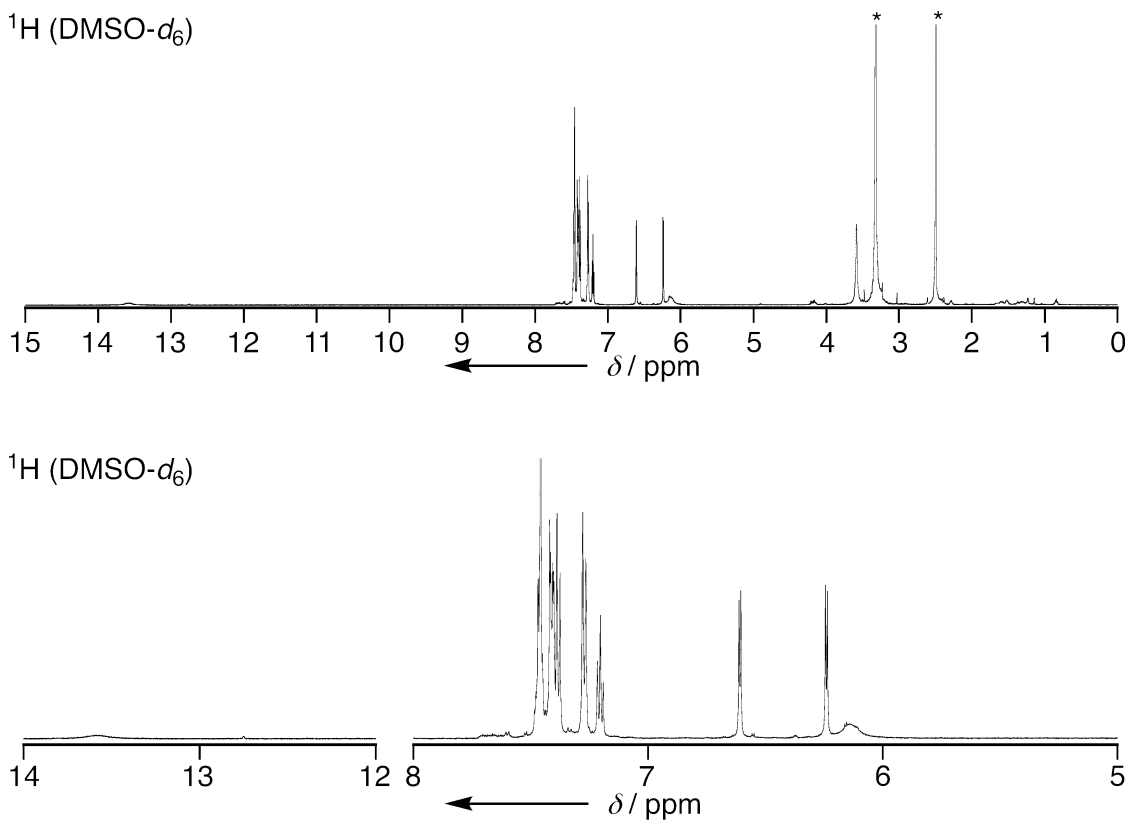

Figure S3-33. ^{1}H NMR spectrum of **11** in DMSO-d_6 at room temperature. * means residual solvent peaks.

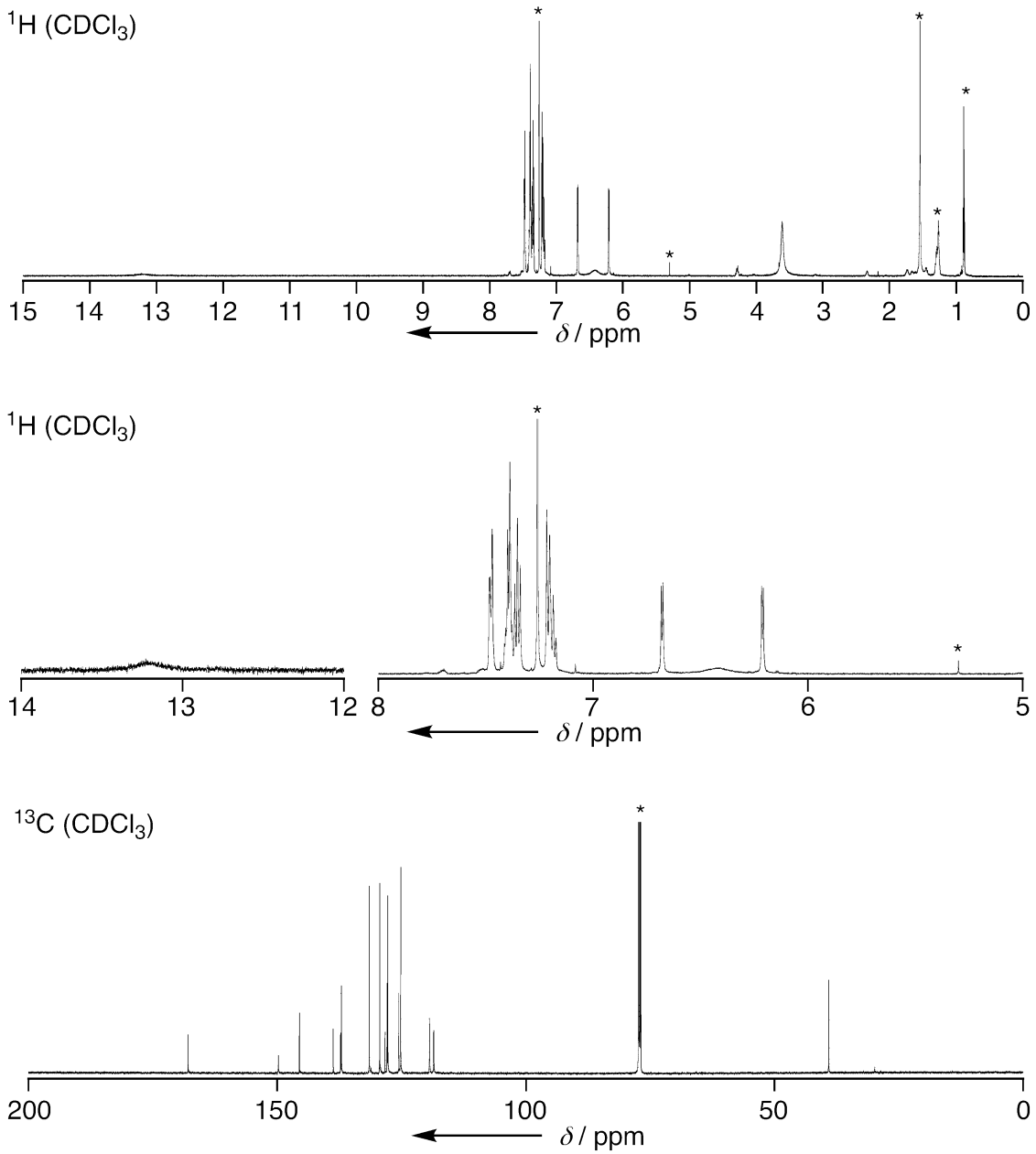

Figure S3-34. ^{1}H and ^{13}C NMR spectra of **11** in $CDCl_3$ at room temperature. * means residual solvent peaks.

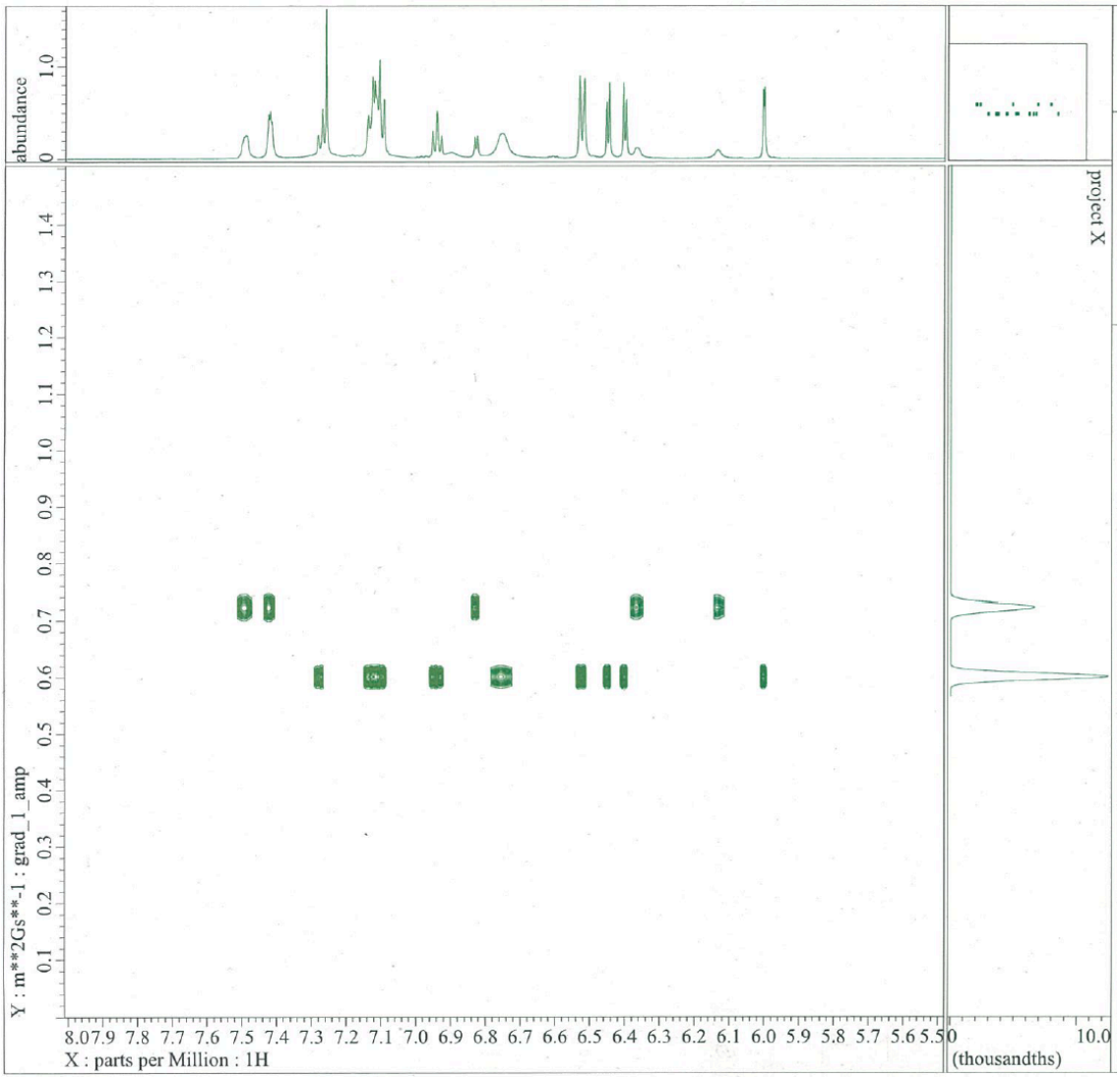

Figure S3-35. ^{1}H NMR DOSY chart of **4** in $CDCl_3$ at room temperature.

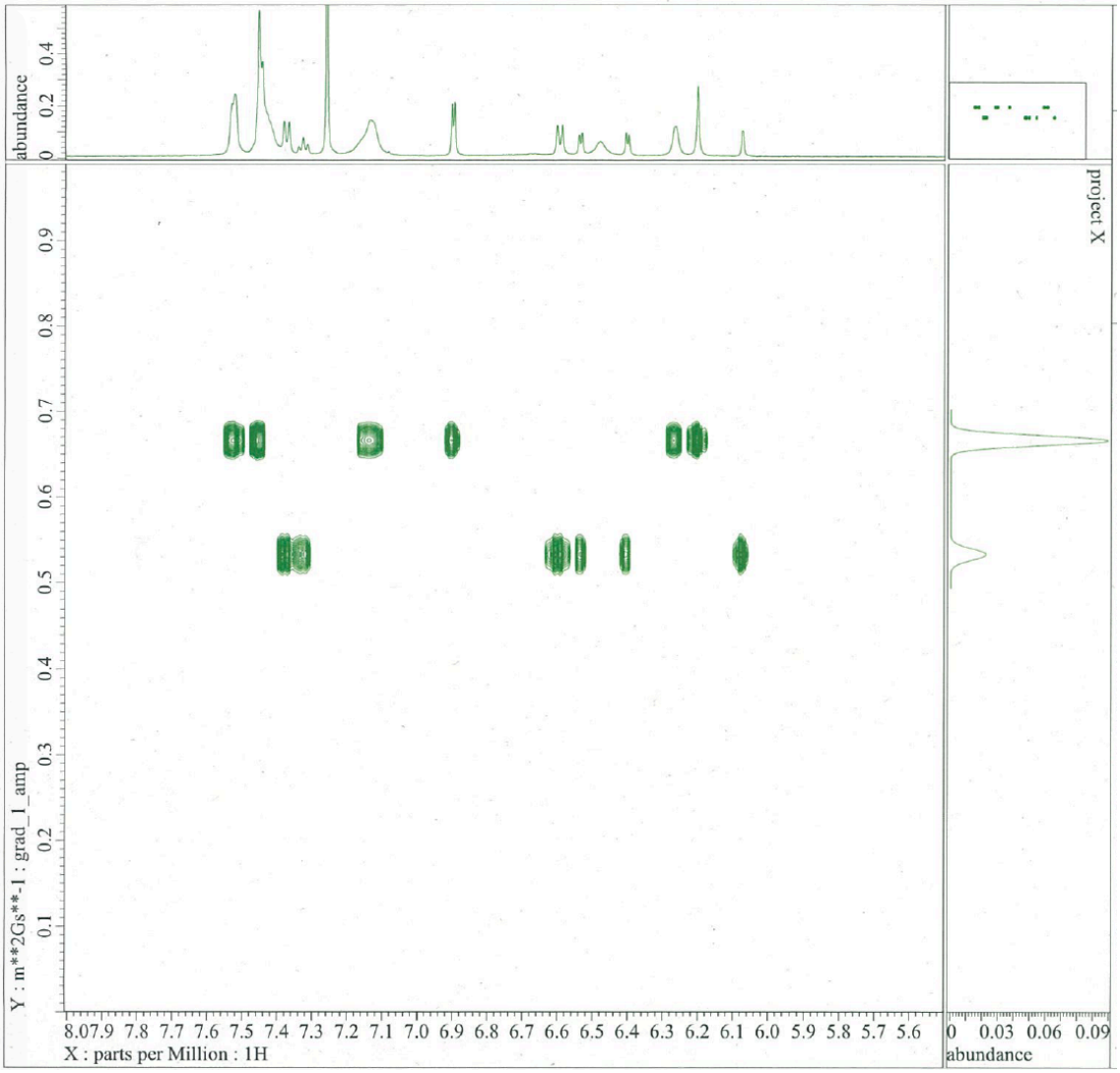

Figure S3-36. ^{1}H NMR DOSY chart of **5** in $CDCl_3$ at room temperature.

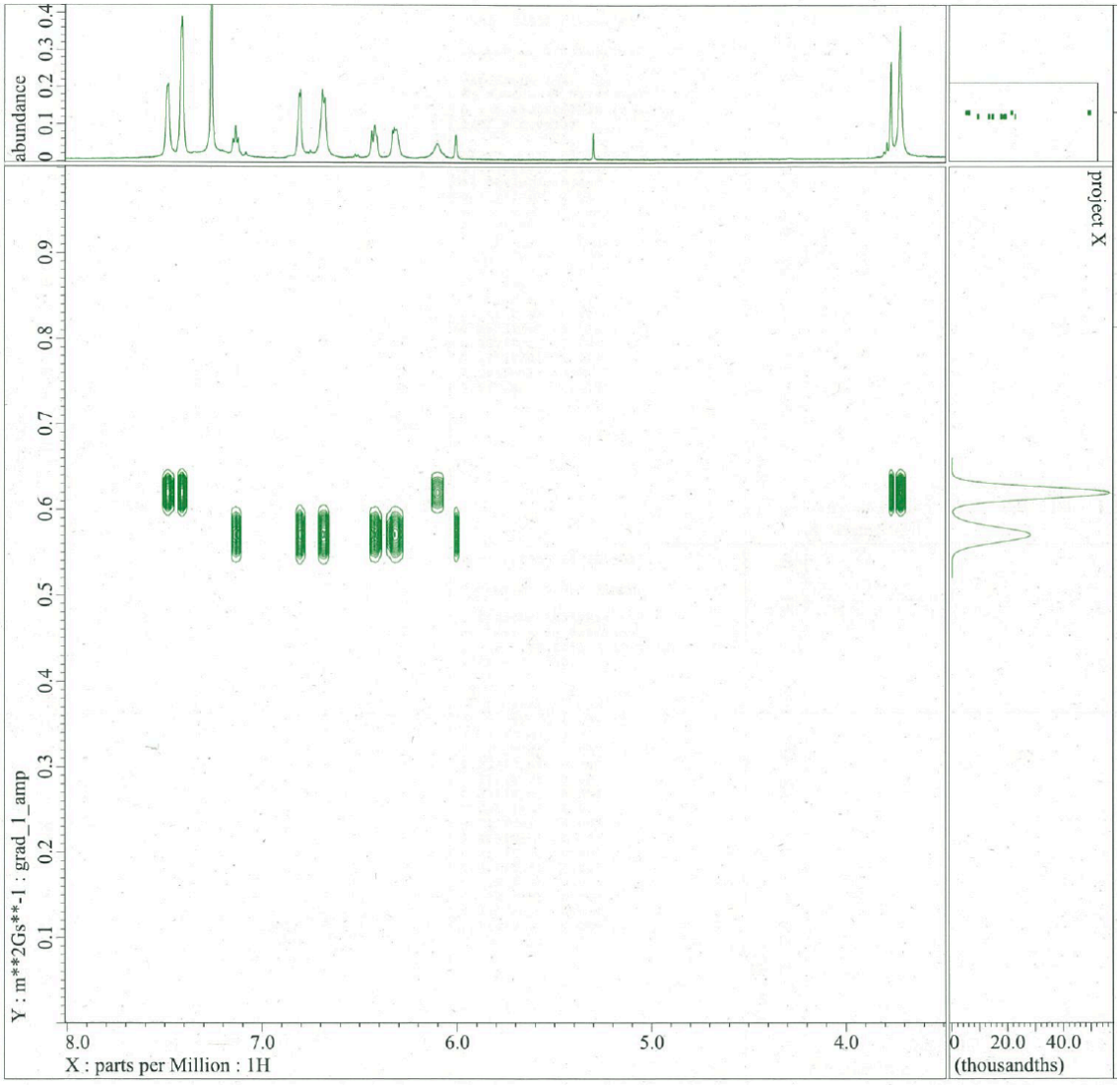

Figure S3-37. ^{1}H NMR DOSY chart of **6** in $CDCl_3$ at room temperature.

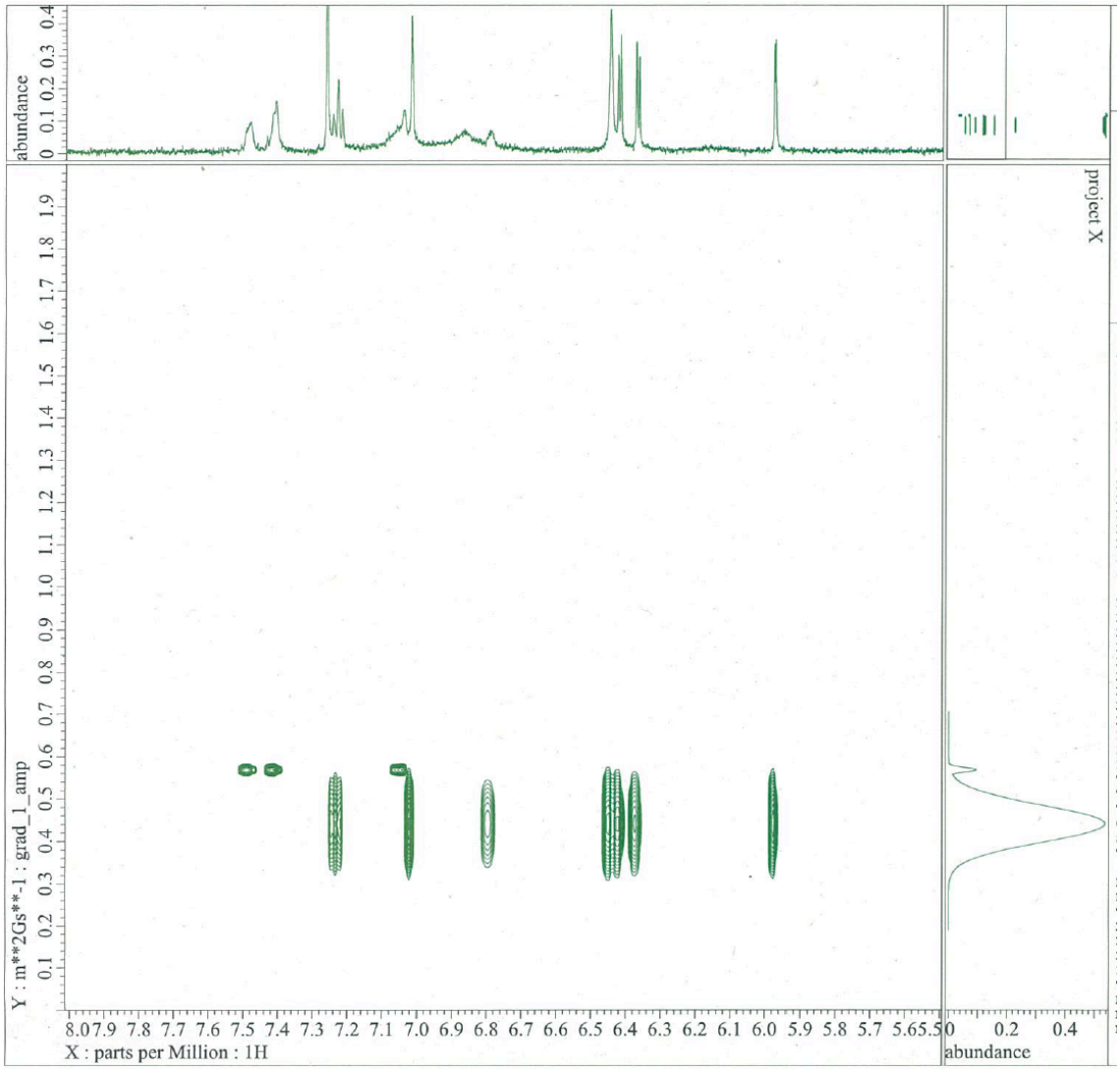

Figure S3-38. ^{1}H NMR DOSY chart of **7** in $CDCl_3$ at room temperature.

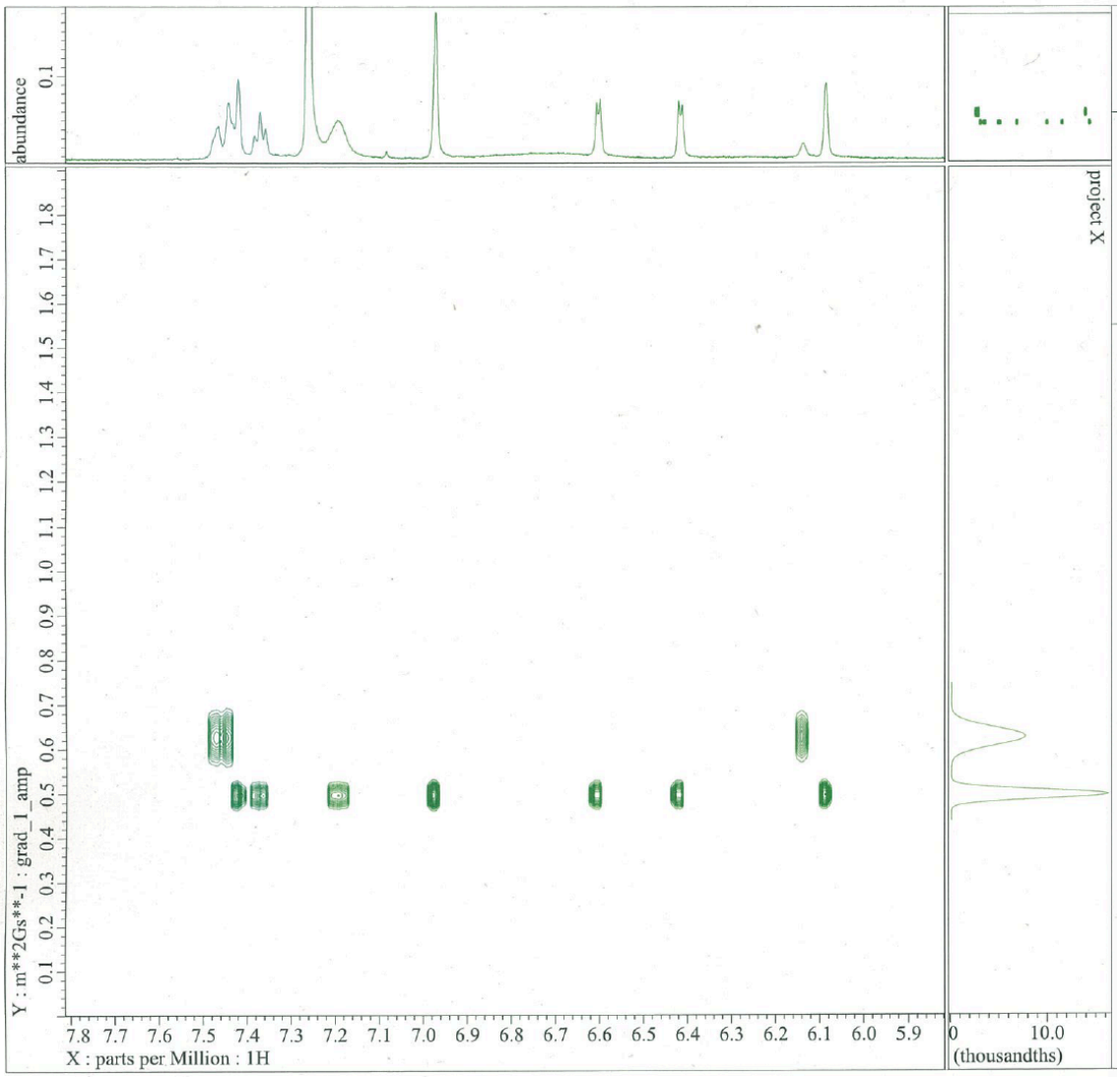

Figure S3-39. ^{1}H NMR DOSY chart of **8** in $CDCl_3$ at room temperature.

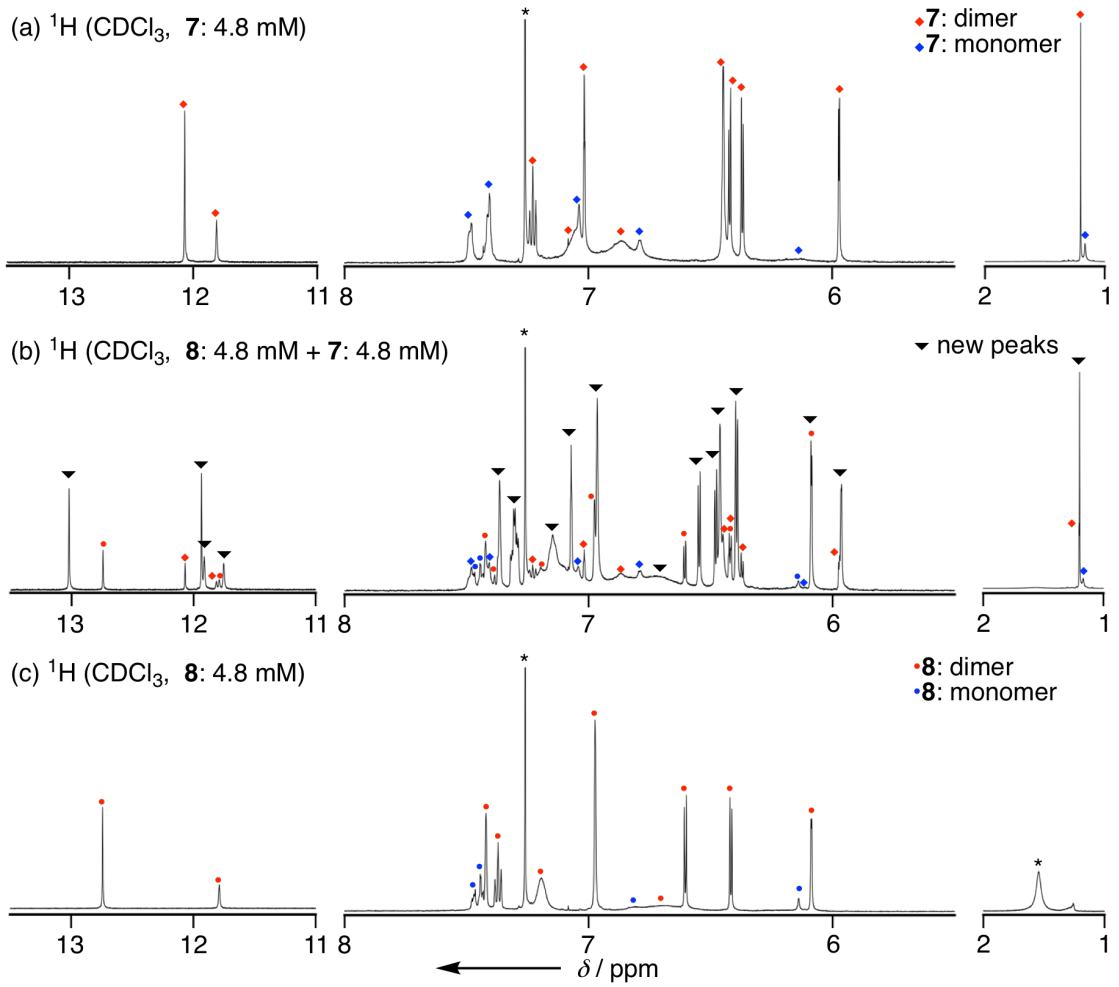

Figure S3-40. ^{1}H NMR spectra of (a) **7**, (b) a 1:1 mixture of **7** and **8**, and (c) **8** in $CDCl_3$ at room temperature.

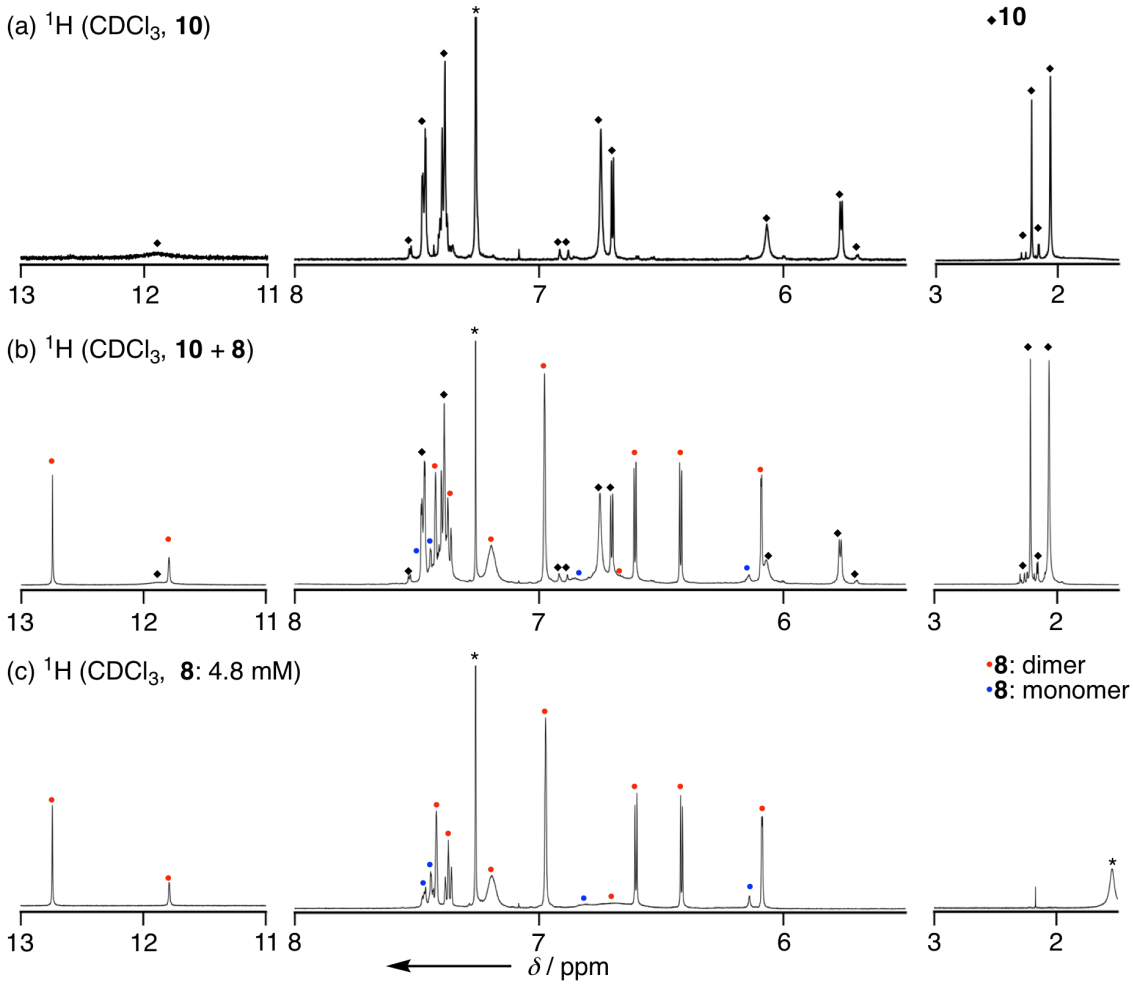

Figure S3-41. ^{1}H NMR spectra of (a) **10**, (b) a 1:1 mixture of **10** and **8**, and (c) **8** in $CDCl_3$ at room temperature.

4. Mass Spectra

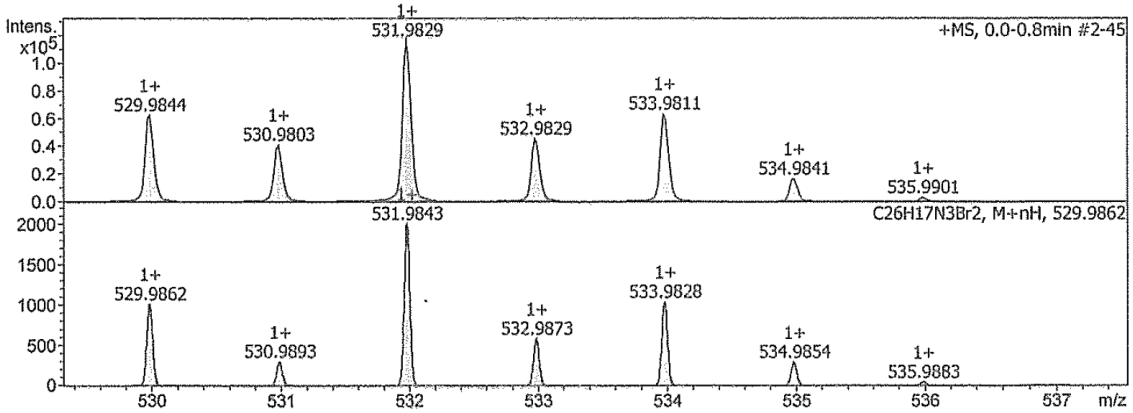

Figure S4-1. HR APCI-TOF-MS of **3**. (Top: observed; Bottom: simulated)

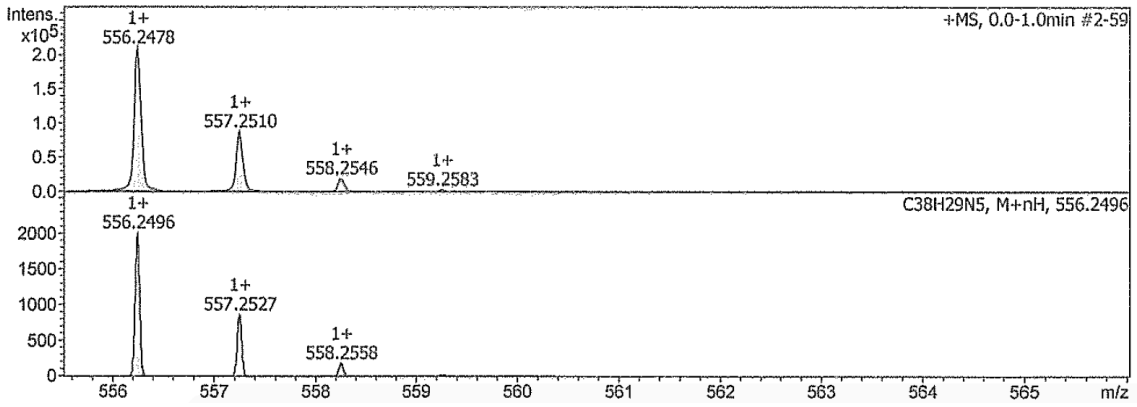

Figure S4-2. HR APCI-TOF-MS of **4**. (Top: observed; Bottom: simulated)

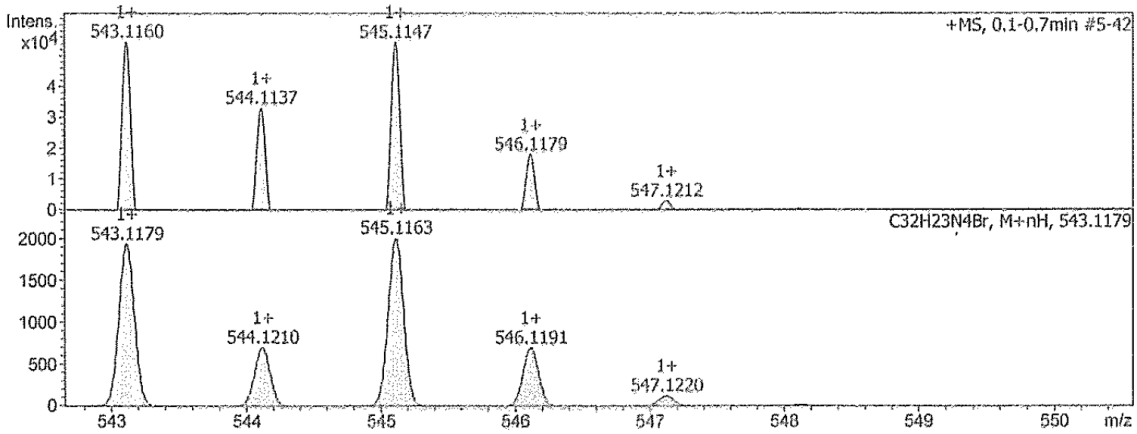

Figure S4-3. HR APCI-TOF-MS of 1-anilino-5,10-diphenyl-14-bromotripyrrin (**S1**). (Top: observed; Bottom: simulated)

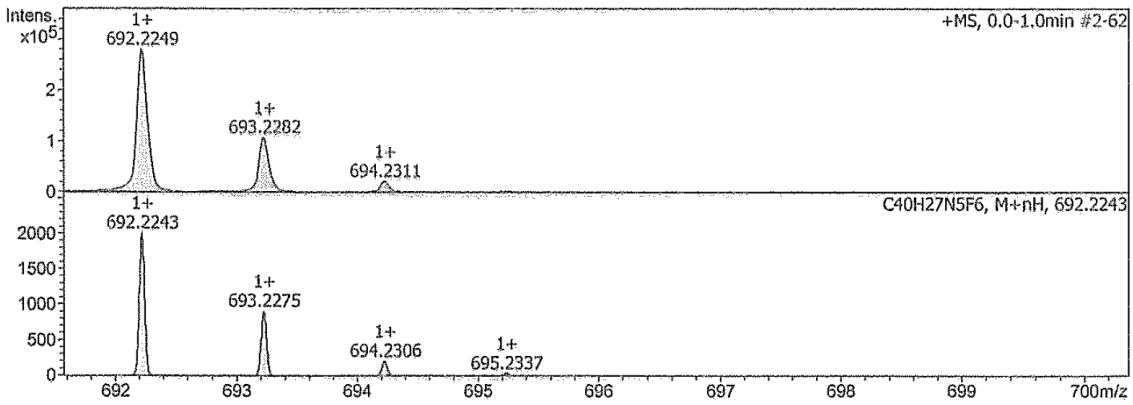

Figure S4-4. HR APCI-TOF-MS of **5**. (Top: observed; Bottom: simulated)

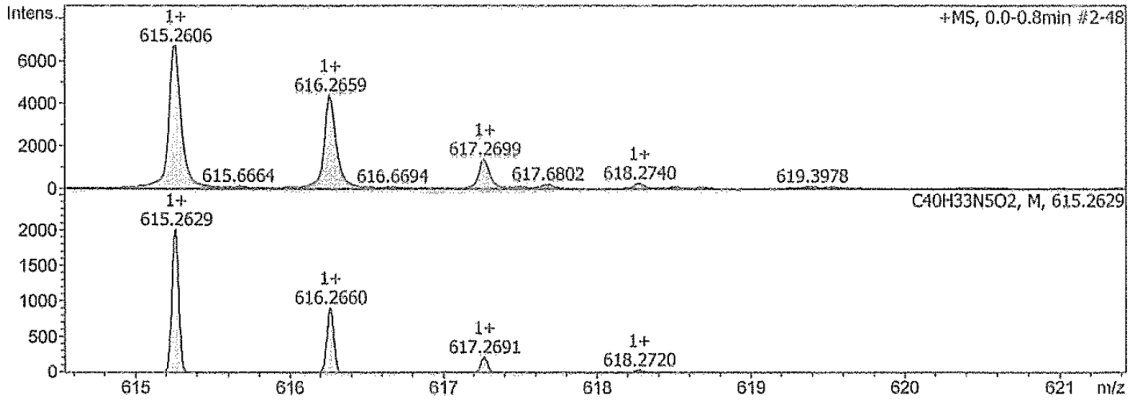

Figure S4-5. HR APCI-TOF-MS of **6**. (Top: observed; Bottom: simulated)

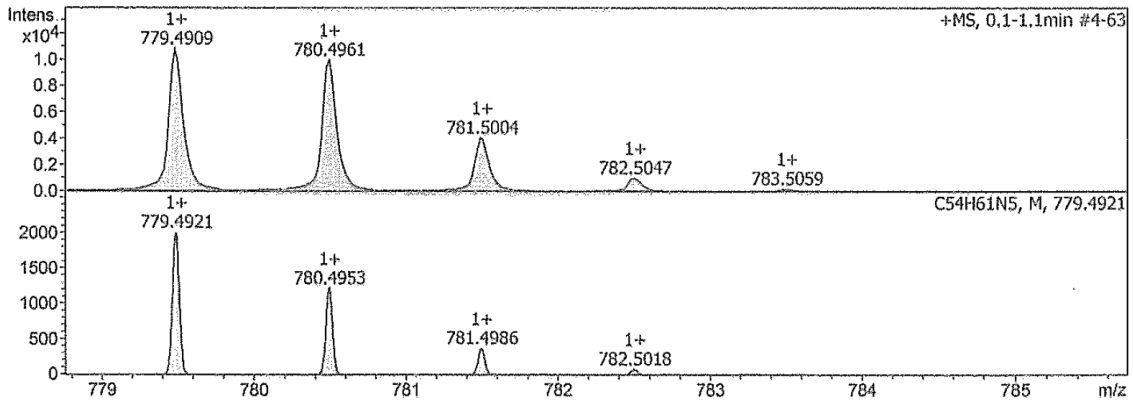

Figure S4-6. HR APCI-TOF-MS of **7**. (Top: observed; Bottom: simulated)

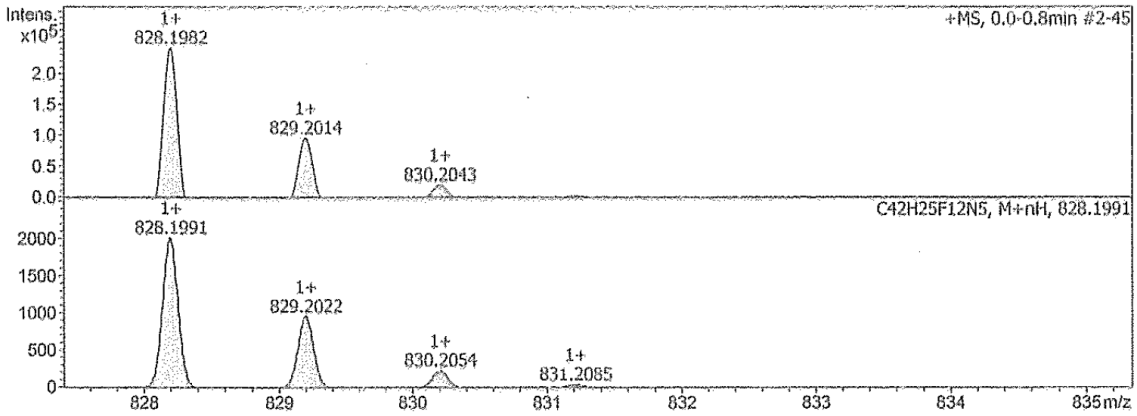

Figure S4-7. HR APCI-TOF-MS of **8**. (Top: observed; Bottom: simulated)

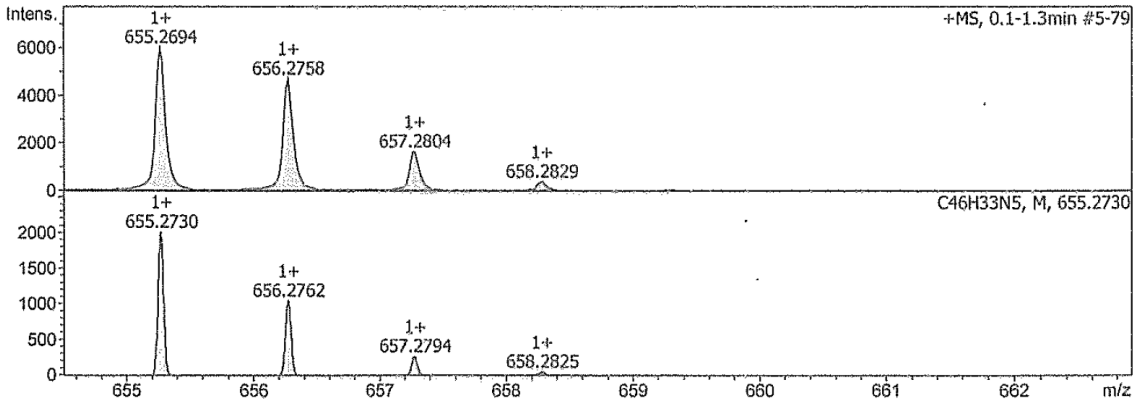

Figure S4-8. HR APCI-TOF-MS of **9**. (Top: observed; Bottom: simulated)

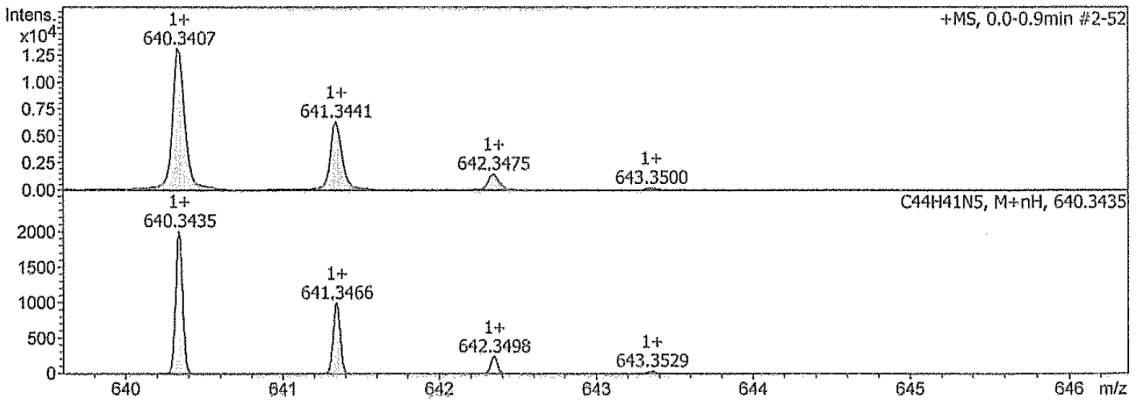

Figure S4-9. HR APCI-TOF-MS of **10**. (Top: observed; Bottom: simulated)

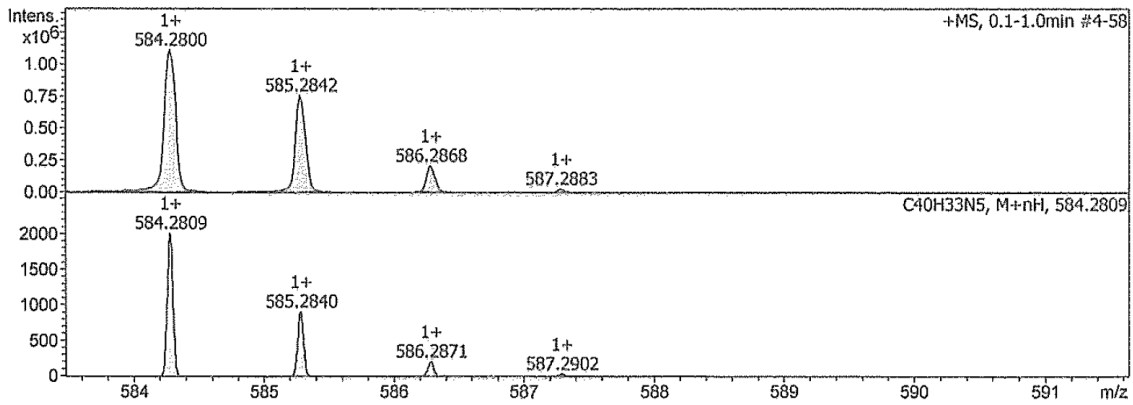

Figure S4-10. HR APCI-TOF-MS of **11**. (Top: observed; Bottom: simulated)

5. X-Ray Crystallographic Details

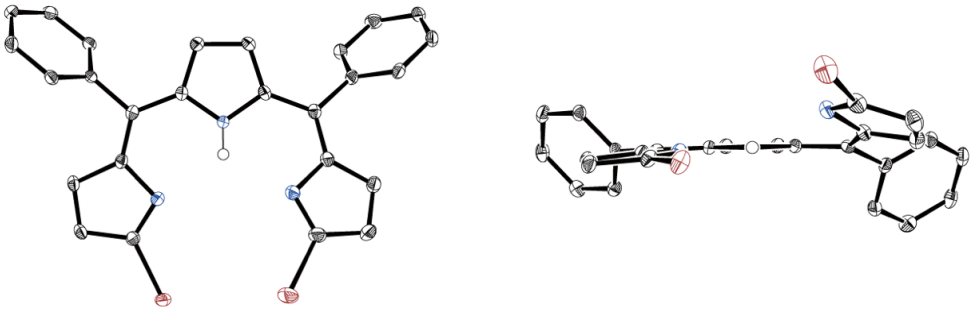

Figure S5-1. X-ray crystal structure of **3**. Hydrogen atoms except for NHs were omitted for clarity. Thermal ellipsoids were scaled to 50% probability.

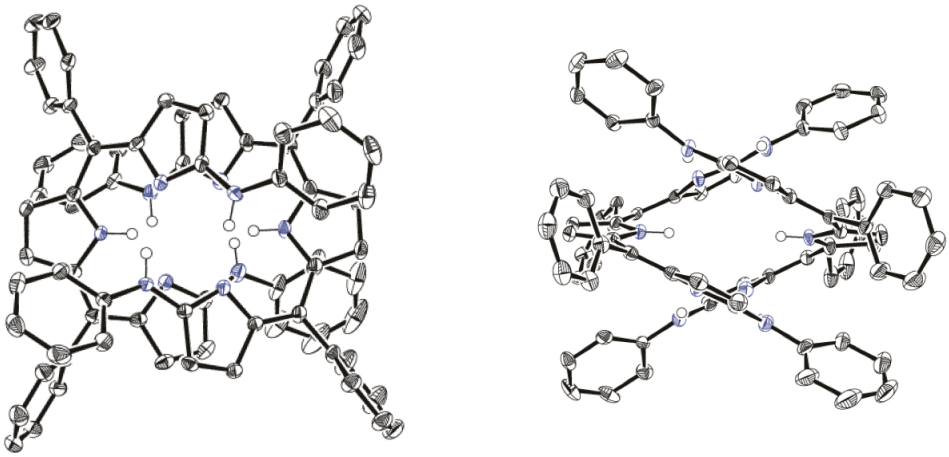

Figure S5-2. X-Ray crystal structure of **4** obtained from $CHCl_3$/*n*-hexane. Hydrogen atoms except for NHs and solvent molecules were omitted for clarity. Thermal ellipsoids were scaled to 50% probability.

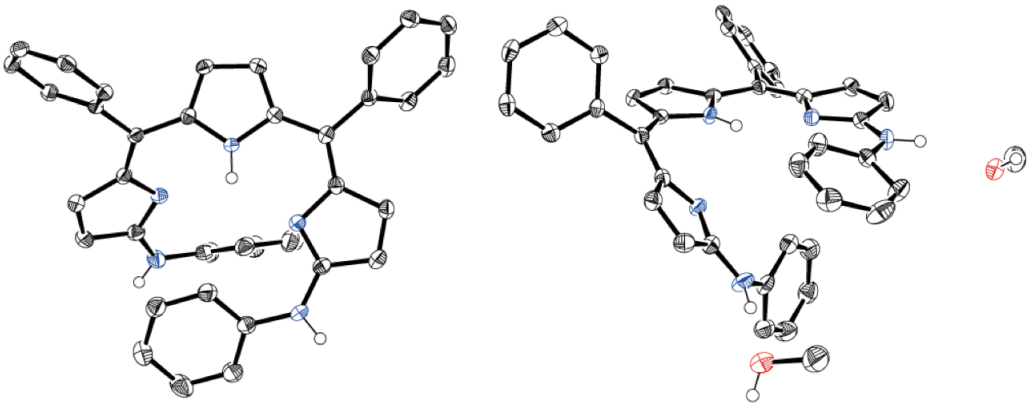

Figure S5-3. X-Ray crystal structure of **4** obtained from MeOH/H_2O. Hydrogen atoms except for NHs were omitted for clarity. Thermal ellipsoids were scaled to 50% probability.

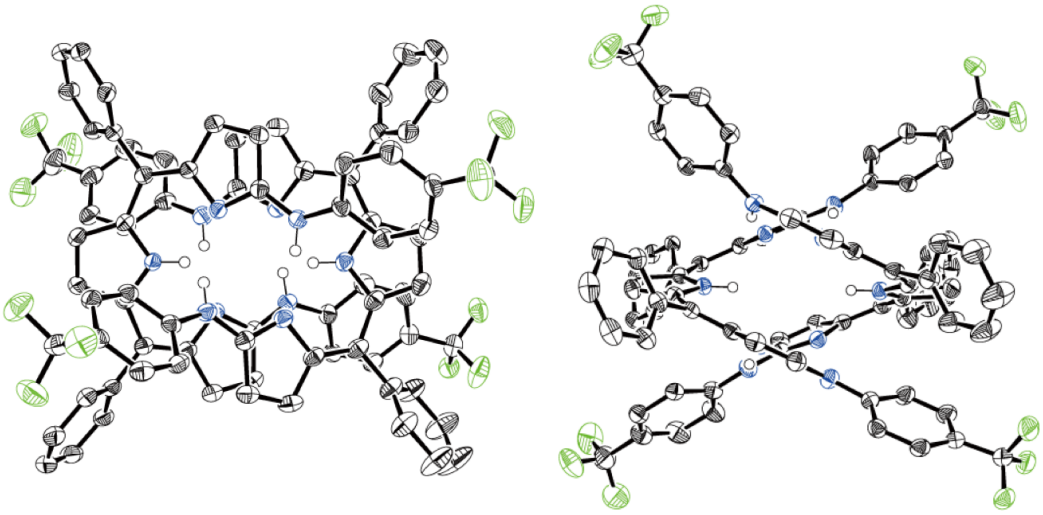

Figure S5-4. X-Ray crystal structure of **5** obtained from *n*-hexane. Hydrogen atoms except for NHs and solvent molecules were omitted for clarity. Thermal ellipsoids were scaled to 50% probability.

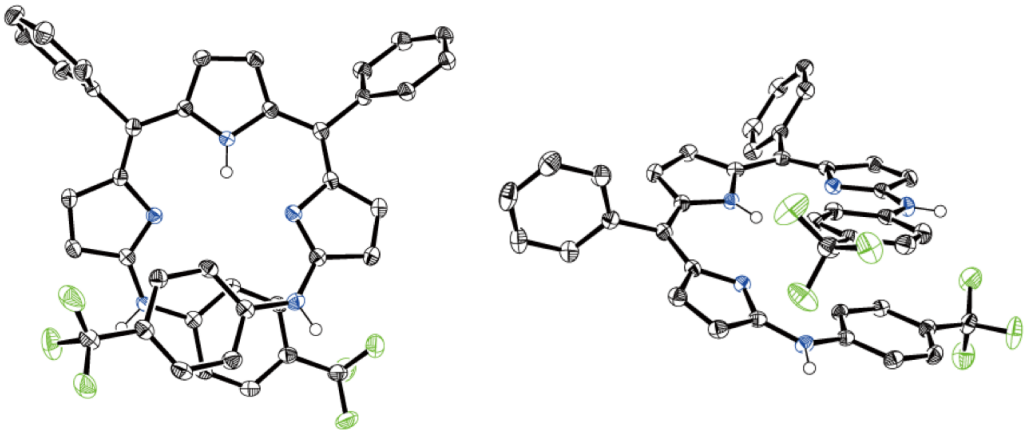

Figure S5-5. X-Ray crystal structure of **5** obtained from MeOH/H_2O. Hydrogen atoms except for NHs and solvent molecules were omitted for clarity. Thermal ellipsoids were scaled to 50% probability.

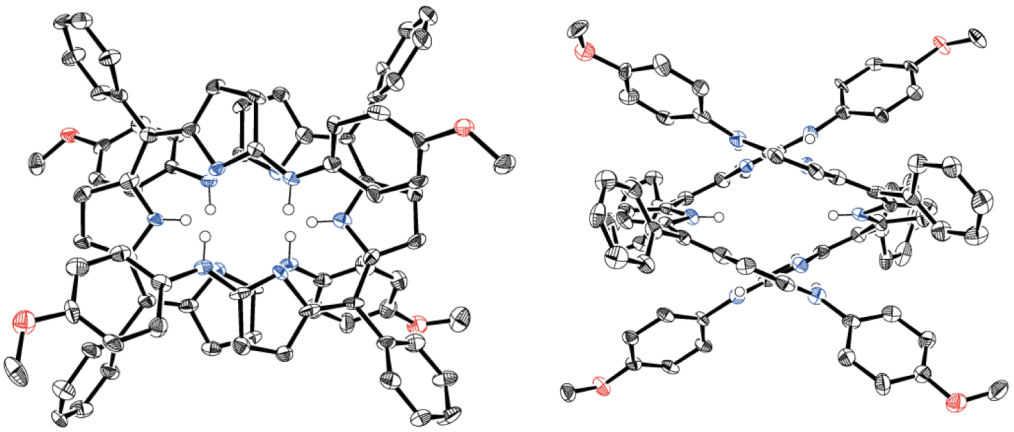

Figure S5-6. X-Ray crystal structure of **6** obtained from $CHCl_3$/*n*-hexane. Hydrogen atoms except for NHs and solvent molecules were omitted for clarity. Thermal ellipsoids were scaled to 50% probability.

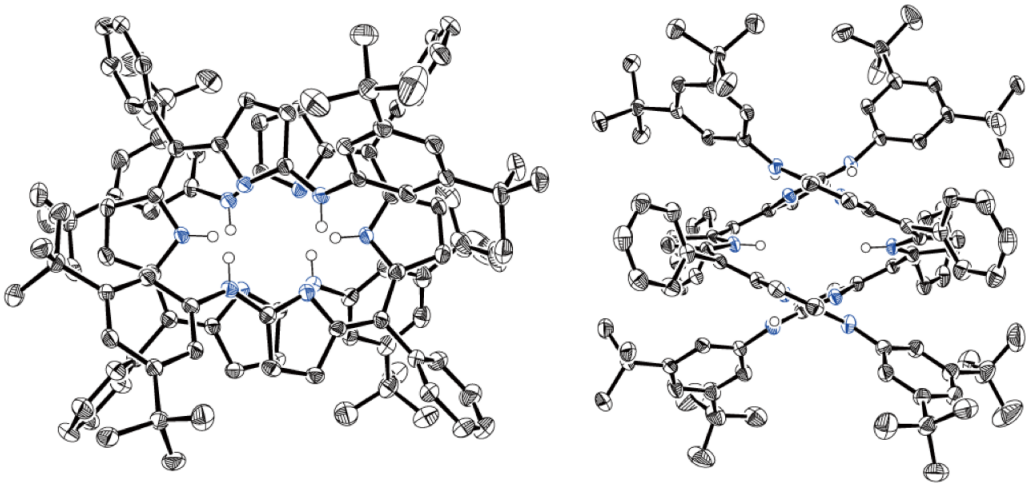

Figure S5-7. X-Ray crystal structure of **7** obtained from $CHCl_3$/*n*-hexane. Hydrogen atoms except for NHs and solvent molecules were omitted for clarity. Thermal ellipsoids were scaled to 50% probability.

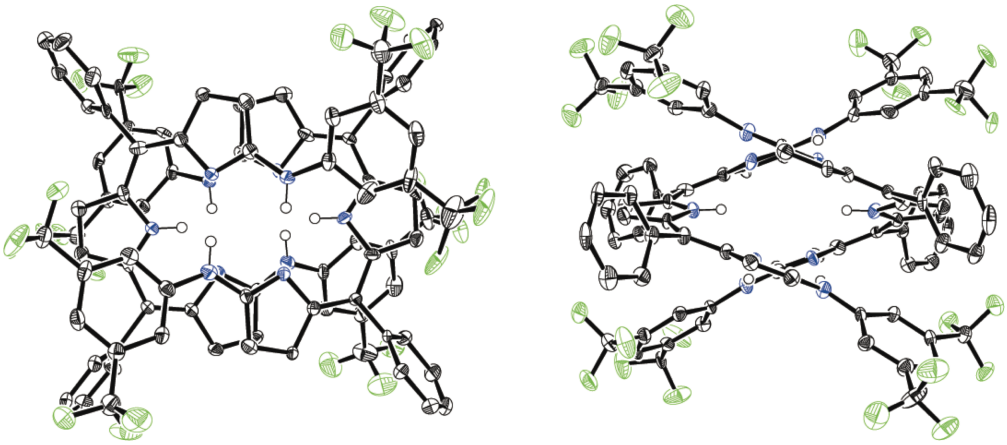

Figure S5-8. X-Ray crystal structure of **8** obtained from $CHCl_3$/*n*-hexane. Hydrogen atoms except for NHs and solvent molecules were omitted for clarity. Thermal ellipsoids were scaled to 50% probability.

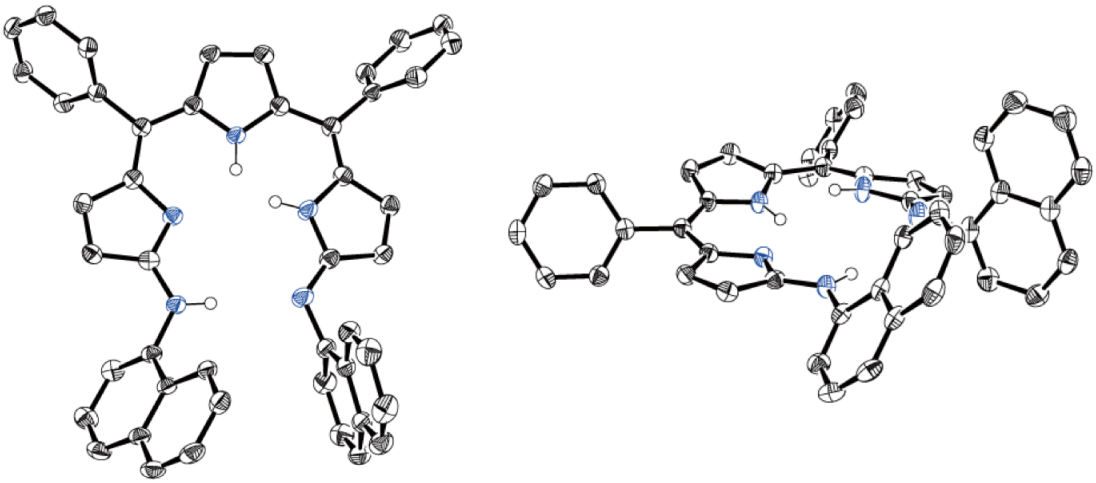

Figure S5-9. X-Ray crystal structure of **9** obtained from CH_2Cl_2/*n*-hexane. Hydrogen atoms except for NHs and solvent molecules were omitted for clarity. Thermal ellipsoids were scaled to 50% probability.

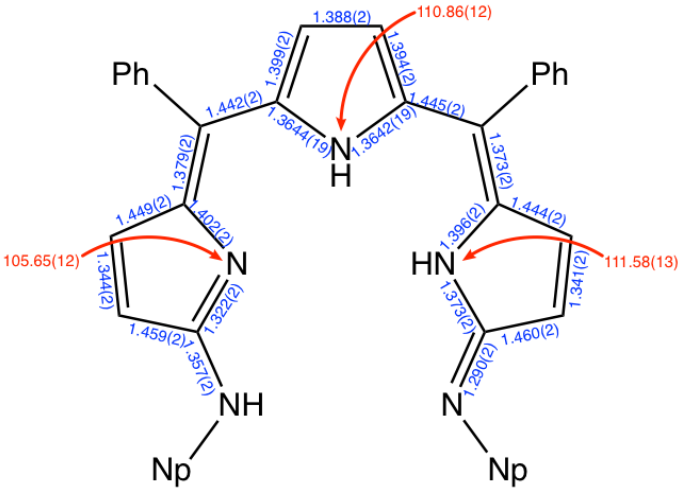

Figure S5-10. Bond lengths(Å) and bond angles(°) of **9**.

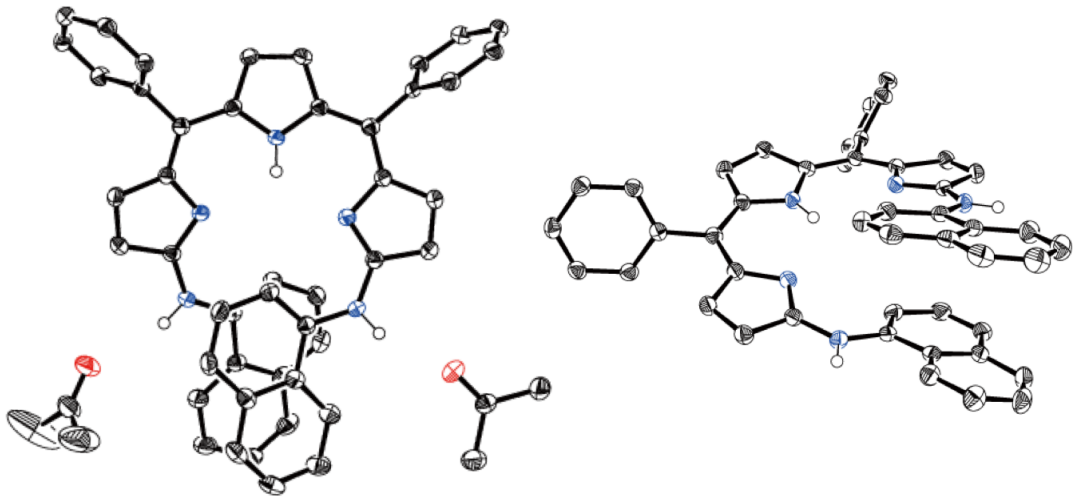

Figure S5-11. X-Ray crystal structure of **9** obtained from acetone/H_2O. Hydrogen atoms except for NHs were omitted for clarity. Thermal ellipsoids were scaled to 50% probability.

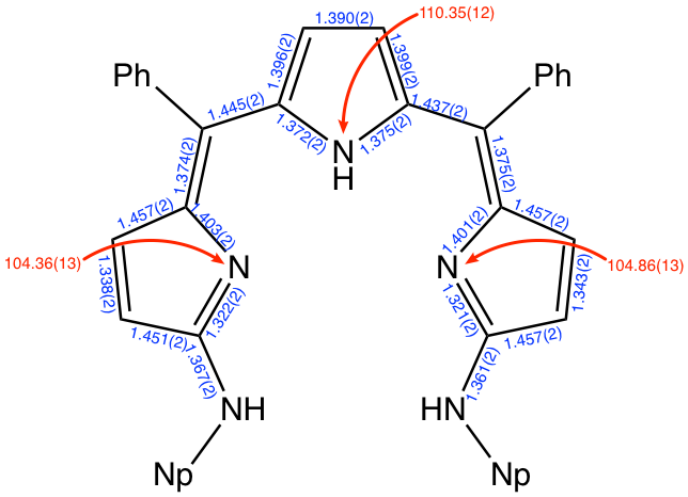

Figure S5-12. Bond lengths(Å) and bond angles(°) of **9**.

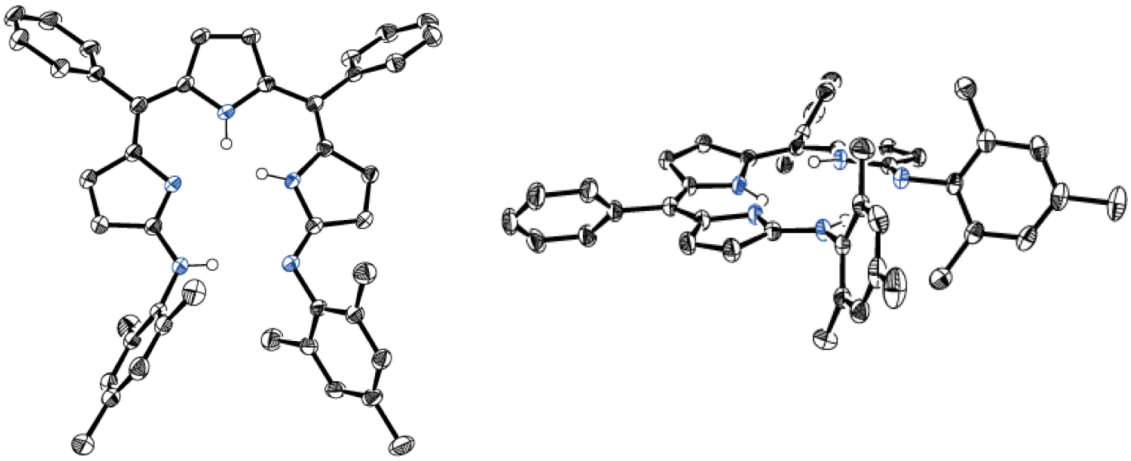

Figure S5-13. X-Ray crystal structure of **10** obtained from $CHCl_3$/*n*-hexane. Hydrogen atoms except for NHs and solvent molecules were omitted for clarity. Thermal ellipsoids were scaled to 50% probability.

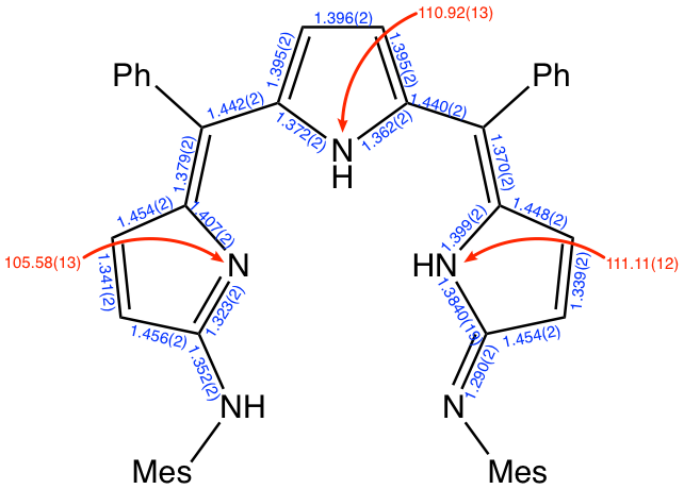

Figure S5-14. Bond lengths(Å) and bond angles(°) of **10**.

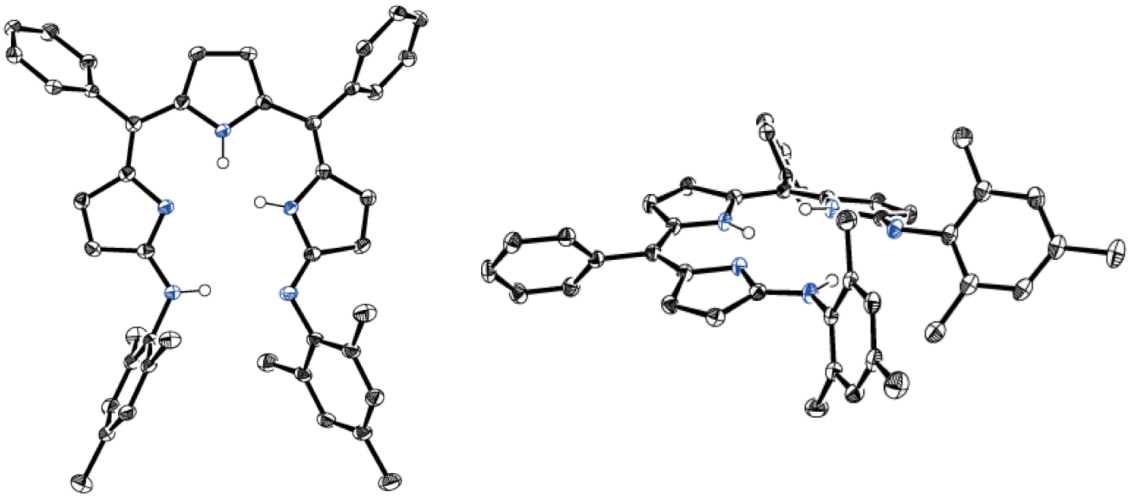

Figure S5-15. X-Ray crystal structure of **10** obtained from EtOH/H_2O. Hydrogen atoms except for NHs were omitted for clarity. Thermal ellipsoids were scaled to 50% probability.

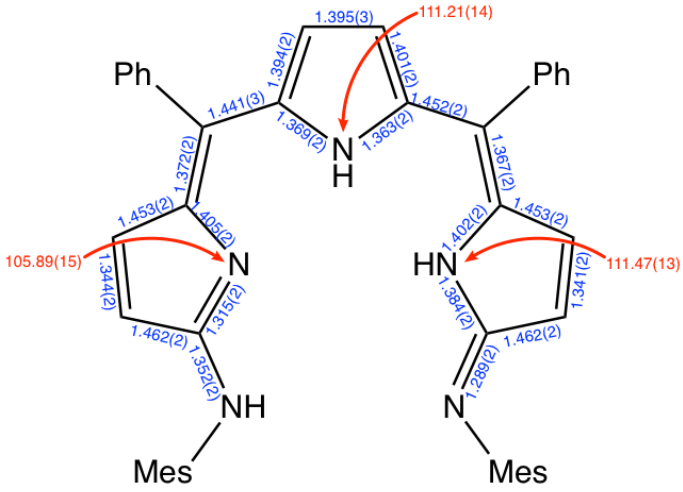

Figure S5-16. Bond lengths(Å) and bond angles(°) of **10**.

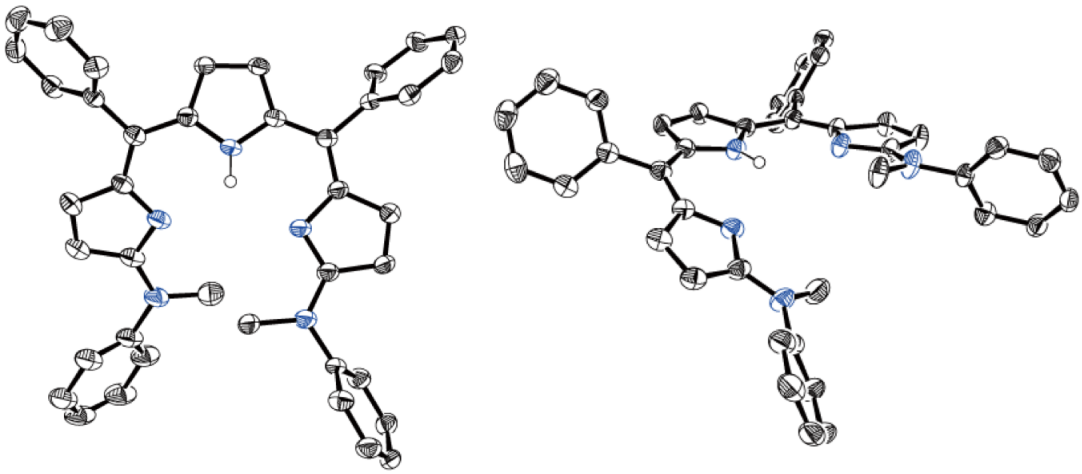

Figure S5-17. X-Ray crystal structure of **11**. Hydrogen atoms except for NHs were omitted for clarity. Thermal ellipsoids were scaled to 50% probability.

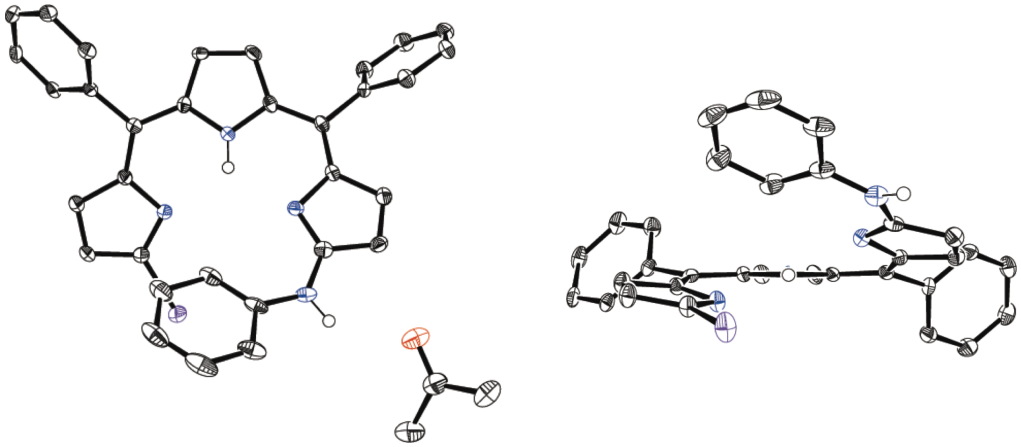

Figure S5-18. X-Ray crystal structure of **S1**. Hydrogen atoms except for NHs were omitted for clarity. Thermal ellipsoids were scaled to 50% probability.

Table S5-1. Crystal data and structure refinements for **3**, **11** and **S1**.

Compound	**3**	**11**	**S1**
Formula	$C_{26}H_{17}N_3Br_2$	$C_{40}H_{33}N_5$	$C_{32}H_{23}BrN_4$, 0.5(C_3H_6O)
M_W	531.24	583.71	572.49
Crystal System	Orthorhombic	Monoclinic	Monoclinic
Space Group	*P c a* 2_1 (No.29)	*P* $2_1/c$ (No.14)	*C* 2/*c* (No.15)
a [Å]	25.043(4)	10.1411(5)	13.751(4)
b [Å]	10.3564(18)	25.4006(11)	15.095(4)
c [Å]	8.256(2)	12.1107(6)	26.536(6)
α [deg]	90	90	90
β [deg]	90	94.978(5)	100.513(4)
γ [deg]	90	90	90
Volume [Å^3]	2141.2(8)	3107.8(3)	1682.1(5)
Z	4	4	8
Density [Mg/m^3]	1.648	1.248	1.404
Completeness	1.73/0.93	0.983	0.987
Goodness-of-fit	1.010	1.012	1.001
R_1 [$I > 2\sigma(I)$]	0.0158	0.0593	0.0421
wR_2 (all data)	0.0414	0.1406	0.1069
Solvent System	$CHCl_3$/MeOH	EtOH/H_2O	acetone/H_2O
CCDC	1849984	1849988	1850026

Table S5-2. Crystal data and structure refinements for **4** and **5**.

Compound	**4** (dimer)	**4** (monomer)	**5** (dimer)	**5** (monomer)
Formula	$2(C_{38}H_{29}N_5)$, $0.497(C_6)$, $CHCl_3$	$C_{38}H_{29}N_5$, $2(CH_4O)$	$2(C_{40}H_{27}F_6N_5)$, C_6	$2(C_{40}H_{27}F_6N_5)$
M_W	1266.48	619.75	1455.39	1383.33
Crystal System	Trigonal	Monoclinic	Monoclinic	Triclinic
Space Group	R –3 (No.148)	$P\,2_1/c$ (No.14)	$P\,2_l/c$ (No.14)	P –1 (No.2)
a [Å]	50.519(7)	18.523(4)	20.794(4)	13.025(3)
b [Å]	50.519(7)	9.319(2)	13.875(2)	14.1499(19)
c [Å]	13.4259(19)	19.109(4)	25.322(5)	18.8806(19)
α [deg]	90	90	90	87.297(14)
β [deg]	90	95.740(5)	102.958(3)	73.304(15)
γ [deg]	120	90	90	82.748(17)
Volume [Å^3]	29674(9)	3282.0(12)	7120(2)	3306.2(10)
Z	18	4	4	2
Density [Mg/m^3]	1.276	1.254	1.358	1.390
Completeness	0.990	0.984	0.973	0.956
Goodness-of-fit	1.004	1.002	1.025	1.094
R_1 [$I > 2\sigma(I)$]	0.0738	0.0457	0.0640	0.0367
wR_2 (all data)	0.2208	0.1228	0.1861	0.1000
Solvent System	$CHCl_3$/*n*-hexane	MeOH/H_2O	*n*-hexane	MeOH/H_2O
CCDC	1850022	1850013	1850011	1850012

Table S5-3. Crystal data and structure refinements for **6**, **7** and **8**.

Compound	**6** (dimer)	**7** (dimer)	**8** (dimer)
Formula	$2(C_{40}H_{33}N_5O_2)$, $CHCl_3$	$4(C_{54}H_{61}N_5)$, $1.521C_6$, $0.479C_6$	$2(C_{42}H_{25}F_{12}N_5)$, CH_2Cl_2
M_W	1350.80	3609.10	1740.29
Crystal System	Triclinic	Orthorhombic	Triclinic
Space Group	*P* –1 (No.2)	*P bca* (No.61)	*P* –1 (No.2)
a [Å]	14.7058(8)	30.1086(3)	12.9577(2)
b [Å]	15.4490(7)	31.9945(4)	14.3835(2)
c [Å]	16.6352(9)	46.8128(7)	20.7824(5)
α [deg]	90.453(4)	90	88.275(2)
β [deg]	101.803(5)	90	83.194(2)
γ [deg]	113.116(5)	90	84.955(1)
Volume [Å^3]	3386.0(3)	45095.2(10)	3830.41(12)
Z	2	8	2
Density [Mg/m^3]	1.325	1.063	1.509
Completeness	0.965	1.000	0.973
Goodness-of-fit	1.111	1.013	1.073
R_1 [$I > 2\sigma(I)$]	0.1689	0.0793	0.1391
wR_2 (all data)	0.4370	0.2596	0.4053
Solvent System	$CHCl_3$/*n*-hexane	$CHCl_3$/*n*-hexane	CH_2Cl_2/*n*-hexane
CCDC	1849994	1849995	184996

Table S5-4. Crystal data and structure refinements for **9** and **10**.

Compound	**9** (tautomer)	**9**	**10** (tautomer)	**10** (tautomer)
Formula	$C_{46}H_{33}N_5$	$C_{46}H_{33}N_5$, $2(C_3H_6O)$	$C_{44}H_{41}N_5$, $0.5(C_6H_{14})$, $0.5(CH_2Cl_2)$	$C_{44}H_{41}N_5$
M_W	655.77	771.93	725.36	639.82
Crystal System	Triclinic	Triclinic	Monoclinic	Triclinic
Space Group	*P* –1 (No.2)	*P* –1 (No.2)	*C* 2/*c* (No.15)	*P* –1 (No.2)
a [Å]	6.5341(12)	11.495(4)	21.584(3)	12.176(10)
b [Å]	12.836(2)	11.813(4)	14.4183(19)	12.713(14)
c [Å]	20.895(3)	16.576(7)	25.314(3)	13.640(9)
α [deg]	106.233(12)	90.499(9)	90	99.304(18)
β [deg]	90.002(15)	110.070(12)	94.247(4)	104.311(8)
γ [deg]	91.44(2)	105.303(9)	90	115.26(3)
Volume [Å^3]	1682.1(5)	2026.9(13)	7856.2(18)	1762(3)
Z	2	2	8	2
Density [Mg/m^3]	1.295	1.265	1.227	1.206
Completeness	0.966	0.962	0.987	0.960
Goodness-of-fit	1.011	1.025	1.054	1.004
R_1 [$I > 2\sigma(I)$]	0.0411	0.0416	0.0418	0.0408
wR_2 (all data)	0.1180	0.1104	0.1139	0.1113
Solvent System	CH_2Cl_2/*n*-hexane	acetone/H_2O	CH_2Cl_2/*n*-hexane	EtOH/H_2O
CCDC	1849993	1849992	1849990	1849991

6. UV/Vis Absorption Spectra

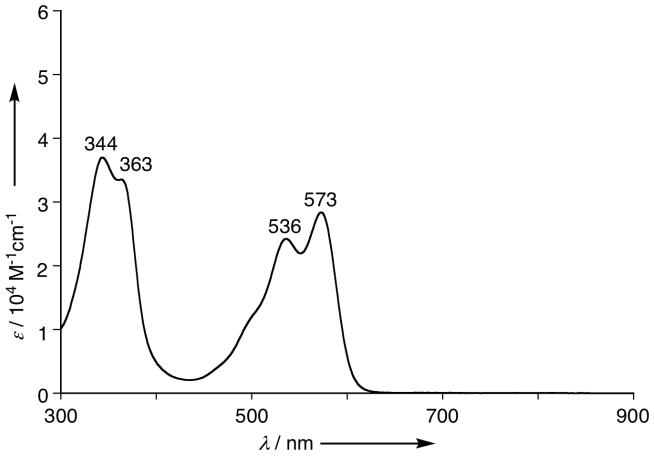

Figure S6-1. UV/Vis absorption spectrum of **3** in CH_2Cl_2.

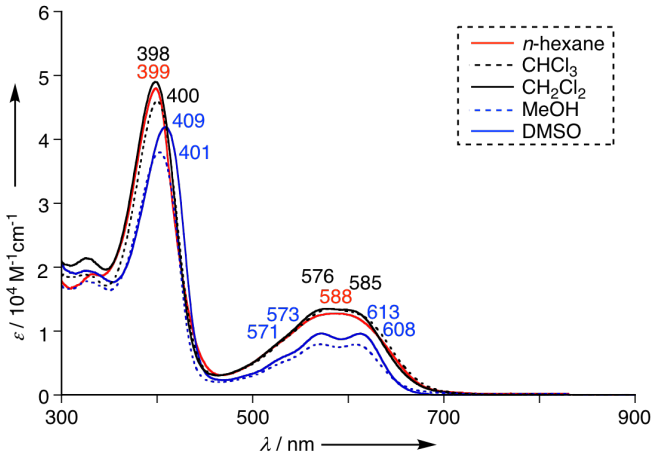

Figure S6-2. UV/Vis absorption spectra of **4** at 1.0 × 10^{-5} M in various solvents.

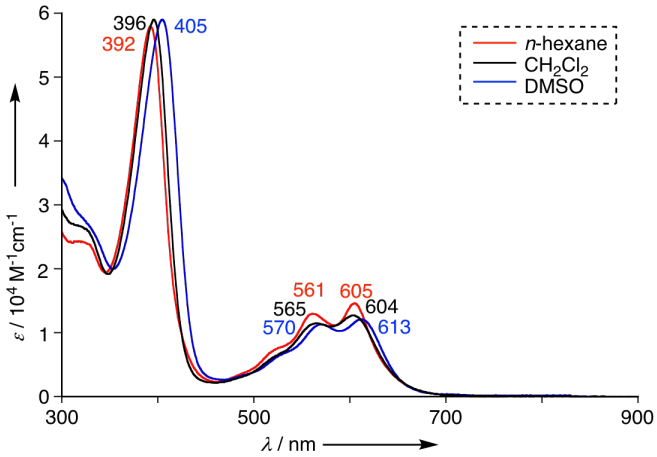

Figure S6-3. UV/Vis absorption spectra of **5** at 1.0 × 10^{-5} M in various solvents.

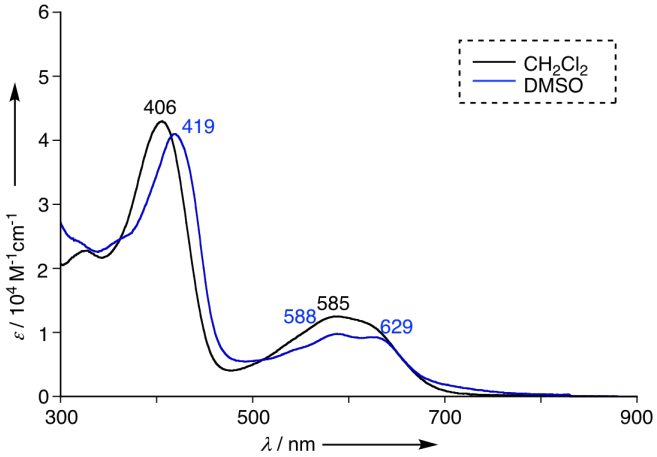

Figure S6-4. UV/Vis absorption spectra of **6** at 1.0 × 10^{-5} M in various solvents.

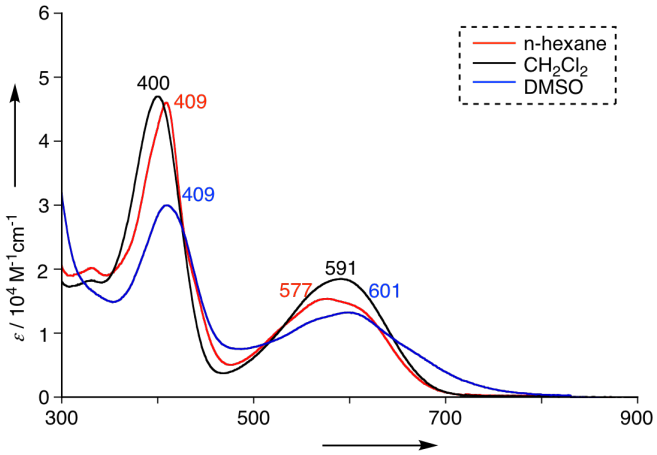

Figure S6-5. UV/Vis absorption spectra of **7** at 1.0 × 10^{-5} M in various solvents.

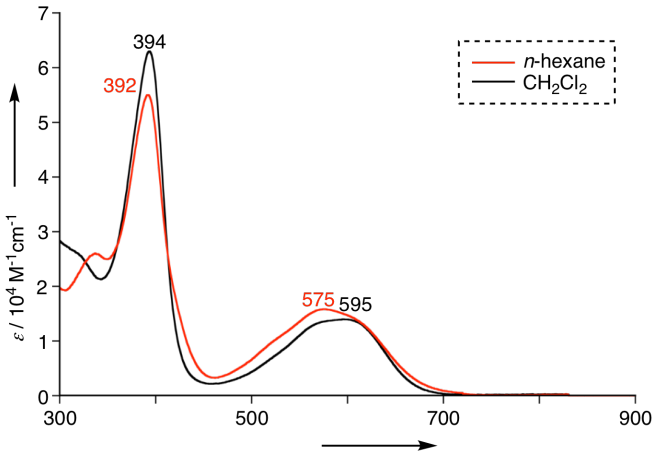

Figure S6-6. UV/Vis absorption spectra of **8** at 1.0 × 10^{-5} M in various solvents.

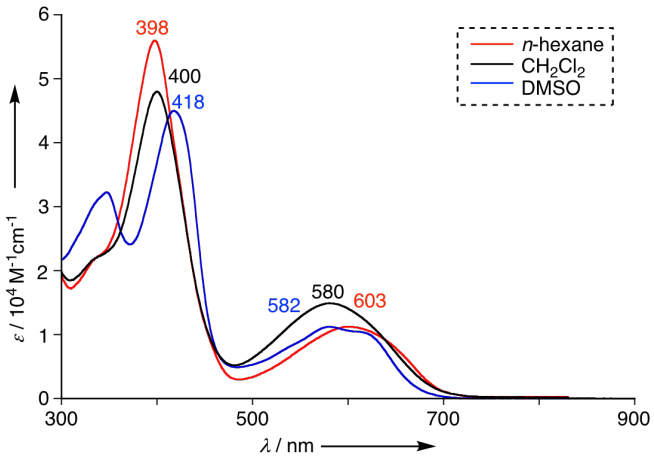

Figure S6-7. UV/Vis absorption spectra of **9** in various solvents.

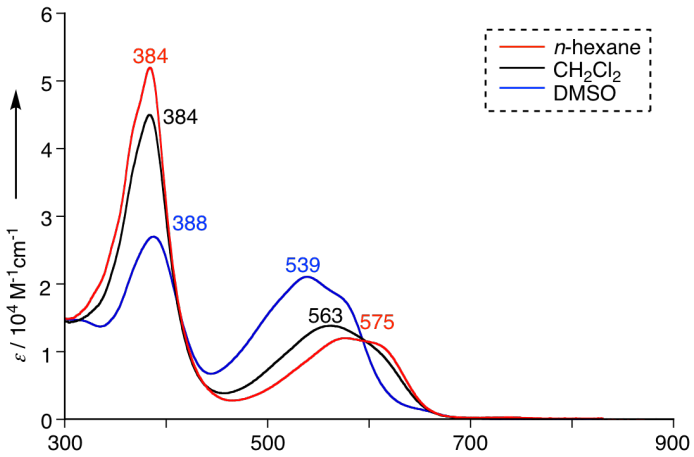

Figure S6-8. UV/Vis absorption spectra of **10** in various solvents.

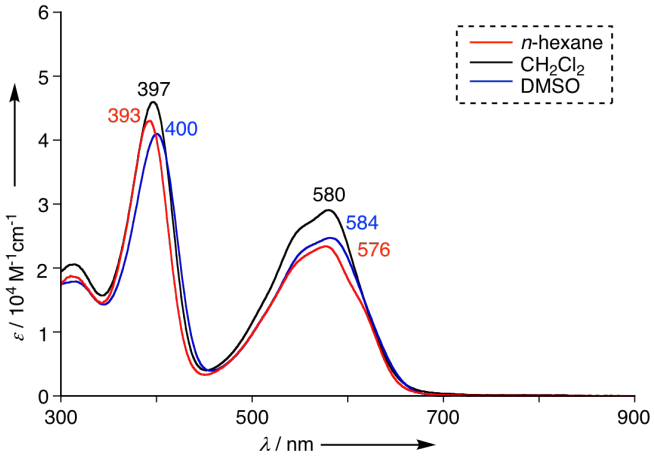

Figure S6-9. UV/Vis absorption spectra of **11** in various solvents.

7. DFT Calculations

All calculations were carried out using the *Gaussian 09* program.[S1] Initial geometries were obtained from X-ray structures. Calculations were performed by the density functional theory (DFT) method with restricted B3LYP (Becke's three-parameter hybrid exchange functionals and the Lee-Yang-Parr correlation functional)[S2] level, employing a basis sets 6-31G(d).

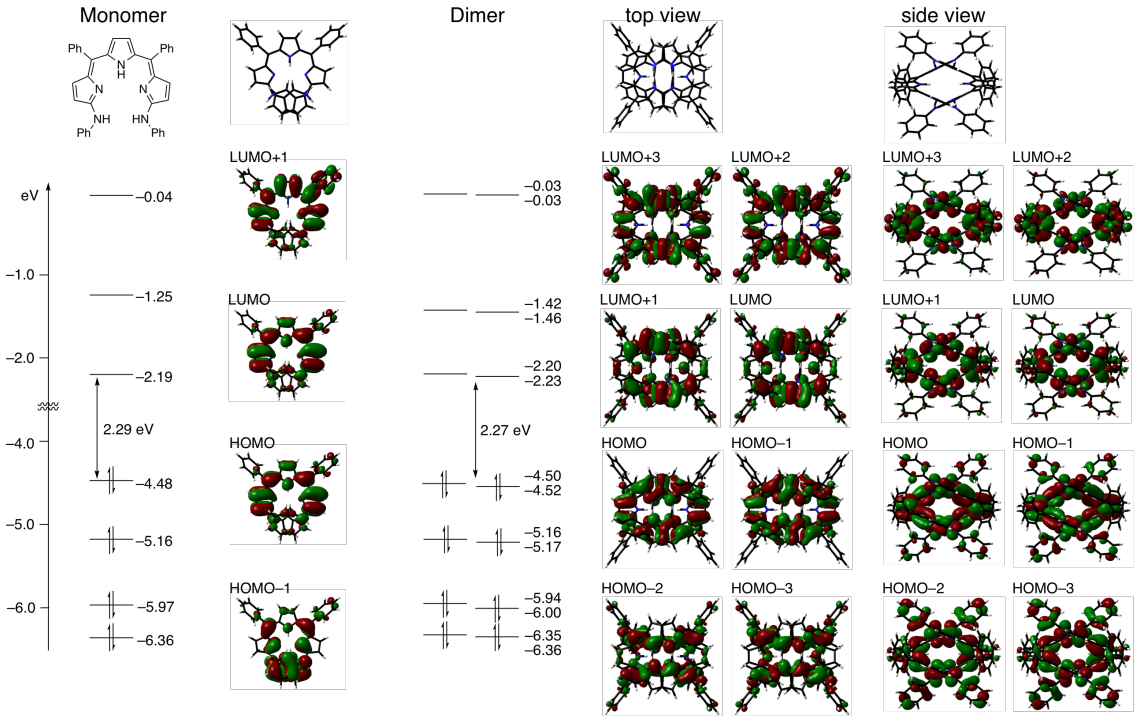

Figure S7-1. Kohn-Sham MO representations and energy diagrams of monomeric and dimeric **4**.

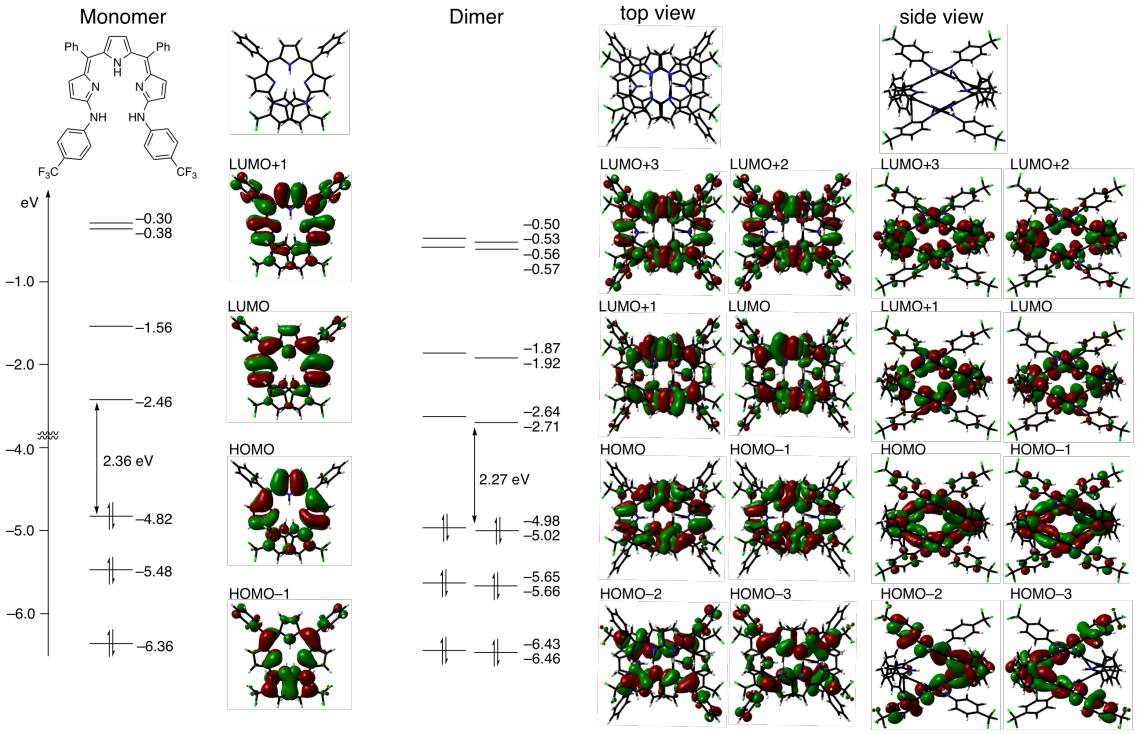

Figure S7-2. Kohn-Sham MO representations and energy diagrams of monomeric and dimeric **5**.

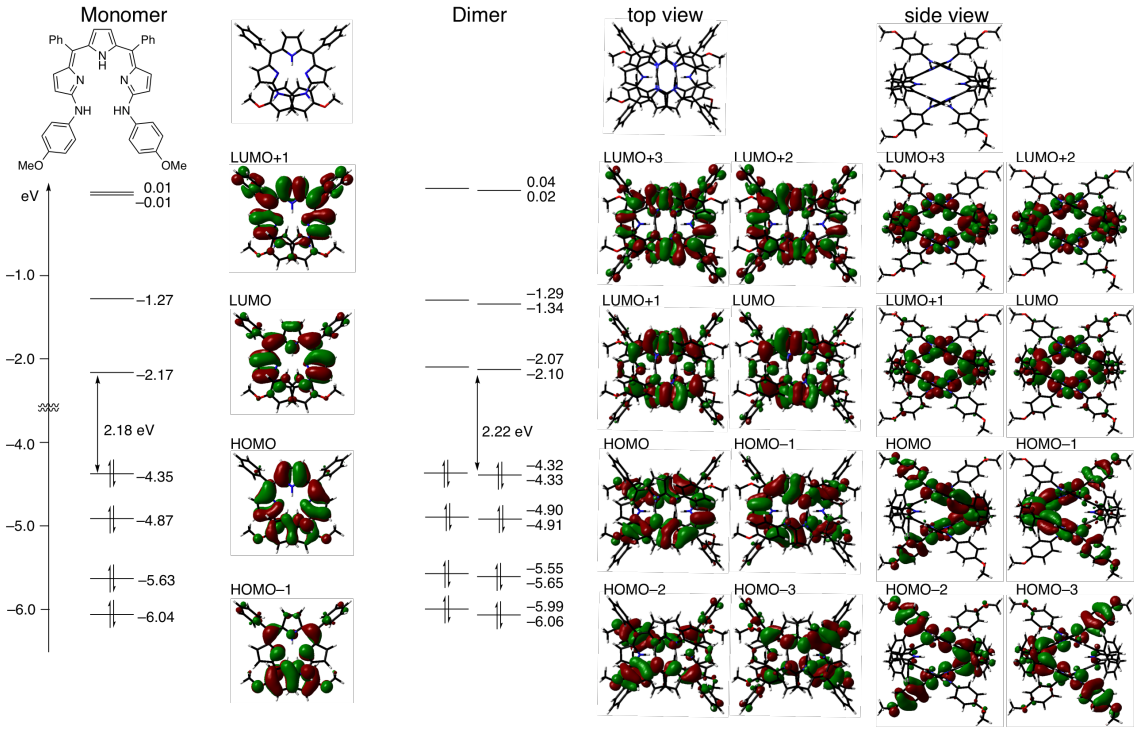

Figure S7-3. Kohn-Sham MO representations and energy diagrams of monomeric and dimeric **6**.

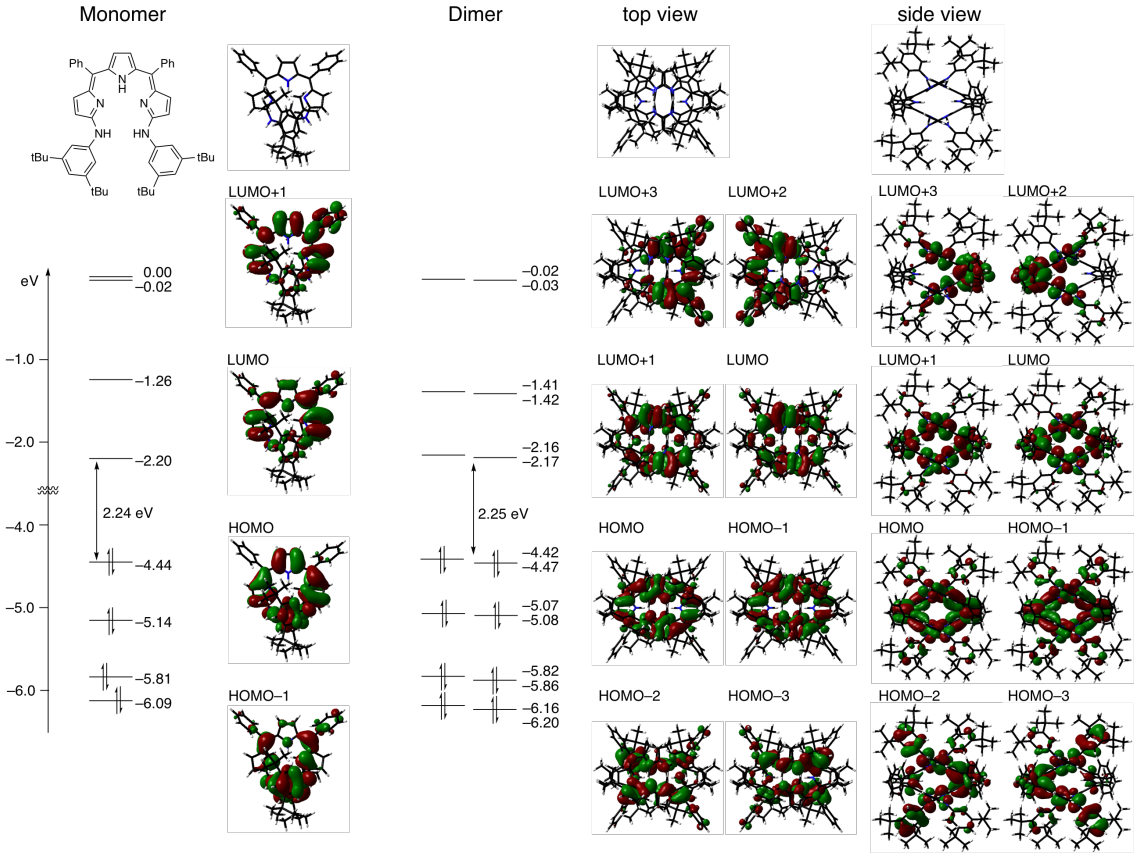

Figure S7-4. Kohn-Sham MO representations and energy diagrams of monomeric and dimeric **7**.

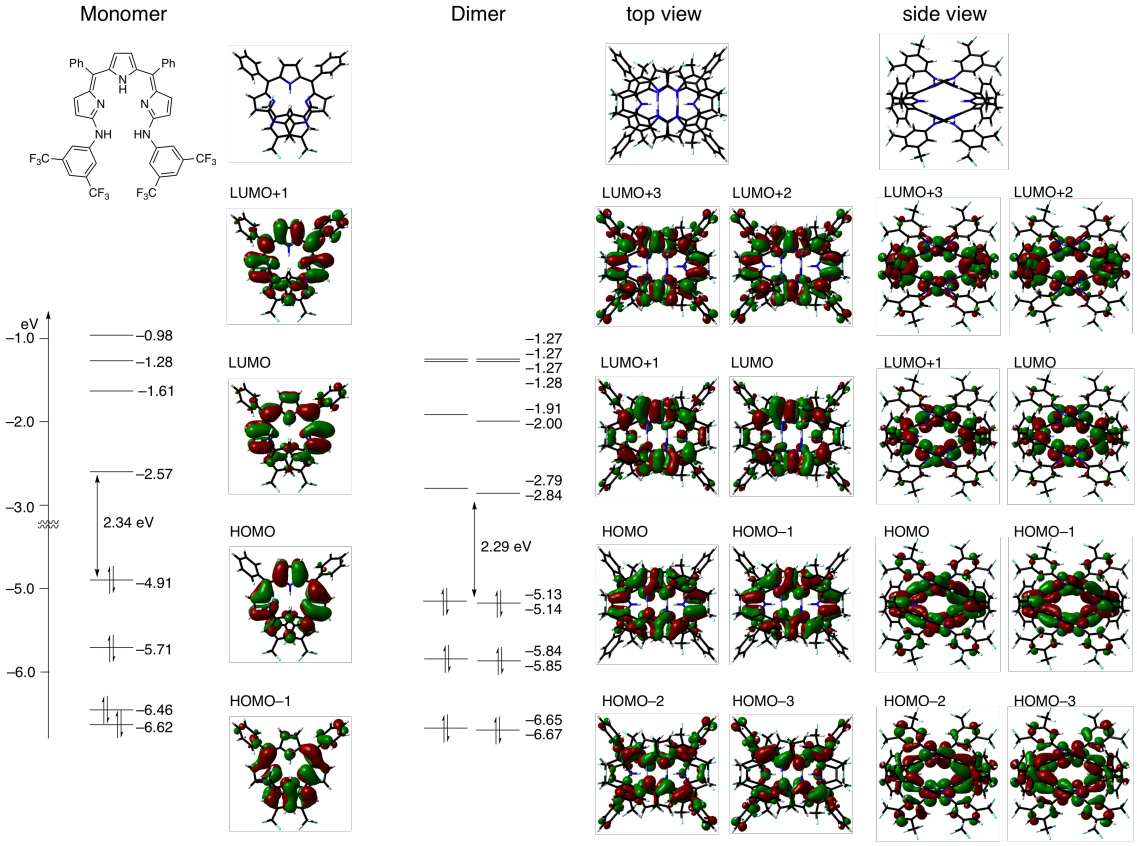

Figure S7-5. Kohn-Sham MO representations and energy diagrams of monomeric and dimeric **8**.

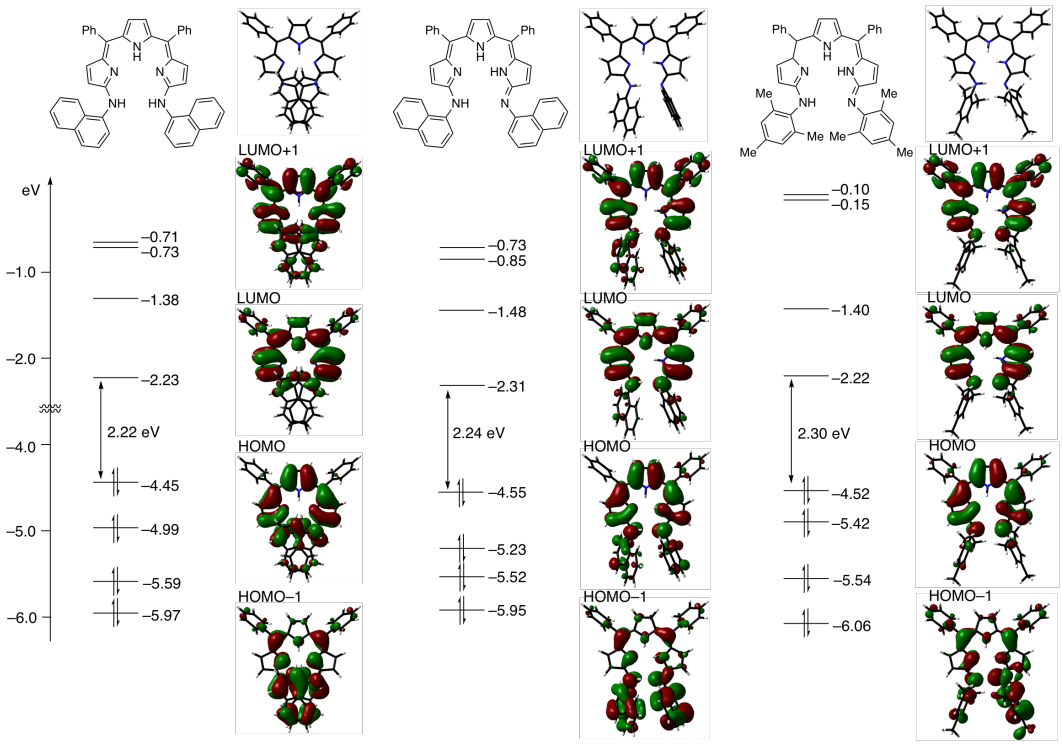

Figure S7-6. Kohn-Sham MO representations and energy diagrams of **9** and **10**.

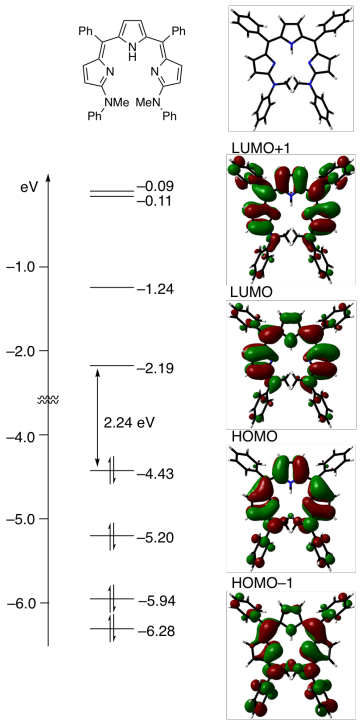

Figure S7-7. Kohn-Sham MO representations and energy diagrams of **11**.

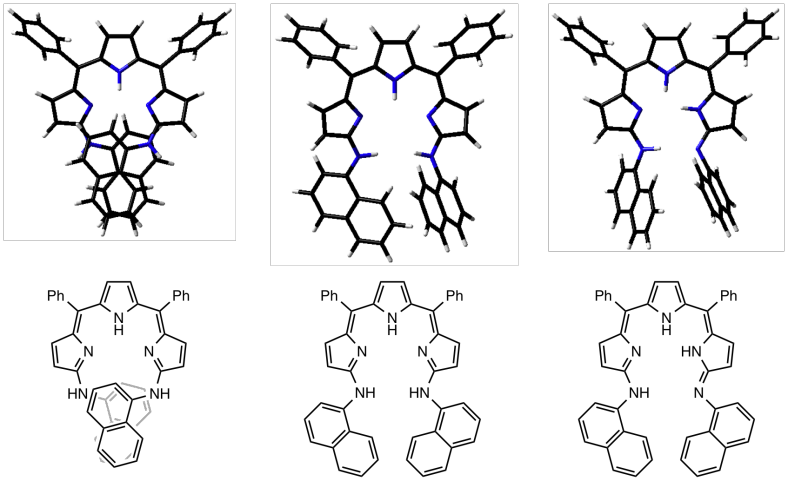

Total energy (hartree)	–2045.867628	–2045.869422	–2045.872461
Relative energy (kcal/mol)	+4.48	+3.35	0

Figure S7-8. Optimized structures and total energy estimation including zero-point energy correction for **9**.

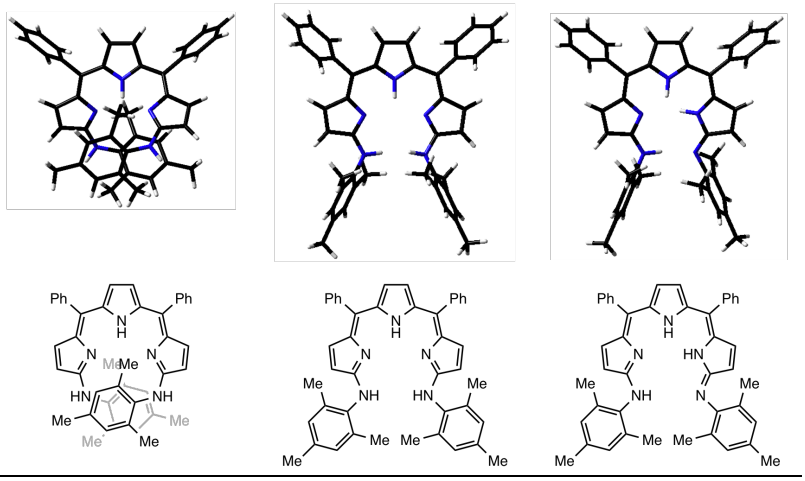

Total energy (hartree)	–1974.403131	–1974.413282	–1074.420924
Relative energy (kcal/mol)	+11.17	+4.80	0

Figure S7-9. Optimized structures and total energy estimation including zero-point energy correction for **10**.

8. Supporting References

[S1] Gaussian09, Revision A.02, M. J. Frisch, G. W. Trucks, H. B. Schlegel, G. E. Scuseria, M. A. Robb, J. R. Cheeseman, G. Scalmani, V. Barone, B. Mennucci, G. A. Petersson, H. Nakatsuji, M. Caricato, X. Li, H. P. Hratchian, A. F. Izmaylov, J. Bloino, G. Zheng, J. L. Sonnenberg, M. Hada, M. Ehara, K. Toyota, R. Fukuda, J. Hasegawa, M. Ishida, T. Nakajima, Y. Honda, O. Kitao, H. Nakai, T. Vreven, J. A. Montgomery Jr., J. E. Peralta, F. Ogliaro, M. Bearpark, J. J. Heyd, E. Brothers, K. N. Kudin, V. N. Staroverov, R. Kobayashi, J. Normand, K. Raghavachari, A. Rendell, J. C. Burant, S. S. Iyengar, J. Tomasi, M. Cossi, N. Rega, J. M. Millam, M. Klene, J. E. Knox, J. B. Cross, V. Bakken, C. Adamo, J. Jaramillo, R. Gomperts, R. E. Stratmann, O. Yazyev, A. J. Austin, R. Cammi, C. Pomelli, J. W. Ochterski, R. L. Martin, K. Morokuma, V. G. Zakrzewski, G. A. Voth, P. Salvador, J. J. Dannenberg, S. Dapprich, A. D. Daniels, O. Farkas, J. B. Foresman, J. V. Ortiz, J. Cioslowski, D. J. Fox, Gaussian, Inc., Wallingford CT, 2009.

[S2] (a) A. D. Becke, *J. Chem. Phys.* **1993**, *98*, 1372. (b) C. Lee, W. Yang, R. G. Parr, *Phys. Rev. B* **1988**, *37*, 785.